Magma Convective Recharge In Volcanic Systems

Thesis

Magma Convective Recharge in Volcanic Systems

A Thesis presented for the degree of
Master of Philosophy

By

Samantha J.N. Aderson
BSc. (Hons)
University of Liverpool

Department of Earth Sciences
The Open University

February 2004

DATE OF SUBMISSION 27 SEPTEMBER 200
DATE OF AWARD 19 MARCH 2004

ProQuest LLC.
789 East Eisenhower Parkway
P.O. Box 1346
Ann Arbor, MI 48106 – 1346

Acknowledgments

It has been a long slog but I have got there in the end so a few thanks to the important people. Thanks to Hazel and Steve for the positive support in the last year. Most of all my thanks to Brian for his endless patience and encouragement. Also thanks to my little allies Frances, Don and Moira.

Abstract

Active lava lakes are not a common phenomenon. Some, such as those found on Kilauea and Erta 'Ale, have stayed active for decades. Remote sensing investigations (Harris et al., 1999; Allard, 1997; Francis et al., 1993) have measured the volatile fluxes from the lava lakes and found that their fluxes were persistently high. Several suggestions have been put forward to explain this. One explanation is that there are large volatile-rich magma bodies at a shallow depth steadily releasing the volatiles. Studies using other geophysical methods such as gravity and seismics have generally not found these bodies (Francis et al., 1993; Allard, 1997). Another suggestion is that volatile-rich magma is constantly being brought up to the surface convectively and when the volatiles have been released the cooler, denser magma sinks allowing replenishment with fresh magma. This is a possible explanation of the longevity of this volcanic feature, but it is not only lava lakes that appear to exhibit this behaviour. There are dykes in places such as Mount Etna that have remained active much longer than expected.

This study will examine this process using contrasting modelling techniques. The first technique involves finite element models to investigate the factors controlling cooling in dykes. The second technique involves using the results of mathematical modelling to design an analogue model in order to study heat distribution within a lava lake – conduit - magma chamber system.

Table of Contents

Chapter 3

Chapter 4

List of Figures

Page

Chapter 1

Chapter 2

Chapter 3

Chapter 4

Figure

Magma Convective Recharge in Volcanic Systems

Chapter 1

1.0 Introduction

The degassing of open vent volcanoes has a huge environmental impact with millions of tonnes of volatiles entering the atmosphere each year (Francis et al., 1993; Allard, 1997; Kyle and Meeker, 1990; LeGuern et al., 1979). Some volcanoes such as Mount Etna in Sicily and Kilauea on Hawaii have been persistently active for considerable periods of time. Fresh magma can be enriched with volatiles and the larger the volume of magma entering the volcanic system the greater the amount of volatiles available to the atmosphere. Estimates from measurements of volatiles in gas plumes and magmas at Mount Etna suggest that there should have been a larger volume of magma, the source of these volatiles, than has been erupted or found at shallow levels (Francis et al., 1993; Allard, 1997). If this is the case how is it possible for volcanoes to be so persistently active? One explanation, which this study examines, is that of convective magma recharge. The suggestion is that gas rich magma rises up to the shallow levels of the volcanic system and degasses. On becoming cooler and denser, it sinks back to the deeper reservoir. Convection then brings more gas rich magma to recharge the upper levels.

In this study the life spans of two parts of the volcanic system are investigated, namely lava lakes and dykes. What is so important about their life spans? If a lava lake comes into existence but then rapidly solidifies it would not pose a big risk, but if it stayed active then there could be several hazards associated with it for surrounding populations. One such hazard may be persistent degassing putting quantities of gases such as SO_2 into the atmosphere. This could lead to respiratory and other medical problems within the local population. These gases could lead to devastation of local vegetation and crops downwind of the plumes.

The study of the life span of lava lakes is clearly important. Whilst a lava lake remains active it remains a risk to surrounding populations, crops, livestock and property.

The threat posed by active dykes is much less obvious. Magma in dykes can either solidify at depth and do no damage or they can feed eruptions with all the associated risks. One example is the 1991-93 eruption on Mount Etna; the main feeder for this eruption was a dyke which intercepted the wall of the Valle del Bove, leading to the largest eruption in the last 300 years (Armienti et al., 1994). It erupted approximately $235 \times 10^6 m^3$ (Rymer et al., 1995) compared to eruptions of $100 \times 10^6 m^3$ in 1983 and $75 \times 10^6 m^3$ in 1971 (Barbieri et al., 1990). Despite the efforts of the Civil Protection force to slow the lava flow it eventually stopped a very short distance from the town of Zafferana.

1.1 Aims

This study will consider several models of magma body cooling as reference points on which to build varied models. Two contrasting modelling methods were used to investigate different magmatic bodies: finite element modelling to examine cooling in dykes, and physical modelling to examine cooling within the lava lake – conduit – magma chamber system.

The first technique that will be examined is the finite element method. This technique enables us to model simple magma bodies on a computer where physical dimensions and material properties can easily be varied. The aims of the finite element modelling will be:

a) To systematically vary the height and width of a 2-D dyke and see its effect on magma cooling rate.
b) To systematically vary different material properties of the magma whilst holding the others constant to see their effect on the magma cooling rate.

By varying the dyke dimensions and magma material properties, this study will also examine whether the magma loses heat by only convection or only conduction.

The second modelling technique involves laboratory and mathematical modelling of a lava lake – conduit – magma chamber system. This modelling technique will also examine the effects of varying the dimensions and material properties of the system and the analogue magma.

From these two modelling techniques we hope to gain an insight into how the physical dimensions of the system and the material properties of the magma combine to facilitate or inhibit convective magma recharge.

1.2 Heat Transfer Mechanisms

As this study examines the cooling of magma bodies it is important to consider various mechanisms that transfer heat to and from a body. The most important types of heat transfer in the volcanic system are conduction and convection.

Conduction of heat happens when molecules collide and transfer energy to one another in a diffusive process. Convection of heat happens when a moving medium transports heat energy. Which of these processes dominates at any given time and place will depend on local conditions and material properties. Figure 1.1 shows an example of heat transfer mechanisms in a schematic cross section of a dyke. At the base of the dyke new hot magma is introduced so heat is transported by forced convection. Near the walls the magma has solidified and here heat is transferred by conduction into the cooler country rock. Between the solidified magma and the inflowing magma there is a thermal boundary layer of partially solidified magma, here heat may be transferred by a mix of conduction and natural convection. Further away from the magma entrance the magma will be well mixed and insulated from the effects of the cooler country rock. Natural convection is entirely due to buoyancy-driven flow within the liquid, e.g. when the magma material expands differentially on heating creating a lower density hence a more buoyant material. It contrasts with forced convection which occurs due to a driving pressure (as at the dyke base) and will not be considered further here.

Whether a fluid convects or conducts can be predicted by the Rayleigh number, when a fluid exceeds a critical Rayleigh number, convection will occur. The Rayleigh number is as given below:

$$Ra = \frac{\alpha \Delta T g \rho d^3}{\kappa \mu}$$ (Brown and Musset, 1995)

Ra = Rayleigh number (dimensionless number) d = thickness of layer (m)

ΔT =Temperature difference between the top and bottom of a layer of thickness d (K).

g = acceleration due to gravity (ms^{-2}) ρ = density (kgm^{-3})

κ = Thermal diffusivity (m^2s^{-1})

where $\kappa = k/\rho c$ k = thermal conductivity ($Wm^{-1}K^{-1}$)

c = specific heat capacity ($J\ kg^{-1}K^{-1}$)

μ = Viscosity (Pas) α = Volume coefficient of thermal expansion (K^{-1})

Ra_{cr} = Critical Raleigh number

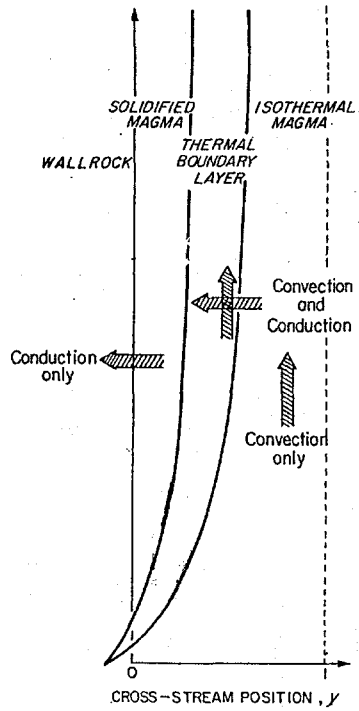

Figure 1.1 Schematic cross section through a dyke showing solidified magma against the wall rock separated by a thermal boundary layer to the well mixed magma within. The dotted line is the vertical symmetry line. (Delaney and Pollard, 1982).

Viscosity is a measure of a fluid's resistance to flow, the more viscous a fluid the more it resists flow. Increasing viscosity leads to a smaller Ra and hence to a reduced likelihood of convection. Density is the mass per unit volume of a material; this occurs in the numerator of the Ra number equation and hence will increase Ra and make convection more likely. Thermal diffusivity is the ability of a material to conduct heat and as it increases, Ra becomes smaller and the material is less likely to convect. The volume coefficient of expansion has an important role in that when a magma has a large volume coefficient then it will expand more, thus decreasing density and increasing instability and buoyancy.

From this it can be seen that there is a fine balance between these material properties and what helps and what hinders convection initiating. Previous studies have shown that the rheology of magma can also be greatly affected by volatiles within the magma. An increase in gas bubbles or vesicles within a magma will increase its viscosity but decrease its density. Previous work done on the thermal effect of vesicles on cooling basalt flows (Keszthelyi, 1994) indicates that thermal conductivity in a magma is reduced as porosity increases. This work also suggested a subtle

lowering of the effect of thermal diffusivity as porosity increases. Increasing porosity of pahoehoe lavas was found to increase their rate of cooling.

1.3 Lava Lakes

Lava lakes are not common phenomena; active lava lakes are particularly rare. Active lava lakes occur where a pool of magma resides over a magma column allowing input from, and discharge to, a lower magmatic system. Inactive lava lakes occur where magma has simply ponded in a topographic depression. Whether or not a lava lake is connected to the magmatic system below, naturally has a marked influence on the longevity of a lake.

1.3.1 Inactive Lava Lakes

Several of the best-studied inactive lakes were formed on the flanks of Kilauea on Hawaii (Peck et al., 1979). In the 1950s and 60s several of these lakes formed, Kilauea Iki in 1959, Alae in 1963, and Makaopuhi in 1965. Kilauea Iki formed by overspills of 17 eruptions over 36 days, this was the deepest of the three lakes and reached depths of over 100m. Alae was the shallowest only reaching a depth of 15m formed during an eruption lasting 3 days. Makaopuhi reached a depth of 83m forming in about 18 days. These lakes were readily accessible and extensively studied using drilled cores. These studies provide data consistent with theories that firstly a thick crust forms on the surface due to cooling by exposure to the elements in particularly the heavy rain. Next a crust at the base of the lake formed and since magma here is relatively insulated the crust is not as thick as the surface crust. Gradually as time progresses the crusts thicken until the lake solidifies completely. Alae was found to have solidified in about ten and a half months whereas Kilauea Iki took about 25 years to solidify completely. It is clear that thicker lava lakes will stay molten much longer than shallow lakes even if they are not connected to a hot magmatic system.

1.3.2 Active Lava Lakes

It is long lived lava lakes such as that on Mount Erebus on Antarctica, Erte 'Ale in Ethiopia, Nyiragongo and Nyamuragira in Eastern Zaire that have stayed active for decades which are the interest in this study. Volcanoes on Hawaii also show examples

of active lava lakes. This outlines some of the work done on these lava lakes and the conclusions that can be drawn from these studies.

Mount Erebus

Mount Erebus is a stratovolcano standing at 3794m on Ross Island in Antarctica and it has an active lava lake that was discovered in 1972 (Giggenbach et al., 1973). Since then it has been the target of several studies using various monitoring methods such as COSPEC and thermal remote sensing (Kyle and Meeker, 1990; Harris et al.,1999; Tazieff, 1994). The lava in the lake is an alkaline anorthoclase phonolitic lava and has been found to be persistently convecting. The lake has demonstrated regular low energy level Strombolian activity although it has on occasions been energetic enough to obscure the lake with debris.

The COSPEC data has been used to investigate sulphur emissions (Kyle and Meeker, 1990). The degassing of the magma on Erebus often gives rise to significant plumes. The phonolite in the Erebus lake is quite viscous and supported particularly big degassing bubbles; one was said to have covered the whole surface of the lake (Tazieff, 1994). It is not suprising that degassing episodes were so distinctive. It is the gases from these plumes and their emission rates that have been measured. In 1983 the lake had a surface area of 11000m^2 and at this time the SO_2 flux was around 200 Mg per day. Over the next few years this dropped to about 16 Mg per day with a lake surface area of 80 m^2. After this the emission rate rose again to 51 Mg per day in 1987 with a lake surface area of 2800 m^2 (Kyle and Meeker, 1990). Clearly this shows that the lava lake has a variable size with volatile fluxes being related to the surface area of the lake. Naturally, Antarctica is a fairly inhospitable place and ground monitoring of the volcano only takes place in the Antarctic summer. These conditions mean that remote sensing methods must be used to examine the lava lake more regularly; this has enabled close regular monitoring of degassing and thermal fluxes. From these data, estimates can be made of the circulation rates of magma chamber – conduit – lava lake system (Harris et al., 1999). These have indicated that fluxes have remained fairly constant; one way of explaining this would be that hot material is constantly emplaced at a shallow level replacing heat lost from the cooling magma. This would imply that the size of a shallow body would be gradually increasing in size, but a deformation survey in the early 1980s showed no evidence of such an intrusion (Otway et al., 1994) An alternative explanation would be that the lake was replenished with hot material and that cold material is removed from the lake.

These studies suggest that there is little shallow level endogenous growth but that a gaseous, relatively viscous magma rises to the lava lake, degasses and then cooler denser material sinks to be replaced by fresh gaseous magma thus maintaining a steady circulatory system.

Erta 'Ale

Erta 'Ale is a shield volcano in the Danakil Depression in Ethiopia in the East African Rift. The active lava lakes in Erta 'Ale's northern lobe are some of the longest-lived of known lakes. Historically it has been a fairly difficult place to access both geographically and politically, temperatures of often over 50°C make field observations particularly difficult (Burgi et al., 2002). In the 1960s scientists began to study it seriously and after an aerial survey showed active lava lakes (Mohr, 1962). In the early 1970s there were two active lava lakes and these were then filled to the level of the caldera floor. (Tazieff, 1994; LeGuern et al., 1979; Burgi et al., 2002) observed the lava lake in the central part of the northern lobe very closely, they observed that instead of gas bubbles buoyantly rising through the viscous magma they rose with the magma. This suggested that there were convecting currents of magma as opposed to only jets of gas bubbles rising through. The surface of the lake was also seen to have currents moving across the surface with down-welling currents at the edge of the lake, reminiscent of a Bernard convection cell. (Tazieff, 1994; LeGuern et al., 1979; Burgi et al., 2002) also observed these surface currents during fieldwork in February 2001 and measured the sideways drift of fire fountains to be around 2-5m per minute. They also observed, as Tazieff did, that the fire fountains and up-welling magma originated from stable areas and down-welled in similarly stable positions. This continual degassing of the lava lake suggested that it might be the renewal of hot magma that helped keep the lake active and molten. Since there was no evidence of volcano growth from within as it continued to have a particularly subdued topography, this model has been favoured (Oppenheimer and Francis, 1998).

As visiting areas such as this has been difficult, they have become ideal targets for satellite remote sensing (Oppenheimer and Francis, 1998). The measurements made show a fairly high, constant heat flux from the lava lakes, it also showed that little magma was lost to eruptions. This again suggests a convective circulation between the lakes through the conduit to a deeper chamber continually replenishing the lake.

Nyiragongo and Nyamuragira

Nyiragongo and Nyamuragira are neighbouring volcanoes in the Virunga volcanic range in Eastern Zaire, which crosses part of the East African Rift.

Nyiragongo, a basaltic shield volcano with a summit elevation of 3058m, was chosen as the African Decade volcano in 1991 as it posed a high risk to the local and refugee populations. It is believed to have had a lava lake for a considerable period from 1894 until 1977 when on January the 10^{th} the lake drained through fissures on the flank, killing 70 people. The lake reappeared in 1982 and by June 1994 it was approximately 40m in diameter but still 150m below the level of the pre-drained 1977 lake. In 2002 there were renewed eruptions causing much damage and now in 2003 a lava lake has again been observed; its diameter is approximately 45m.

There were several field visits to these volcanoes in the 1960s and 1970s. The level of the lakes varied during this study period. It was observed that little heat was lost from the gas moving through the lakes but like that of Erta 'Ale it was more of a slow convection of magma bringing gas bubbles with it. This again suggested that degassing is the result of magma convection rather than the cause.

Nyamuragira, also a basaltic shield volcano, also had a long-lived lava lake from at least 1921 until it drained in 1938. It is also one of the most active African volcanoes.

Kilauea

Kilauea on Hawaii has had several long-lived lava lakes; some are inactive lava ponds such as Alae and some that have been very active such as Kilauea Iki. Two of the currently most active are Pu'u 'O'o and Kupainaha. They formed during an eruptive episode between July 1986 and November 1991 (Heliker et al., 1998). They are slightly different to the other active lakes discussed here as they are flank lava lakes as opposed to summit lava lakes. They are believed to be linked by a dyke-like reservoir, which in turn is connected to the main Kilauea reservoir. It has been observed that a decrease in activity at one lake will lead to increased activity at the other lake (Heliker et al., 1998; Harris et al., 1999). At flank lava lakes it is not unusual for magma to be erupted rather than recirculated (Harris et al., 1999). The lakes on Kilauea have frequently filled, drained, collapsed and then refilled, this has meant that the dimensions of the lakes have varied over time.

Satellite remote sensing of these lakes showed that Pu'u 'O'o had a high heat flux, it was suggested that this may be due to overturning of the magma. It has also been

proposed that magma degassed at Pu'u' O'o being denser, sank and then mixed with the Kupainaha magma and was then erupted through that vent. See figure 1.1 taken from (Harris et al., 1999). Again, like the lava lakes discussed above this suggests that these lava lakes remain molten because of convective circulation.

1.3.3 Lava Lakes – Summary

There are two main types of lava lakes:

- **Inactive** – Inactive lakes are merely ponds of magma with no fresh input after the initial formation of the lake.
- **Active** – Active lava lakes have been shown to have remained molten and active for many years even decades.
    - *Mount Erebus* – A phonolitic persistently degassing, convecting lava lake with little evidence of endogenous growth (Tazieff, 1994).
    - *Erta 'Ale* – A persistently degassing basaltic convective lava lake, again surveys suggesting no endogenous growth (LeGuern et al., 1979).
    - *Nyiragongo and Nyamuragira* – Basaltic convective lava lakes.
    - *Kilauea* - There have been several long-lived active lava lakes on the flanks of Kilauea. Magma from Pu'u O'o is believed to have been convectively recycled and extruded from Kupainaha.

All the active lava lakes discussed here show some evidence for a circulating system. Thus a process of heat loss by conduction cannot fully explain the longevity of the active lava lakes.

Whether this continual heat flux is a result of recycling or continual replenishment by intrusion of more and more magma is unknown at this time. Little geophysical evidence has been seen (e.g. deformation, seismics and gravity) for shallow intrusions leading to endogenous growth (Francis et al., 1993).

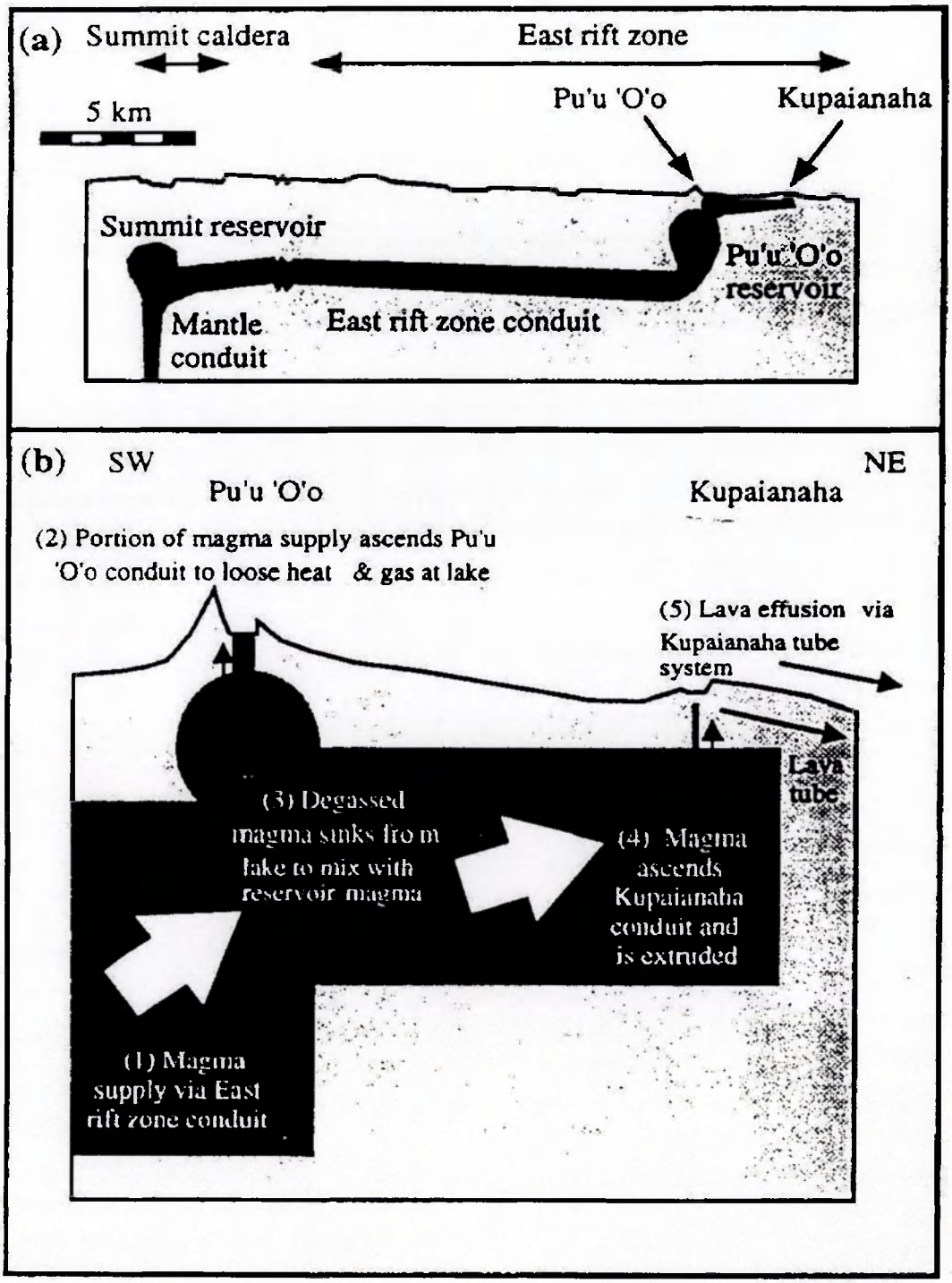

Figure 1.2 This shows how the lava lakes of Pu'u 'O'o and Kupainaha are thought to be connected. One or both can be active at the same time feeding off each other keeping them molten and hence active for long periods. (Harris et al., 1999).

1.4 Heat Transfer in Dykes

In the previous section I introduced lava lakes, which can be thought of as windows onto the magmatic system. In this next section I examine dykes that are a part of the magmatic system that is usually hidden. Dykes are discordant igneous bodies that are usually more or less vertical and sheet like. Dykes may occur in any part of the magmatic system though they commonly branch off from magma chambers (McLeod and Tait, 1999). Dykes are often detected by geophysical methods such as microgravity, magnetic surveying and ground deformation studies. Generally, dykes cool and solidify in a matter of hours or days but this is not always the case. Dykes can stay sufficiently molten and be efficient feeders for eruptions when they intersect the land surface; it was a dyke that fed the 1989-91 eruption on Mount Etna. So, like lava lakes, the longevity of dykes can be very important to surrounding communities.

1.4.1 Dyke Width and Magma Viscosity

Dykes occur when the driving pressure of the magma exceeds the elastic stresses in the surrounding country rock and creates magma-filled fractures, although sometimes the fractures can be pre-existing and the magma simply fills them. Obviously, higher pressures can create wider dykes but it is believed that the viscosity of a magma can also be a determinant of dyke width. Work by (Wada, 1994) suggests that mafic magmas of viscosities of around 10^1-10^2 Pas would form dykes of widths of approximately 1m whereas felsic dykes of viscosities 10^6-10^7 Pas could form dykes of widths up to 100m.

Basic Tertiary dykes in Mull, Scotland, have an average width of 1.5m (Bailey et al., 1924), though some were wider than 50m. The Chief Joseph swarm of dykes that were thought to have fed the Columbia River Basalts have a much higher average thickness of 6m (Pollard and Delaney, 1982). Some flood basalts were fed by dykes of widths greater that 100m (Wada, 1994). This is thought mainly to be due to extremely high driving pressures. Generally speaking the thinner the dyke, the quicker it will solidify. The heat within a relatively thin dyke has a shorter distance to travel and hence dissipate into the surrounding country rock. The initial width of a dyke can be critical (Huppert and Bruce, 1990). Assuming pressure is constant, if a dyke is too narrow then as the heat of the magma is transferred to the cooler country rock. Viscosity will increase and the magma will begin to solidify and narrow the dyke,

eventually the flow of magma may be blocked. The steeper the temperature gradient between the magma and the country rock then potentially the faster the heat transfer will be. However if it is wider than the flow rate can carry in more heat than is lost to the walls and this may even lead to the walls being melted back widening the passage and allowing the flow rate to be further increased. The models of (Huppert and Bruce, 1990) Figure 1.3 suggest that the wider the dyke the longer it will take to block and solidify. The top graph in figure 1.3 illustrates, for different length dykes, there are critical initial widths. A dyke a few tens of centimetres narrower than this critical width could block and therefore halt a potential eruption. This graph also shows the importance of the initial temperature of the country rocks. A dyke emplaced into hot rocks can maintain its flow at much narrower widths than if it had been emplaced into cooler rocks. This is not unsurprising as the temperature gradient between the magma and the hot country rocks would be shallower and hence the heat loss and ensuing solidification would be less. For longer dykes the width needs to be greater for meltback to be achieved possibly due to an increased surface area of cooler rocks.

The lower graph in figure 1.3 shows the time taken for a dyke to block with given initial widths. This illustrates that very narrow graphs solidify in a matter of days but as the initial width of a dyke approaches the critical value it takes increasingly longer for this blocking to occur. The graph also illustrates, how for different length dykes with an initial width of less than a metre, there is little difference between the time taken for them to block.

1.4.2 Intrusion of Magma into Dykes

How a dyke is filled and the rate at which the magma enters the system is critical to a dyke's longevity. If magma is simply intruded and left to cool purely by conduction then numerical models (Jaeger, 1968) indicate that dykes will cool rapidly in hours or days so clearly there are other factors to consider. For dykes to remain viable and feed eruptions, the heat input needs to be greater than the heat output to the cooler country rocks (Huppert and Bruce, 1990). So, if magma is not simply emplaced an alternative is for magma to be intruded in pulses, but is there any evidence for this? Work by (Maaloe, 1998; Parfitt et al., 2002; Wada, 1992) indicates that intrusion in a pulse-like fashion is likely to keep magma hotter for longer. (Wada, 1992) observed phenocrysts

in the feeder dyke of the 1983 eruption of Miyake-Jima, Japan that implied that the magma entered in three distinct pulses, the last pulse being intruded vertically.

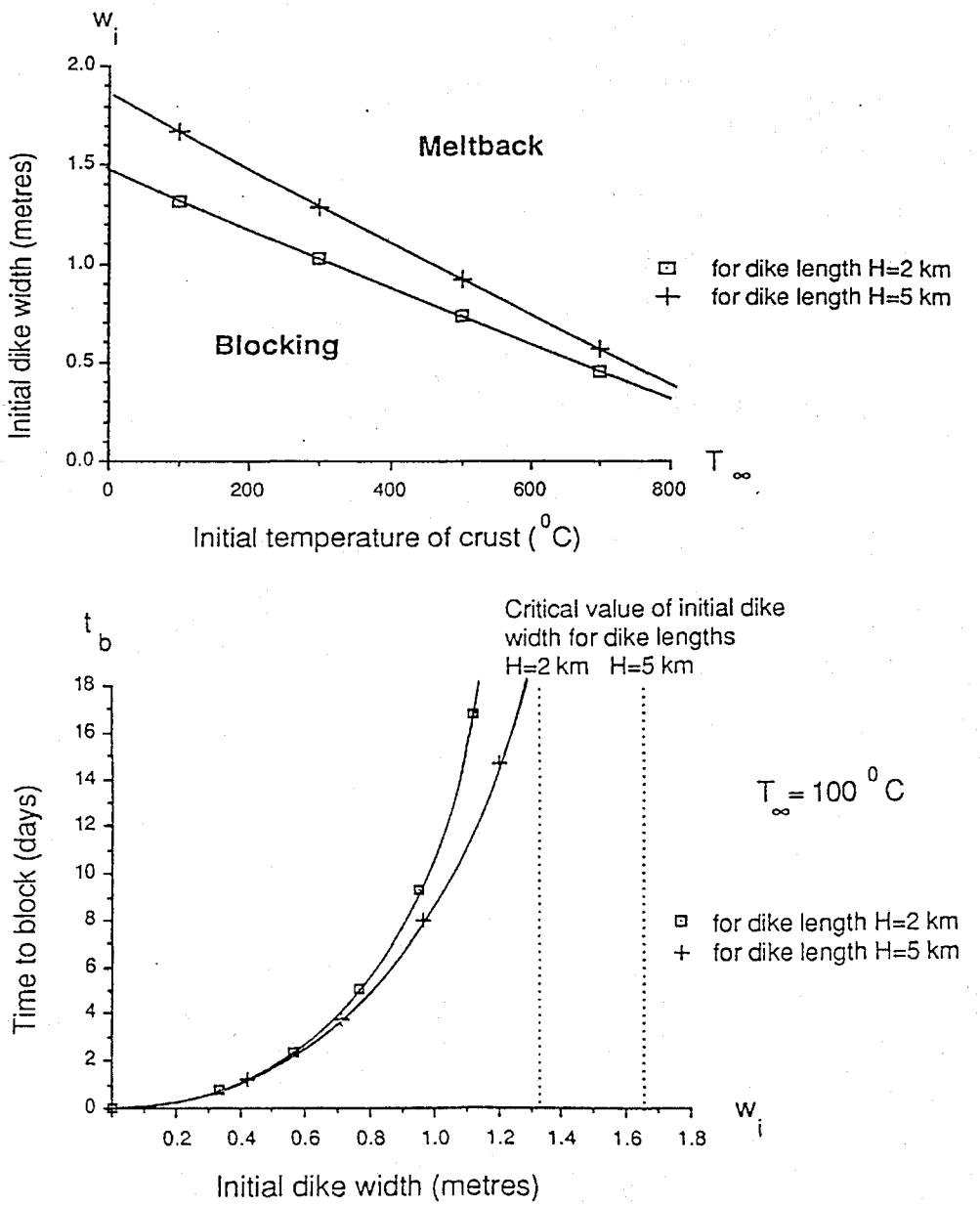

Figure 1.3 The top graph (a) shows the region in which meltback or blocking may occur. The lower graph (b) shows the time for a dyke to become blocked as a function of initial dyke width. The time to block becomes infinite for initial widths approaching the critical value for meltback to occur. (Huppert and Bruce, 1990).

(Maaloe, 1998) suggests that the feeder dykes on Kilauea, Hawaii are supplied by a succession of magma pulses. How the magma flows in to the dyke system not only has an effect on the thermal viability of a dyke but can also affect the style of

eruption. (Parfitt et al., 2002) compared sub-aerial and submarine eruptions at Kilauea and their implications for thermal viability of feeder dykes. These eruptions were classified into five types: Type 1 – short-lived fissure eruptions that had significant eruptive active for up to 13 hours, Type 2 – longer lived fissure eruptions typically lasting around 5 – 15 days, Type 3 – fissure eruptions that evolve to a central vent, Type 4 – episodic eruptions that start as fissure eruptions but evolve to give distinct deposits, and Type 5 – long-lived, steady state eruptions. (Huppert and Bruce, 1990) suggested that feeder dykes were either in a state of active cooling and solidification or a state of active melting back (Parfitt et al., 2002). Type 1 activity tends to lead to rapid cooling and solidification and therefore dykes of this type are not viable feeders, Type 2 are more viable but still soon block the feeder dyke. Type 3 activity leads to feeder dykes similar to those suggested by (Huppert and Bruce, 1990) where as the dyke begins to narrow and solidify the magma flow becomes localised into a central vent. Type 4 activity seems more typical of longer lived dykes with pulses or episodes of eruptive activity keeping the magma in the dyke hotter for longer and possibly leading to some thermal erosion. As it begins to cool, if the magma pressure in the magma chamber increases enough after the initial input, then the pathway may be viable enough for another episode to occur. Type 5 activity with its steady state keeps dykes viable and able to feed long-lived eruptions such as the Mauna Ulu 1972-74 eruption.

1.4.3 Dykes on Mount Etna, Sicily and Tolbachik, Kamchatka

Mount Etna on Sicily is Europe's largest active volcano and is easily accessible. Many studies have been carried out there over hundreds of years. In the 1980s and 1990s a lot of gas emission data were collected using COSPEC (Allard, 1997). From these data, Allard calculated that there must be large amounts of degassed magma stored within the plumbing system of Mount Etna because only about 10-20 percent of this degassed magma was extruded. Estimates from other geophysical surveys suggest the storage capacity of the upper plumbing system to be only about 0.6 km^3 (Allard, 1997). In 1979 a gravity network was set up to monitor changes in microgravity in the summit region of Mount Etna (Sanderson, 1982). From the gravity changes observed the movement of magma can be inferred. Where magma is stored prior to eruption and where it comes from is important to our understanding of

eruption mechanics. These early gravity surveys from September 1979 to August 1980 indicated gravity increases, which were accompanied by little seismic activity. It was therefore suggested that the magma filled pre-existing fractures passively. These results were modelled in terms of an intrusion with depth to the top of the intrusion at approximately 500 m with a height of 1 km and a width of about 1 – 5 m. Some 7 months later, in March 1981 there was a massive flank eruption fed by this intrusion. So how did this intrusion manage to drain after sitting for at least six months? Why did it not solidify?

More recent gravity surveys on Mount Etna showed a similar situation (Rymer et al., 1993). In 1989, activity led to several fissures developing to the north and the south-southeast of the South East crater. Various detection methods including seismic and gravity indicated that the SSE fracture did not fill with magma at that time. Further surveys carried out between June 1990 and June 1991 (Rymer et al., 1993) showed a gravity increase over the area of the fracture zone. This increase was modelled as a dyke (Rymer et al., 1993), which had passively filled the void left by these fractures. In December 1991 this modelled dyke intercepted the wall of the Valle Del Bove and there was a flank eruption that fed the most voluminous lava flow of the 20th century. The amount of degassed magma erupted during the 1991-1993 eruption was about 5km^3, which is an order of magnitude more than the earlier estimates of storage capacity. The volume was much greater than the volume of the proposed dyke that fed it. So how did the magma in this dyke stay hot enough to allow magma to pass through after sitting there for up to 18 months?

Geophysical techniques such as microgravity and ground deformation (Rymer et al., 1995), confirmed that there was no shallow intrusion of this volume of this material. This implies that there must be some kind of circulation, connecting to a deeper reservoir where degassed magma must sink to be emplaced at depth. Mount Etna is persistently degassing, therefore hot gassy magma must rise up to degass in the upper levels before sinking again.

The 1975 Tolbachik eruption lead to the intrusion of a shallow dyke; twenty years later this dyke was investigated by (Connor et al., 1997). The temperature of this dyke was measured and twenty years after the intrusion they found temperatures of up to 475°C, this was measured at a depth of 1.75-2.0 m. These temperatures were not expected so they constructed thermal models to examine several aspects of the cooling. Firstly they examined the thermal conductivities of the dyke and the scoria,

they suspected the porosity of the scoria to have an impact. They also examined the effect of a larger intrusion detected at a depth of around 80m. They found that the porosity of the scoria was indeed a key factor and significantly affected the bulk thermal conductivity. They showed the bulk thermal conductivity of the scoria at 0.1-0.5 $W/m^{o}C^{-1}$ was much lower than that of the pure basalt at around 2 $W/m^{o}C^{-1}$. This suggests that the scoria effectively acts as an insulator only transferring heat slowly. (Connor et al., 1997) proposes according to their models that this dyke will take over 100 years to cool to a temperature of below 100°C. They found that the magma body below had little thermal effect on the dyke.

They did not discount the possibility of some natural convection taking place within, but their models showed that with the right conditions and materials the dyke could have cooled to its current temperature by losing heat conductively over the 20 year period.

1.4.4 Dykes – Summary

From a review of the literature regarding cooling in dykes, it is clear there are several aspects that require investigation to enable a better understanding of the longevity of these magma bodies:

- **Dyke dimensions** – Dimensions have been argued by several workers to be a key factor. (Huppert and Bruce, 1990) showed that there is a critical initial width of dyke. This could indicate whether it rapidly cools and solidifies or whether the heat balance is such that the magma can actually begin to erode and meltback the walls of the country rock. Generally speaking the wider the dyke the greater its longevity, that is the length of time that it remains able to feed an eruption.
- **Material Properties** – Viscosity and other material properties such as thermal conductivity, density and thermal diffusivity of magmas have various effects on the longevity of dykes. (Wada, 1994) suggested that the more viscous a dyke magma, then the wider it will be. It was also shown that a steep temperature gradient between the walls of the country rock and the magma led to a more rapid increase in viscosity leading to blocking and eventually stopping the flow of magma. Viscosity along with the other material properties also intrinsically affect how the magma itself will cool.

- **Intrusion of Magma** – How the magma is intruded is also critical, whether the magma is simply intruded and left to stagnate or whether further intrusions or episodes occur (Maaloe, 1998; Parfitt et al., 2002; Wada, 1992).

1.5 Lava Lakes, Dykes and Convective Magma Recharge

As studied in section 1.3 at inactive lava lakes e.g. Kilauea Iki, (Oppenheimer and Francis, 1998; Harris et al., 1999; Swanson et al., 1972), where lava has ponded and there is no new influx, the lava rapidly (within a few years) solidifies losing heat to its surroundings. Active lava lakes such as that at Erta 'Ale can stay hot for around 90 years (Oppenheimer and Francis, 1998). This may be because the lava lake sits on top of a conduit filled with hot magma (Swanson et al., 1972) providing a continual influx of heat. One of the main explanation of how these active lakes manage to stay so hot for so long, where does the heat come from and where does it go?

Gas emission studies of volcanoes have lead to theories about how persistent degassing can be due to magma convection; gas-rich magma will depressurise as it rises allowing bubbles to exsolve. One such study is by (Kazahaya et al., 1994) and their investigations of Izu-Oshima volcano. It led to the idea of a convective recharge within the conduit. Whether this convection was driven by the degassing or whether the degassing was a result of the convection was not determined. Two models were proposed, one a Pouiseulle flow model where a column of gassed magma rose up the centre of a conduit and the degassed magma descended the walls of the conduit. The other model proposed consisted of discrete spheres of gassed magma ascending through degassed magma. Experiments carried out by (Stevenson and Blake, 1998) looked at the dynamics and thermodynamics of degassing. The experiments demonstrated a concentric double walled flow resulting from the over-turned magma.

Remote sensing observations show that active lava lakes generally have a fairly sustained heat flux (Oppenheimer and Francis, 1998; Harris et al 1999). The sustained heat flux that has been observed suggests a continual supply of hot magma or hot magma forming large subsurface bodies. Ground-based geophysical methods such as microgravity can detect shallow magma bodies and bodies such as these have not been detected. So is there another explanation? In a convective system, hot buoyant relatively gas-rich magma could rise up a conduit and as it gets closer to the top it would cool and degas becoming denser, it would then sink and either be emplaced

within or below the edifice, (LeGuern, 1987; LeGuern et al., 1979; Oppenheimer and Francis, 1998; Francis et al., 1993). Alternatively it may sink back into a hot reservoir to be recycled (Harris et al., 1999) and rise again, another possibility is that there may be new hot fresh magma ready to takes its place and rise up providing a fresh heat and mass flux.

If we take a schematic view of a lava lake system (figure 1.4) we can see heat and gas being lost to the atmosphere and the surrounding country rock. Heat will be transferred into the lava lake through any mass influx rising up the conduit into the lake or by conduction from hot magma below. Therefore, for the lava lake to stay active a density difference between the lava lake and the magma chamber must be maintained. If the lake and conduit magma had the same density, convection could not occur and therefore no fresh influx of heat and gas would prevent solidification. These ideas of convective recharge as a mechanism for sustaining lava lakes over periods in excess of several decades form the foundation for this investigation.

Studies on the dykes of Mount Etna have shown that dykes can remain viable for months after intrusion and feed eruptions. This again raises the question why some magma bodies can stay hotter for longer than others and the conditions that permit this. This has been summarised into the following points:

- Can magma stay hot without a mass heat/influx i.e. in a closed system? By conduction or convection?
- Does natural convection occur in a closed system and how does this affect cooling rates?
- Does a single episode intrusion explain the longevity of some dykes and other magmatic bodies, or is convective magma recharge essential to this longevity?

1.6 Aims

In this study, persistently active volcanoes will be considered using computer, mathematical and physical analogue methods. The following points will examined:

- Whether dykes can remain molten over long periods of time without a heat influx.
- Whether natural convection occurs in dykes when it is a closed system.
- How the dimensions of dyke can affect their convection and cooling rate.

- Which material properties are the most influential in enabling convection and the effect on the cooling rate.
- How the dimensions of a lava lake – conduit – magma chamber system affects the cooling rate of both lava lake and magma chambers.
- How the cooling rate is affected by convection within the system.
- The material properties of a magma and how this affects the cooling rate.

Chapter 2
Finite Element Modelling of Dykes

2.0 Introduction

In chapter 1 I discussed the longevity of dykes on Mount Etna and how they could potentially feed large eruptions. The aim of this chapter is to examine the key factors in the cooling of basaltic dykes as found on Mount Etna. The main areas to be examined are the height and width of the dykes and also the material properties of the magma.

Many studies have assumed that the material properties of a magma varying with temperature is not significant, but this may not be the case. The properties that I have examined are density (ρ), viscosity (μ), specific heat capacity (c) and thermal conductivity (k). To vary all these properties with temperature makes calculations very difficult without a specialist computer program. To help with these calculations researchers use finite element computer packages such as Ansys and NACHOS II (Carrigan et al., 1992; Emery and Lee, 1999). Carrigan specifically looked at thermal and dynamical regimes of single and two-phase magmatic flow in dykes, whereas others examined natural convection of fluids in rectangular boxes and cylinders. These packages are commonly used by engineers looking at thermodynamics.

In this chapter I have used the Ansys Finite Element Analysis package, which is essentially an engineering package that can be used to investigate natural convection in fluids (Emery and Lee, 1999). I used Ansys to first examine conductive heat transfer models and then examine convective models, finally comparing the two.

To just use FEA models in isolation would be unrealistic, so I have looked to compare these models with other methods. Jaeger and Carslaw did extensive work on conductive cooling in magma bodies (Carslaw and Jaeger, 1959; Jaeger, 1968). Extracts of this work will be used to compare to the Finite Element Models of conduction. The convective FEA model will be compared to the laboratory models of (Jaupart and Brandeis, 1986). Jaupart and Brandeis looked at natural convection within a plexiglas tank. These tanks represented magma chambers so that they could examine how convective plumes penetrated the bottom boundary layers and hence affect the crystallisation taking place there. Their tanks were filled with silicone oils

and the sides were insulated and the top and base held at a constant temperature. The initial temperature of the oil was hotter than the walls. The experiments showed evidence of natural convection and temperatures taken at points within the box were compared to equivalent Finite Element Models convective models.

2.1 Methods

2.1.1 Finite Element Analysis (F.E.A.)

In F.E.A. the object to be modelled is divided into a mesh of subdivisions called elements and the corners where these elements interconnect are called nodes (figure 2.2). Variables such as temperature and velocity are assumed to act over the element in a predefined way. After the object has been broken down into elements the governing equations for each element are calculated and combined to give the equations for the whole system (Fagan, 1992), The more elements and nodes the longer the processing time. Then it is simply a matter of applying initial and boundary conditions, material properties and other loading conditions. The F.E.A. package Ansys-flotran has been used here as it allows material property values to be entered as functions of temperature (Ansys.Inc, 1994). Using F.E.A we can model dykes and sills, which can be approximated in 2D by a rectangle (Figure 2.1).

2.1.2 Initial and boundary conditions

The initial conditions of a model are its most critical parameters. For the model dyke, a basaltic magma is assumed to be instantaneously emplaced within the void. The temperature of the magma was initially set at 1250K and the temperatures of the walls were fixed in each model. There were two main sets of thermal boundary conditions used as shown in figure 2.2. One set creates a thermal gradient between the inlet and outlet of the model. This gradient was varied to assess its importance. The other set of conditions keeps all the walls at the same temperature. At all the walls in all the models no-slip boundary conditions apply i.e. the magma at the boundary walls will have the same velocity as the boundary walls. As Ansys calculates iteratively it is necessary to set the number of global iterations in each load set, so that the solution converges quickly but not so that processing time is unnecessarily increased.

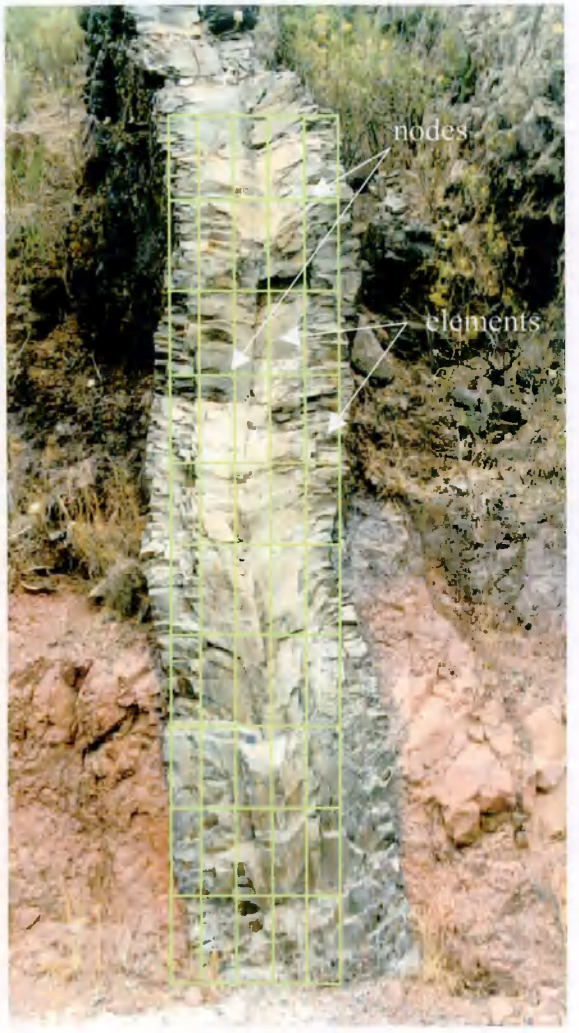

Figure 2.1 A dyke approximated as a rectangle and broken down into a mesh of elements

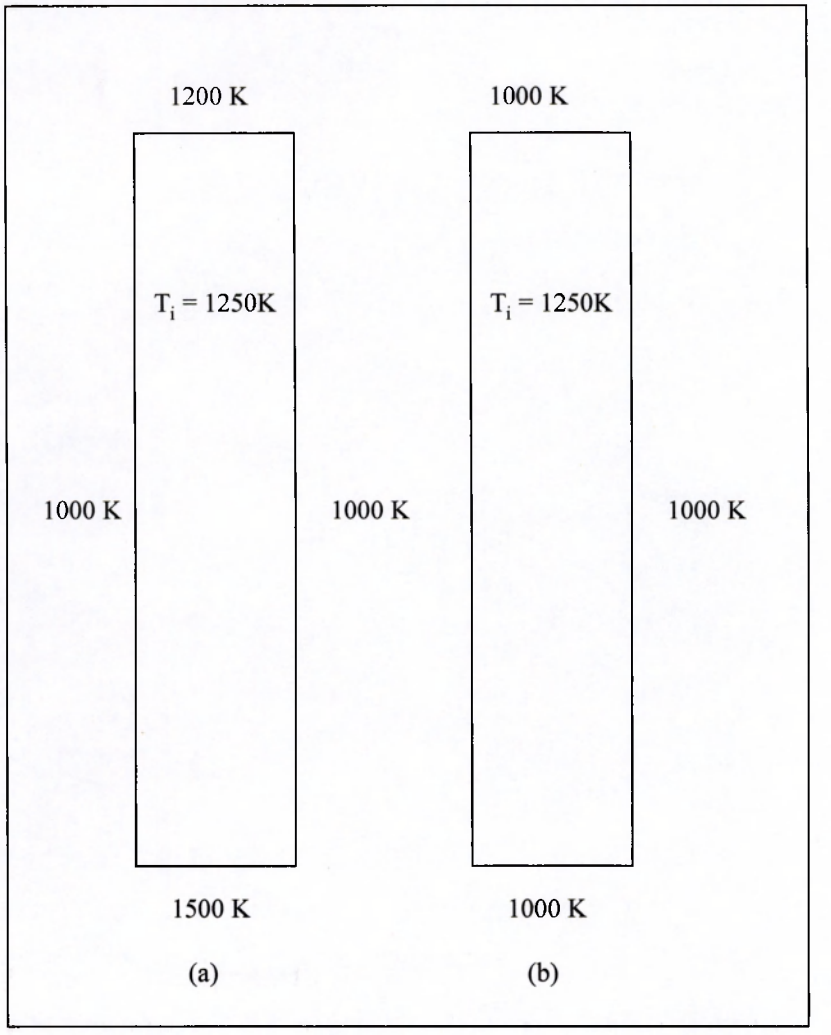

Figure 2.2 This figure shows the initial and boundary temperature conditions (a) lower wall at 1500K and upper one at 1000K, side walls at 1000K. (b) All walls at 1000K. Initial magma temperature 1250K. The top of the models are assumed to be near the crust surface.

2.1.3 Mesh

The resolution of the mesh is very important as the more nodes used the more accurate the solution will be. The disadvantage of having a great many nodes is that it takes longer to resolve the simulation, so a balance between the two needs to be found. To find the most efficient mesh several models were run gradually increasing the mesh density until the resolution showed no noticeable improvement. We want to use the least nodes that give the greatest accuracy (see figure 2.3). In this figure we have 1m x 10m models showing vertical velocities (V_y (m/s)), the reds are upward velocities and the blues and greens the downward velocities. From left to right the mesh density increases, the first 2 × 10 element mesh will have elements of 50cm × 100cm and the 100 × 10 mesh will have elements of 1cm × 100cm. It can be seen that the coarser meshes show very little detail and the distribution is very angular. As the meshes become finer they become much smoother and more detailed. This figure purely illustrates the effect mesh density can have on the resolution of these models, all the other parameters were held the same and only the number of elements within the mesh were varied. The figure does not relate to actual models used in this investigation. The boundary and initial conditions were as illustrated in figure 2.2(a).

The shape of the elements used in the models described below depended on what was being investigated, if width were being studied then the number of elements across the body was increased as the width increased. Ideally elements should be square, but on some of the larger models to do this would mean very long calculation times and for the required accuracy it was not necessary so in most models rectangular elements were used. For models that are symmetrical we need only model part of them. This saves computing time/allows more nodes to be used. For example a pipe may be modelled as an axi-symmetric rectangle. The models here have used 2-D meshes. For all the models here, tests were run to obtain the mesh density for the appropriate dimensions of the model and thereafter each model of that dimension had the same mesh for comparison.

2.1.4 Variations of material property values with T (K)

As can be seen from figures 2.4 – 2.7 the material properties of magmas such as viscosity and density do vary considerably with temperature. The values used in the F.E.A. models have been obtained from a variety of sources as follows. Specific heat

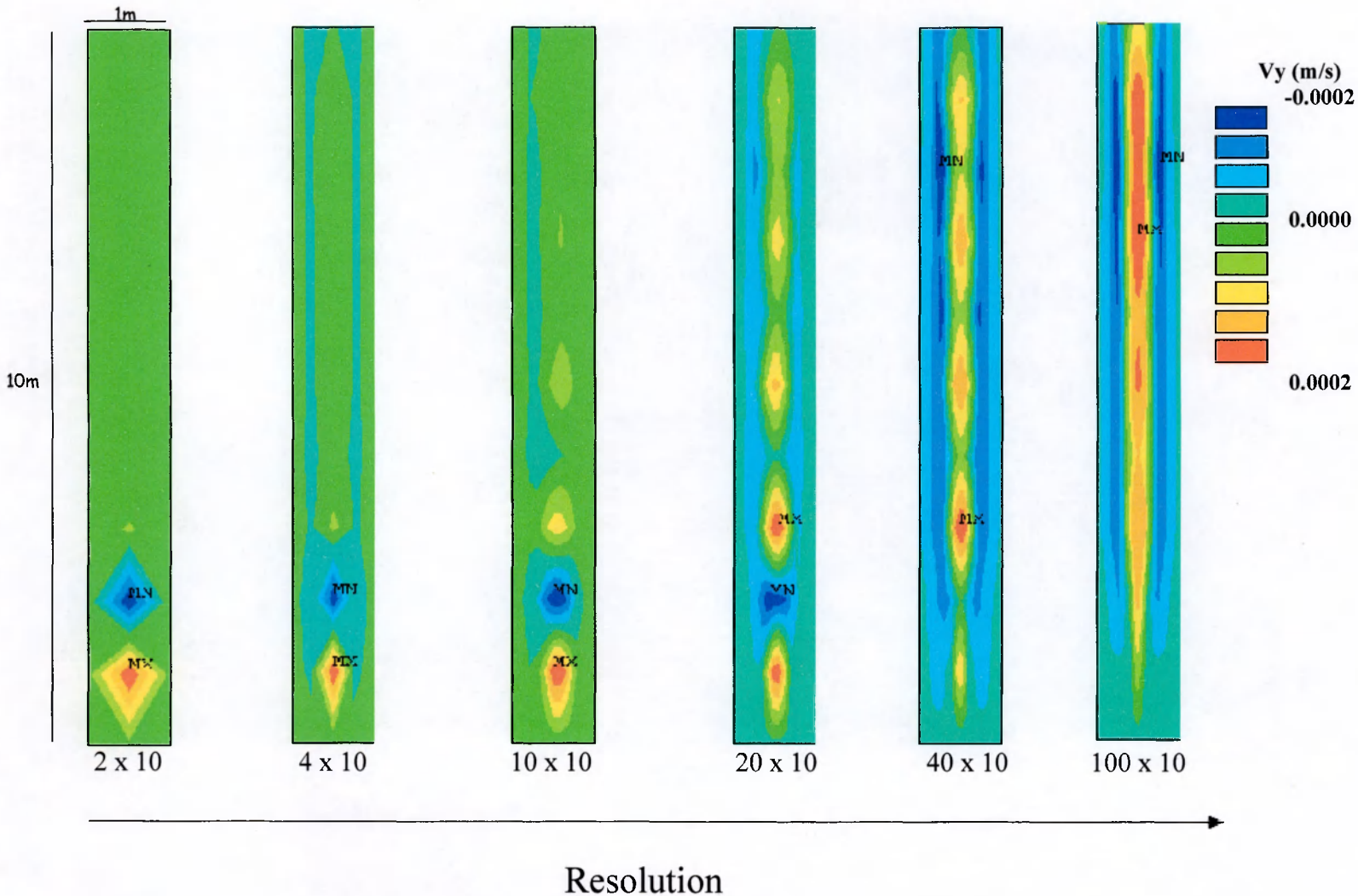

Figure 2.3 This figure shows how detail improves with increasing mesh density. A × B where A is the number of elements horizontally and B the number of elements vertically. The boundary conditions used were as figure 2.2 (a) . The next model in the sequence, 200 × 10 showed little difference in resolution to the 100 × 10.

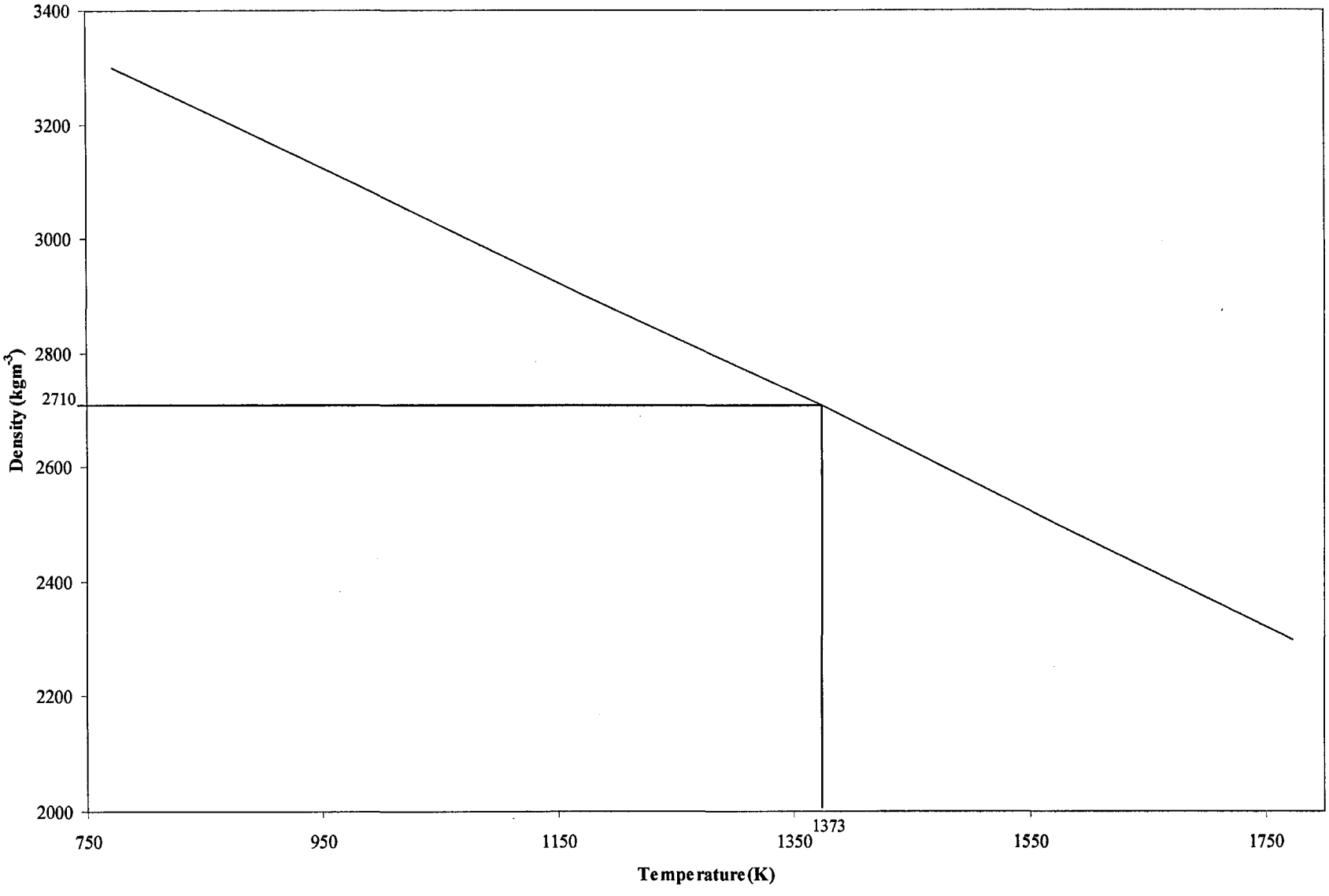

Figure 2.4 Variation of density with temperature

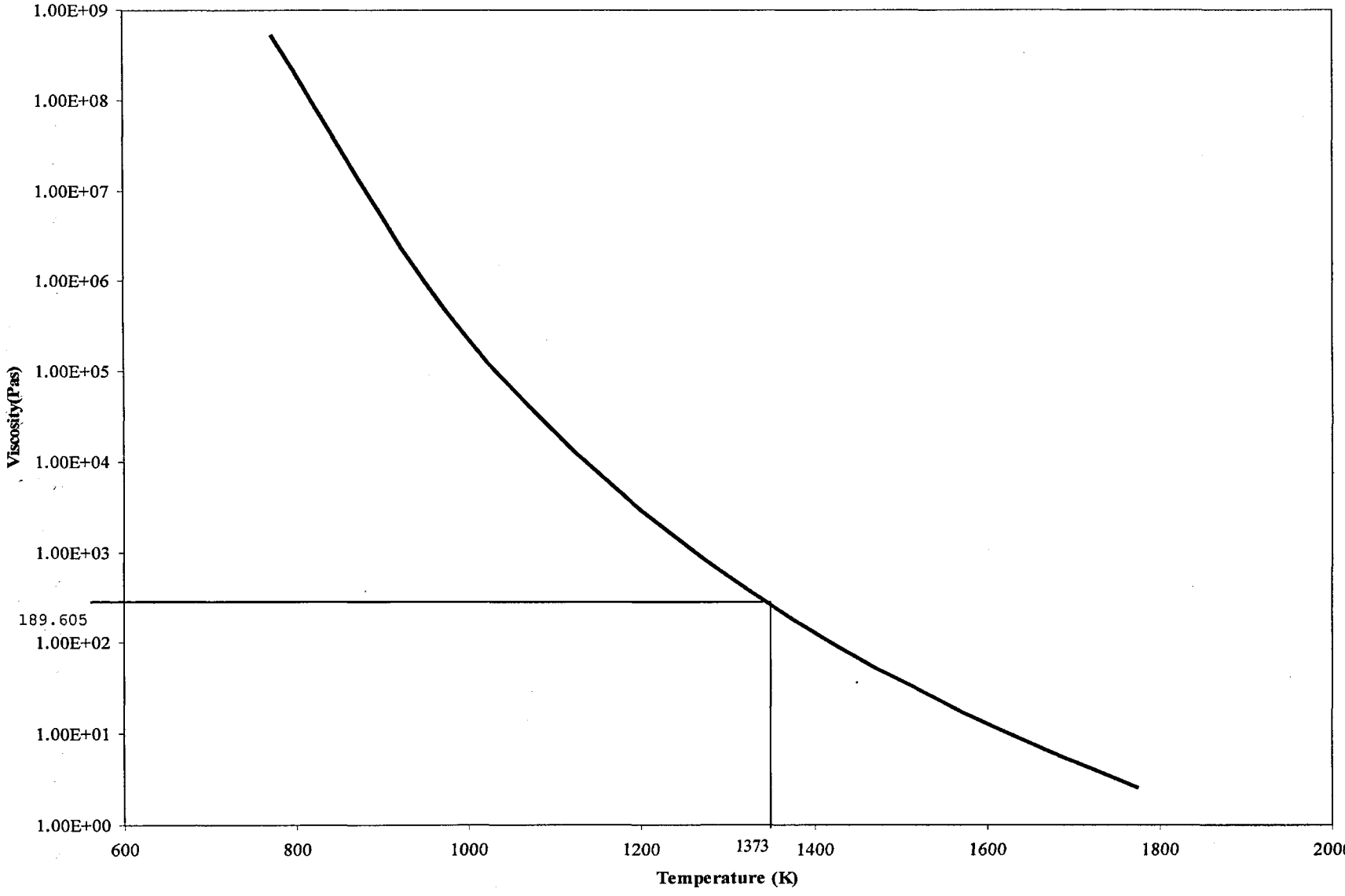

Figure 2.5 Variation of viscosity with temperature

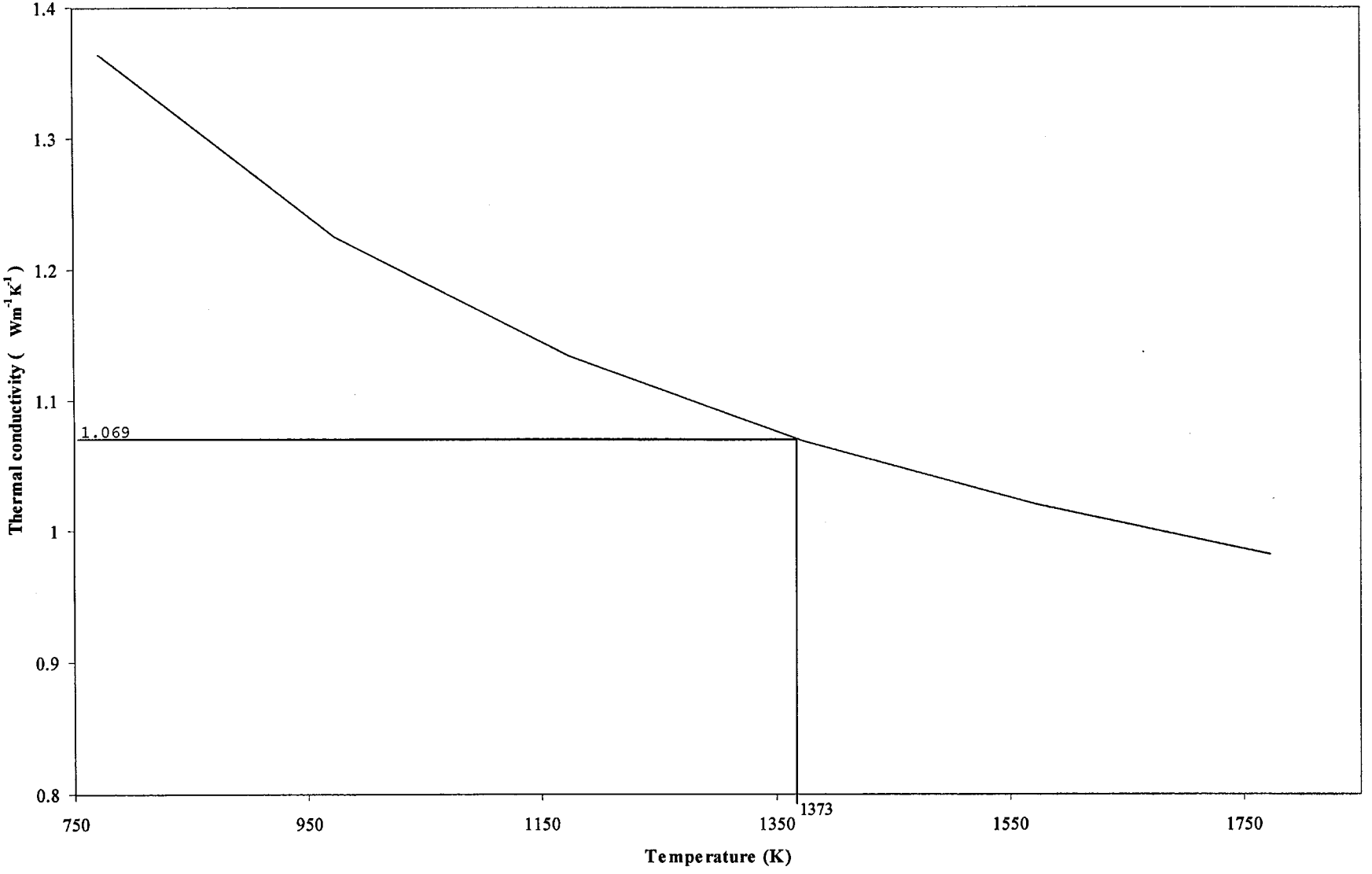

Figure 2.6 Variation of thermal conductivity with temperature

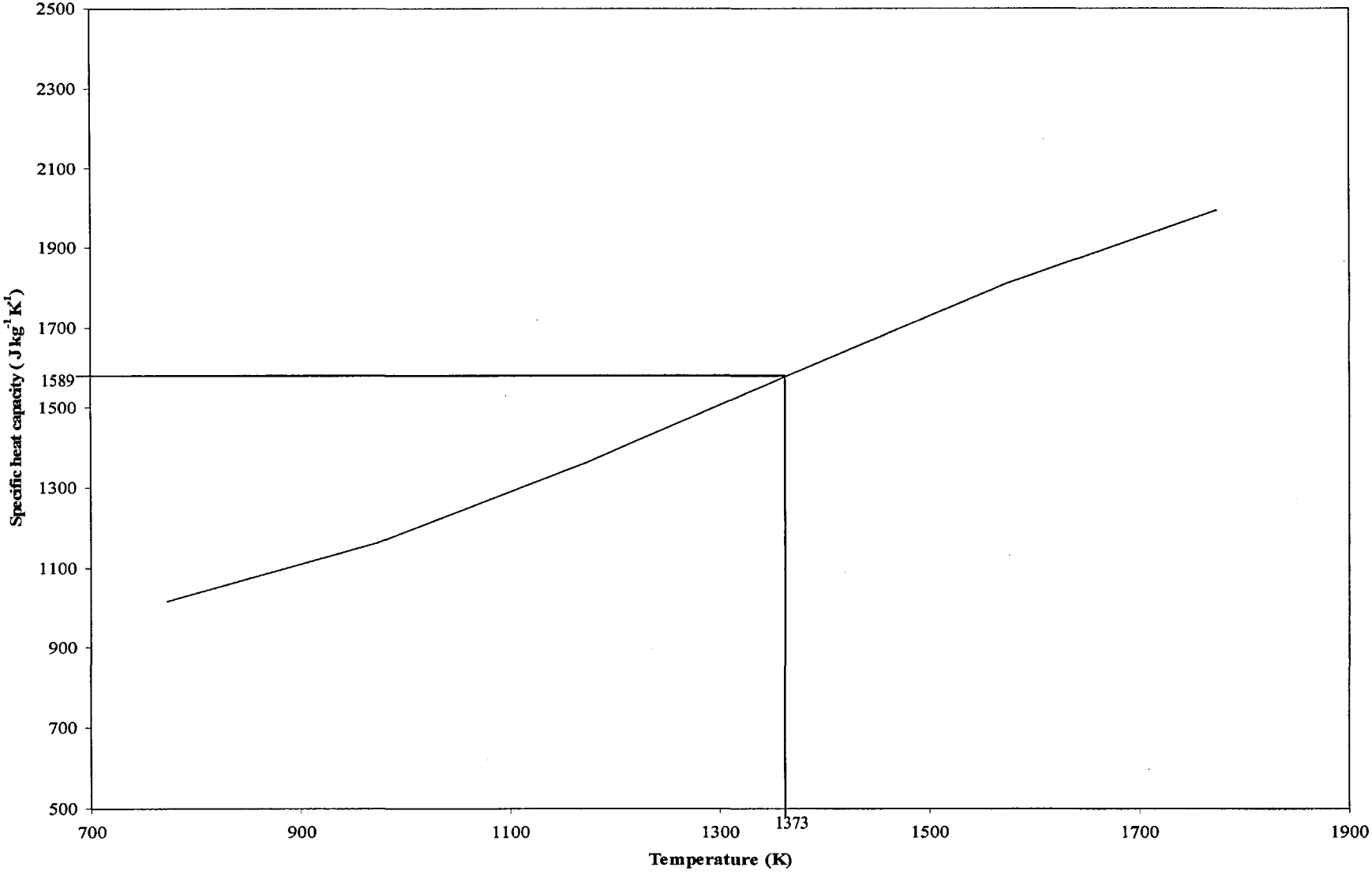

Figure 2.7 Variation of specific heat capacity with temperature.

capacity (cp) is obtained from (Buttner et al., 1998). Thermal conductivity (k) uses the relationship:

$$k(T) = 0.689 + \left(\frac{522}{T}\right) \text{ Wm}^{-1}\text{K}^{-1} \qquad \text{(Carrigan et al., 1992)}$$

Density (ρ) uses the relationship: $\rho = \rho_o (1+\alpha(T_o-T))$

ρ = density at specified temperature (kgm^{-3})

ρ_o = density at initial temperature (kgm^{-3})

T = specified temperature (^oK)

T_o = initial temperature (^oK)

α = coefficient thermal expansivity $=5 \times 10^{-5}\,^oC^{-1}$

k = thermal conductivity ($Wm^{-1o}K^{-1}$)

Viscosity for basalt uses the relationship: $\mu = 1.0 \times 10^{-6} \exp(26170/T)$ (Carrigan et al., 1992)

2.1.5 Models

The main aim in this investigation is whether magma can stay sufficiently hot within a dyke to feed eruptions several months after emplacement and whether convection makes a difference to the cooling period. To do this the following models were produced:

- Conductive models: comparing previously published analytical models with new F.E.A. models.
- Convective models: comparing Ansys F.E.A. models with the Jaupart/Brandeis laboratory experiments
- Convective models: comparing F.E.A. with the Jaupart/Brandeis theoretical models
- Convective models: looking at dykes; their material properties and dimensions

2.2 Conductive models: old and new

The first objective is to determine whether F.E.A. will produce the same results as those obtained by previous analytical solutions calculated by Carslaw and Jaeger. For the conductive models all the material property values are constant. The values used

were the ones for 1373K as shown on figures 2.4 – 2.7. Models were run for up to the equivalent of 90 days. The initial and boundary conditions shown in figure 2.2 were both used. The assumption is that if we can reproduce Carslaw and Jaeger's results, then we can have confidence to construct complex models.

To compare the two models the following method was employed:
First a temperature profile was taken from Ansys. This was done by selecting nodes from the centre of a dyke model out to the walls. The temperatures at these nodes were converted to dimensionless temperatures using the following relationship:

$$\theta = \frac{T - T_w}{T_i - T_w}$$

Where T = temperature at a particular node (K)
T_i = initial magma temperature (K) = 1250K
T_w = temperature at wall (K) = 1000K

The position x across the profile was converted into dimensionless distance using the relationship $\frac{x}{l}$ where x = distance from dyke centre and l = half width of the model dyke. For this comparison the measurements were taken after the equivalent of 20 and 50 days. The data from these measurements were plotted as θ v $\frac{x}{l}$. The data from the Carslaw models were taken from figure 10, page 98 (Carslaw and Jaeger, 1959). To find the data curve for the same cooling times the following relationship was used:

$$\tau = \frac{\kappa t}{l^2} \qquad \text{Where} \quad \kappa = \frac{k}{\rho c}$$

k = thermal conductivity = 1.069$Wm^{-1}K^{-1}$
ρ = density =2710 kgm^{-3}
c_p = specific heat capacity = 1589 $Jkg^{-1}K^{-1}$
l = 2m
t= 1728000s (= 20 days) or t = 4320000s (= 50 days)
Data taken from an Ansys 4m x 1km conductive model.
Therefore $\tau_{20} = 0.11$ $\tau_{50} = 0.27$ Where τ_x = dimensionless time
x = days

A comparison was also made using the temperature of the central node from the Ansys model and centre of the Carslaw solution cooling over a period of 75 days.

2.2.1 Results

The conductive models cool from the outside, as can be seen in figure 2.8 which shows the temperature field of a 4m x 1km model, where the reds are the hotter areas and the blues the cooler areas. Where the walls all have the same temperature the cooling is completely symmetrical as would be expected. The data from this temperature field were taken as a profile across the centre of the dyke (figure 2.9). This naturally shows a symmetrical distribution where the hottest part is in the centre and the temperature drops off to its lowest points at the walls. In the model where the inlet is set at 1500K and outlet at 1200K the temperature distribution is symmetrical only about the vertical axis. This is to be expected as heat will come in from the inlet and be lost at the outlet.

The dimensionless distance (x/l) from the centre of the model was plotted against dimensionless temperature (θ) for both the Ansys and the Carslaw models. The data were extracted for temperatures after 20 and 50 days.

The upper two curves on figure 2.10 show the results for 20 days of cooling and it can be seen that the two curves are virtually coincident. The lower two curves are those for 50 days of cooling and again they are almost coincident. This is the result that had been predicted. As a further check, cooling over time of the central part of the two models were compared (figure 2.11), this too showed that they were essentially coincident.

2.2 Summary

- The Ansys F.E.A. conductive model accurately reproduces the results as given by the Carslaw and Jaeger analytical solution.
- These results give us confidence that Ansys F.E.A. can be used to model more complex magma body cooling.

2.3 Convective models: comparing F.E.A. and laboratory models

It is important to find a way to check if F.E.A. convective models are reasonable and can be used to address the questions posed in section 1.6. To do this, the Ansys

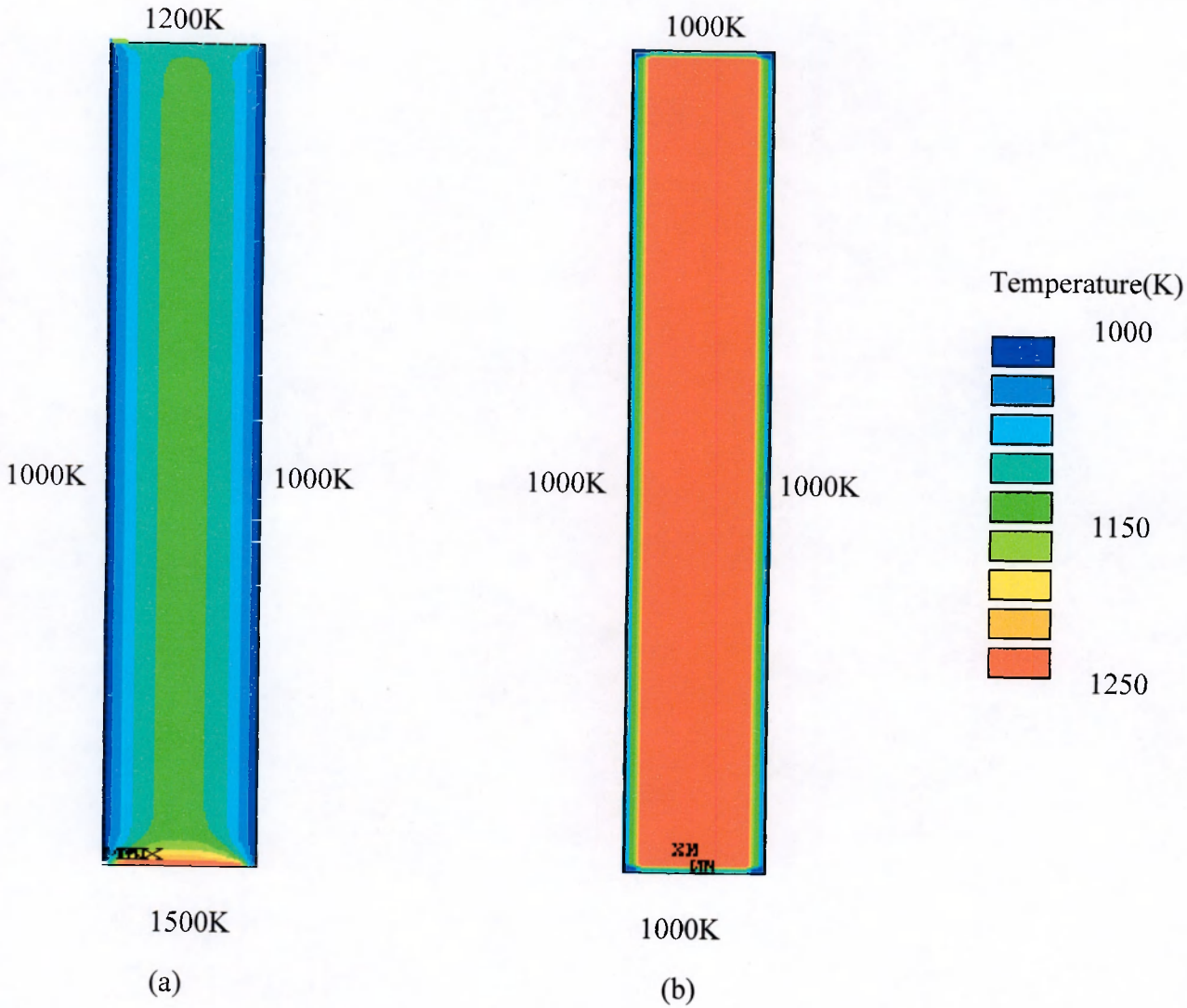

Figure 2.8 This shows the temperature distribution of 4m x 1km conductive models with differing boundary conditions. (a) lower wall temperature at 1500K, upper wall at 1200K and side walls 1000K. (b) All wall temperatures set at 1000K. In the corners of the models there is a difference in thickness, this is probably due to numerical instability at the the corners of the mesh.

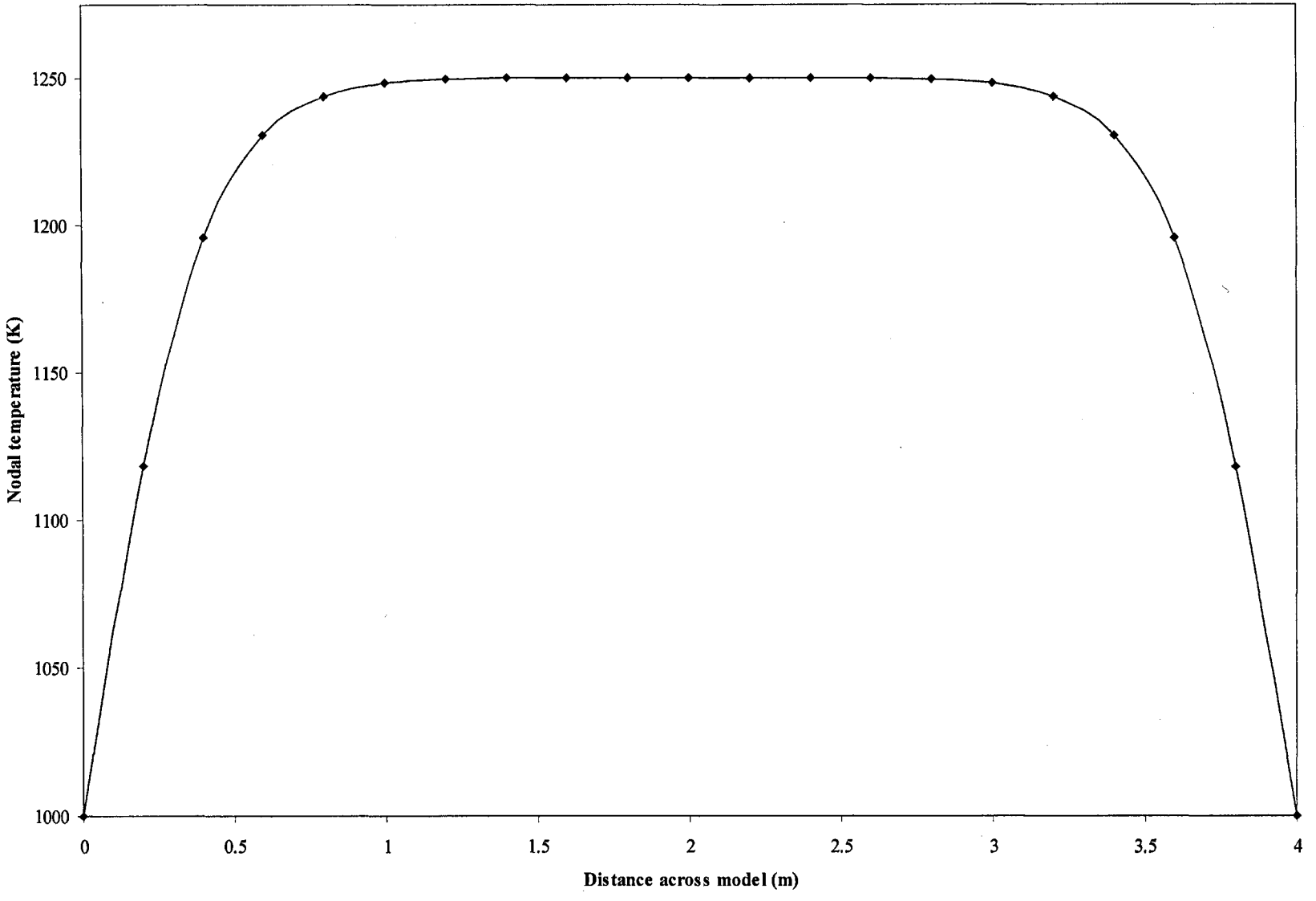

Figure 2.9 This shows the temperature profile across the centre of a 4m wide conductive model figure 3.1a,(b).

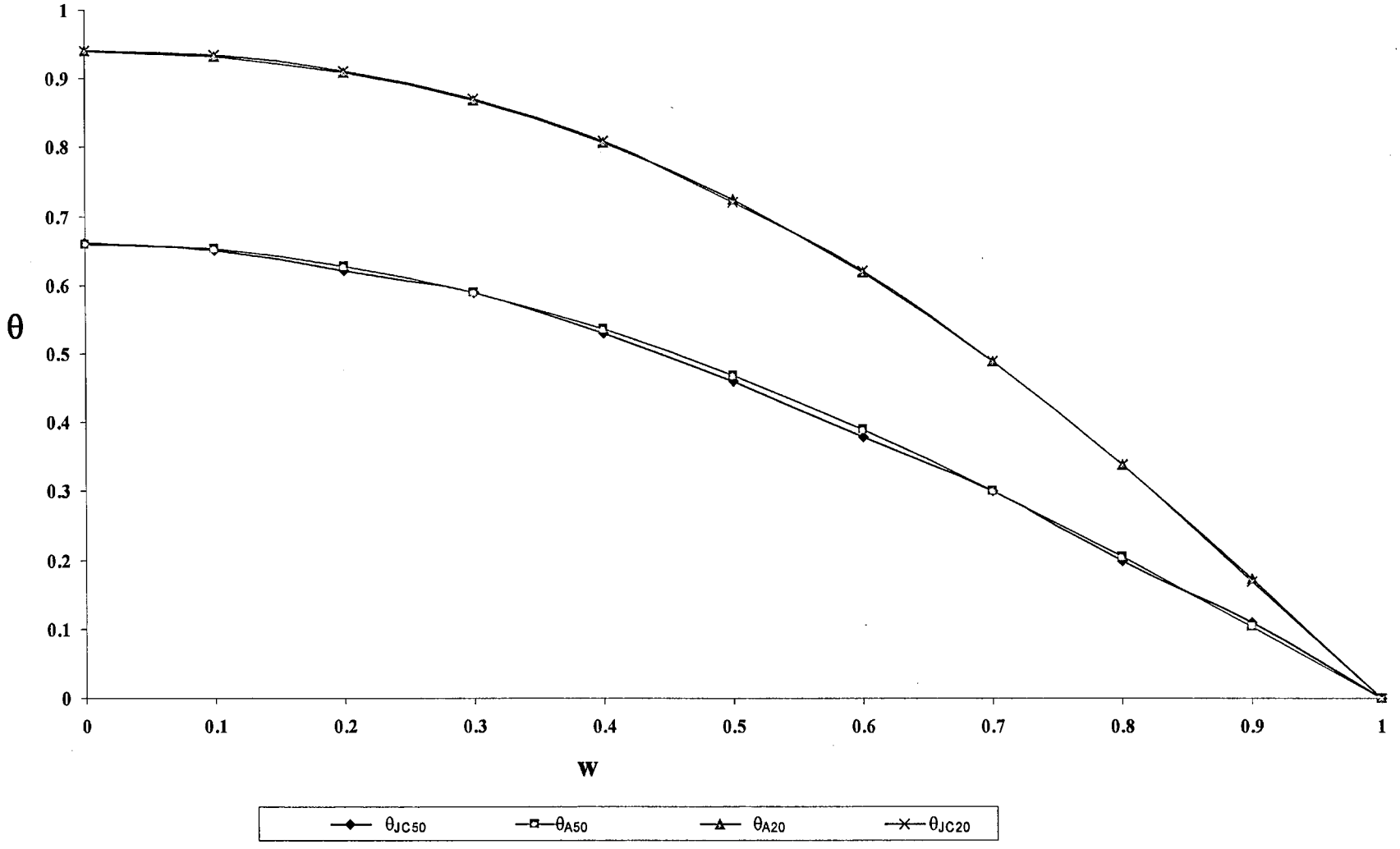

Figure 2.10 Comparing Carslaw analytical conductive model with Ansys F.E.A. conductive model. The vertical axis shows dimensionless temperature (θ) and the horizontal axis shows dimensionless distance (w) from the centre of the dyke. θ_{JC50} - Jaeger/Carslaw model after 50days. θ_{JC50} - Jaeger/Carslaw model after 20 days. θ_{A50} -Ansys model after 50 days. θ_{A20}-Ansys model after 20 days.

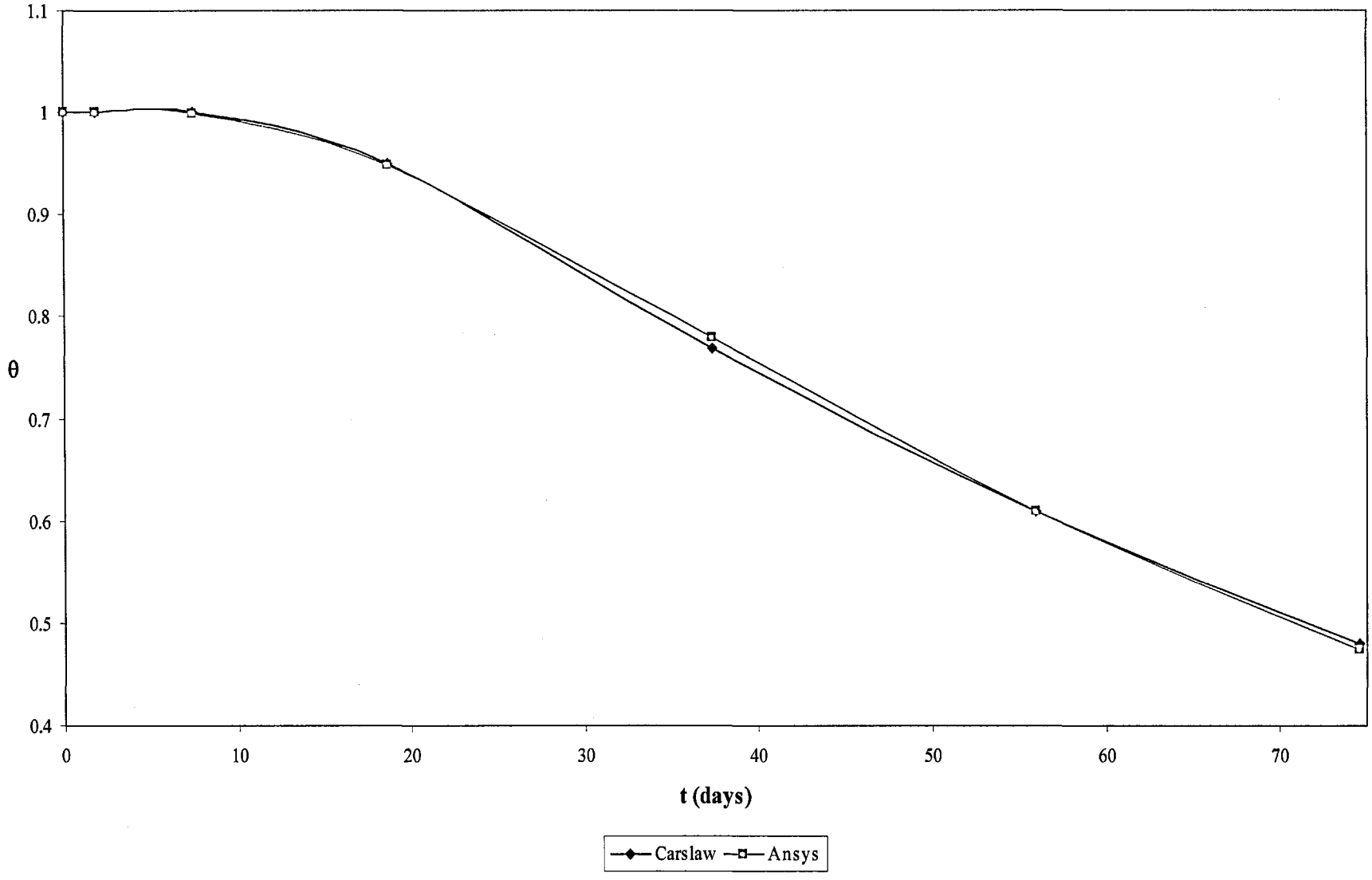

Figure 2.11 This compares the temperature of the central node over time for both Carslaw and Ansys conductive models. The vertical axis showing dimensionless temperature (θ) and the horizontal axis showing time (t) in days.

F.E.A. program was used to model a laboratory experiment performed by (Jaupart and Brandeis, 1986). I recreated their experiment number 8 using Ansys. In their experiment a rectangular 2D box with dimensions of 25cm long by 10cm high was used, it was filled with silicone oil with properties as below:

$\mu = 1.35 \times 10^{-2}$ Pas

$\rho = 965\ (1\text{-}9.45 \times 10^{-4}(T\text{-}20^{\circ}C))\ kgm^{-3}$

$c_p = 913.19\ Jkg^{-1}K^{-1}$

$k = 0.16\ Wm^{-1}K^{-1}$

$\alpha = 9.45 \times 10^{-4}\ ^{\circ}C^{-1}$

The top and bottom of the box were held at a temperature of 27.6 °C and the initial temperature of the silicone oil was 49.4 °C. The side walls were insulated. Both the Ansys and the Jaupart/Brandeis (J/B) experiment were run for the equivalent of 33 minutes. When this time period had elapsed, the temperatures from both were horizontally averaged and plotted as dimensionless temperatures against dimensionless vertical position. The data from the J/B experiment was taken from the graph figure 5(a) from (Jaupart and Brandeis, 1986). Results were compared for times of 12 and 21 minutes.

2.3.1 Results

Figures 2.12, 2.13 and 2.14 show the results obtained from running the J/B simulation. The horizontal axes show θ dimensionless temperature and the vertical axes show the vertical position within the model. The temperatures of nodes in the Ansys model were taken from across a horizontal section, the same as in the J/B experiment. These were then averaged before being made dimensionless as done in the laboratory experiment. The two curves shown in figure 2.12 are for the laboratory experiment and F.E.A. simulation after a time of 12 minutes. These show that the experimental curve is symmetric about the centre of the model whereas the F.E.A. simulation shows that the curve reaches a temperature peak in the upper half of the model. After a time of 21 minutes in figure 2.13 the experimental curve is again symmetric and the simulation peaks in the upper half of the model. The curves are a similar shape above the dimensionless vertical distance z =0.95 and below z =0.15. It is noticeable from these results that the F.E.A simulation is on average hotter in the central area of the model. Figure 2.14 shows the average of the temperatures plotted against time. This shows that both the F.E.A. and J/B models show very similar rates

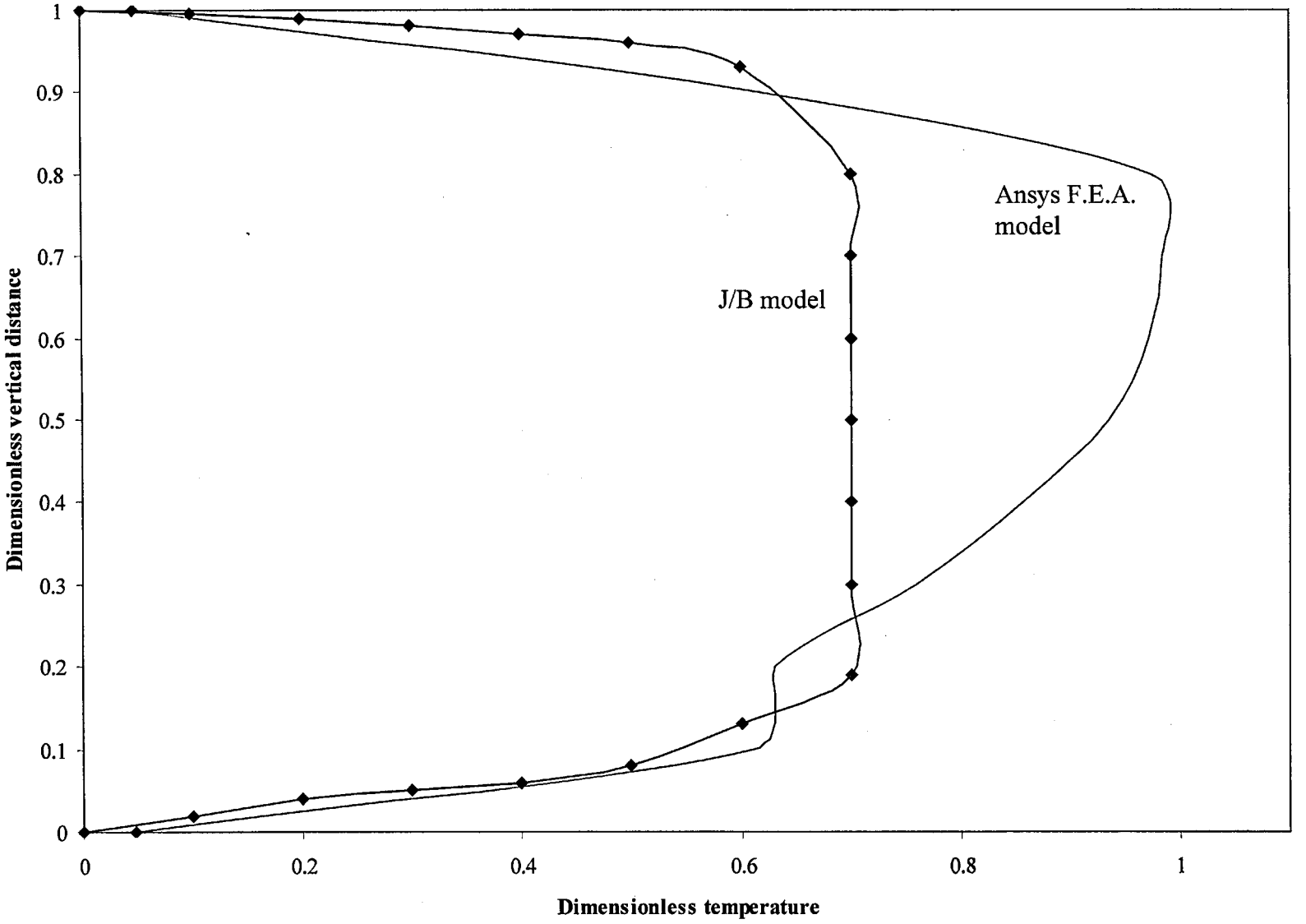

Figure 2.12 J/B model compared with the Ansys F.E.A. model after 12 minutes

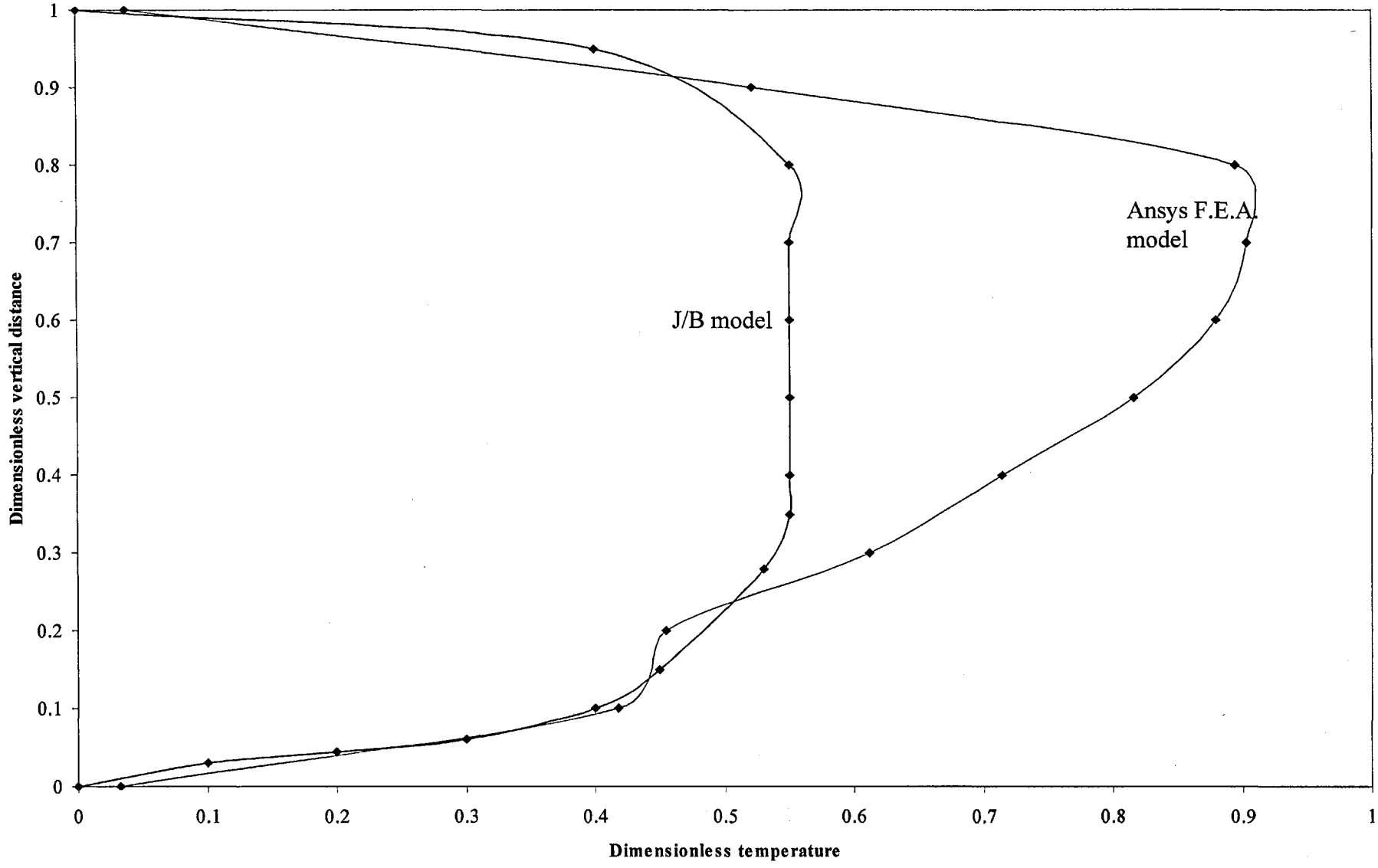

Figure 2.13 J/B models compared with Ansys F.E.A. model after 21 minutes

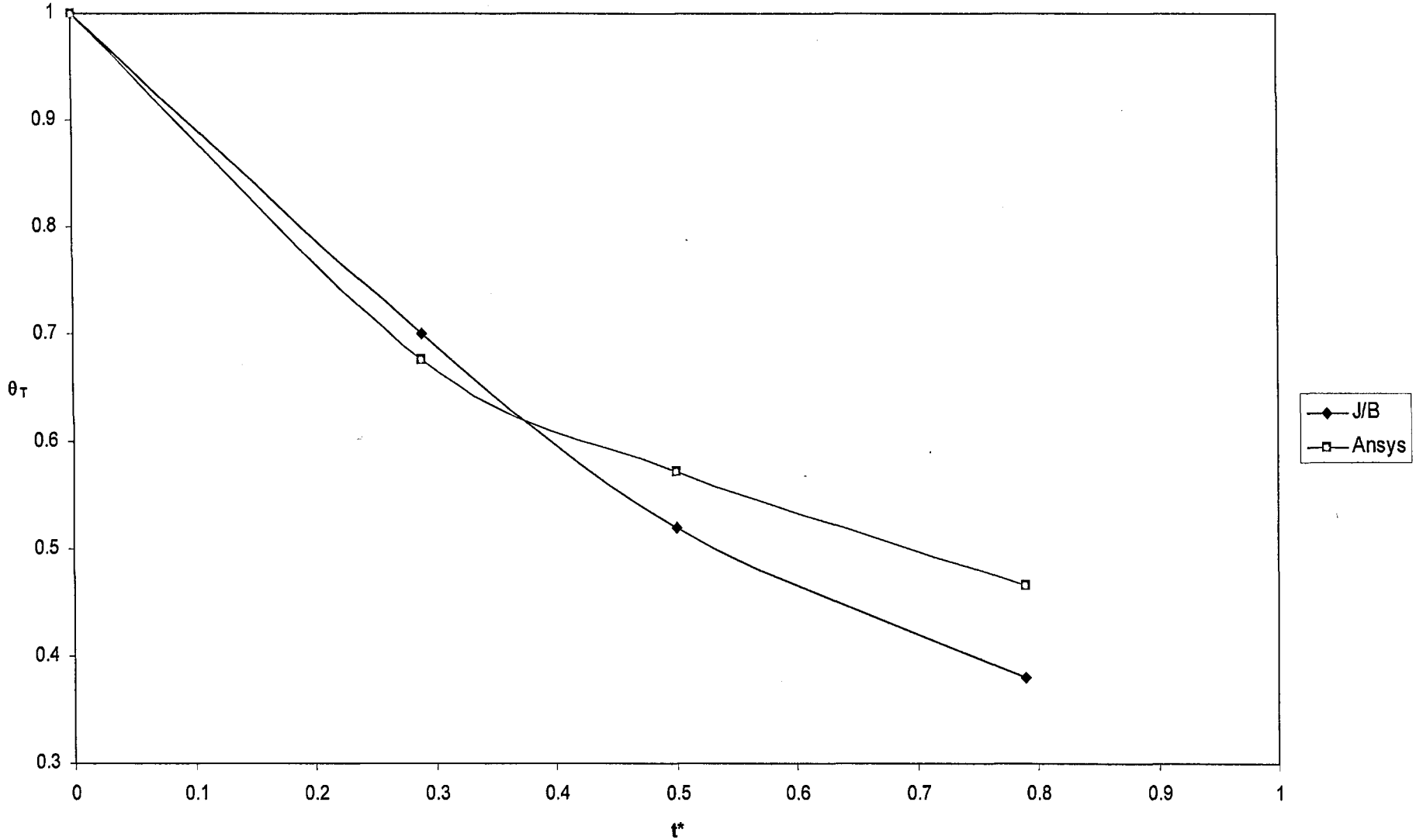

Figure 2.14 Cooling of laboratory model compared with Ansys F.E.A. model. θ is the average dimensionless temperature. t* is dimensionless time.

of cooling. Initially they both cool at around 0.6 $^{0}Cmin^{-1}$ and after about 15 minutes they slow to around $0.2^{0}Cmin^{-1}$. To try to explain the asymmetry of the Ansys model a series of snapshots, taken at 60-second intervals, were taken as the model ran. Figure 2.15 shows the 25cm wide by 10cm high Ansys model. The colours represent the temperature distribution with the blues being the coolest going up to the reds as the hottest material. The walls were insulated so there is no loss or gain there. From this figure it can be seen that the roof layer changes little in thickness and if fairly flat. The base layer is more variable, the layer is generally thicker and as time progresses central plumes form and off centre the base layer appears to show variable thickness.

2.3.2 Summary

- Both the Ansys model and the J/B model show similar temperature distributions.
- J/B model has a very similar cooling rate to that of the Ansys model, Ansys cooling very slightly slower after 15 minutes.

Increasing the mesh density and the number of global iterations used may smooth the curves but would be unlikely to remove the asymmetric nature of the Ansys model.

The difference in temperature between the two may be due to several factors. The insulation of the sidewalls in the F.E.A. model is such that no heat will be lost to the sidewalls unlike in the J/B model though Jaupart/Brandeis believes these losses to be small (Jaupart and Brandeis, 1986). There are also some errors within the experimental reading process itself, again though Jaupart/Brandeis believe them to be small.

The snapshots may explain some of the asymmetry of the Ansys model. As the model progressed the base layer became thicker at the base than at the roof. These layers contain cooler material and this would naturally reduce the average temperatures in the lower half of the model and may contribute to the asymmetry of the model.

2.4 Convective models: Comparing F.E.A. with theoretical models

(Jaupart and Brandeis, 1986) compared their experimental laboratory models with the theoretical models of people such as (Deardorff et al, 1969). In this section data from the F.E.A. simulation section are also compared with the theoretical models. This comparison is for high Rayleigh numbers ($>10^{9}$) where convection can easily occur. From (Jaupart and Brandeis, 1986) and using equations 16a-c and 17;

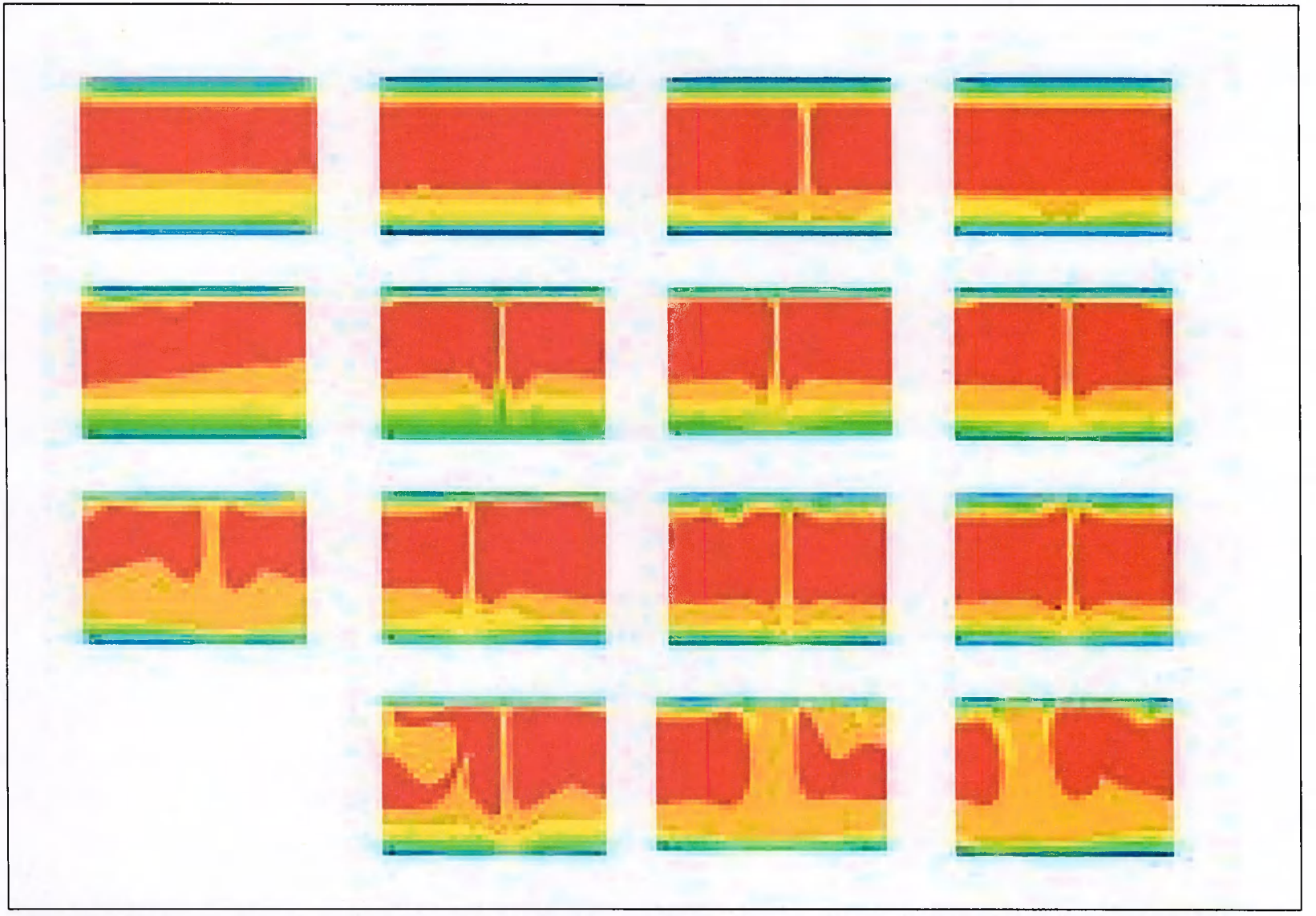

Figure 2.15 This figure shows snapshots at 60s intervals taken from an Ansys model of a J/B experiment Jaupart(1986) The roof and base are held at a temperature of 27.6 °C. The initial temperature of the oil is held at 49.4°C and the walls are insulated.

$$\tau = \frac{3d^2}{m\kappa} Ra_0^{-1/3} \qquad (16a)$$

$$\theta = \left(\frac{T_0 - T_{wall}}{T - T_{wall}} \right) \qquad (16b)$$

$$t^* = \frac{t}{\tau} \qquad (16c)$$

and $$\theta = (1 + t^*)^{-3} \qquad (17)$$

where τ = timescale d = width of model m = constant

κ = thermal diffusivity θ = dimensionless temperature t^* = dimensionless time

Ra_0 =Rayleigh number at t = 0

Take 16a and 16c and equate

$$\frac{t}{t^*} = \frac{3d^2}{m\kappa} Ra_0^{-1/3} \quad \Rightarrow \quad t^* = \frac{m\kappa t}{3d^2 Ra_0^{-1/3}} \qquad (A)$$

Then take 16b and 17 and equate

$$\left(\frac{T_0 - T_{wall}}{T - T_{wall}} \right) = (1 + t^*)^{-3} \quad \Rightarrow \quad t^* = \left(\frac{T_0 - T_{wall}}{T - T_{wall}} \right)^{\frac{1}{3}} - 1 \qquad (B)$$

Now equate (A) and (B)

$$\Rightarrow \quad \left(\frac{T_0 - T_{wall}}{T - T_{wall}} \right)^{1/3} - 1 = m \frac{\kappa t}{3d^2} Ra_0^{1/3}$$

This gives the equation of a straight line of the form y = mx going through the origin

Where $$\left(\frac{T_0 - T_{wall}}{T - T_{wall}} \right)^{1/3} - 1 = y$$

And $$x = \frac{\kappa t}{3d^2} Ra_0^{1/3}$$ where m is the gradient of the line

Using data from the F.E.A. model plotting x against y will enable m to be compared between methods. m has been empirically found (Deardorff et al, 1969) to range from 0.1 to 0.2. Though some, (Ho-Liu et al, 1985), have found values of up to m= 0.327.

T_0 = average temperature T at t = 0

T_{wall} = temperature at the wall = 27.6 °C

d = 0.1m

$\kappa = 1.14 \times 10^{-7}\ m^2s^{-1}$

$$Ra_0 = \frac{g\alpha\Delta T\rho d^3}{\mu_0\kappa} \qquad \text{where } g = 9.81 ms^{-2}$$

Other values as in section 2.2.

2.4.1 Results

The data from the F.E.A model was taken and put in to the above equations to obtain figure 2.16. Data from the J/B model was also plotted on this graph. The horizontal and vertical axes are x and y as above. The graph shows reasonably straight lines, when extrapolated the J/B model goes virtually through the origin and the F.E.A. model cuts the y-axis at around 0.05. The gradient of the F.E.A. model is approximately m = 0.3 which is a little over the predicted value. The J/B model however gives m as approximately m= 0.5.

2.4.2 Summary

- The Ansys F.E.A. and the J/B models compare reasonably well with the J/B theoretical model.

2.5 Convection in dykes

In section 1.4 it was shown that there have been occurrences of dykes remaining hot for longer than expected and that perhaps it was convective recharge that was the process responsible for this behaviour. A closed system, whereby we assume that there is no mass flux into or out of the body, will be considered first before moving on to an open system.

2.5.1 Varying material properties with temperature

In order for convection to occur, density at least must vary with temperature. Four models were run where the material properties; viscosity, thermal conductivity and specific heat capacity were systematically varied with temperature whilst holding the others (except density) constant. The purpose was to see how each property individually affected the thermal behaviour of the magma. A model where density only varied was created so that comparisons could be made.

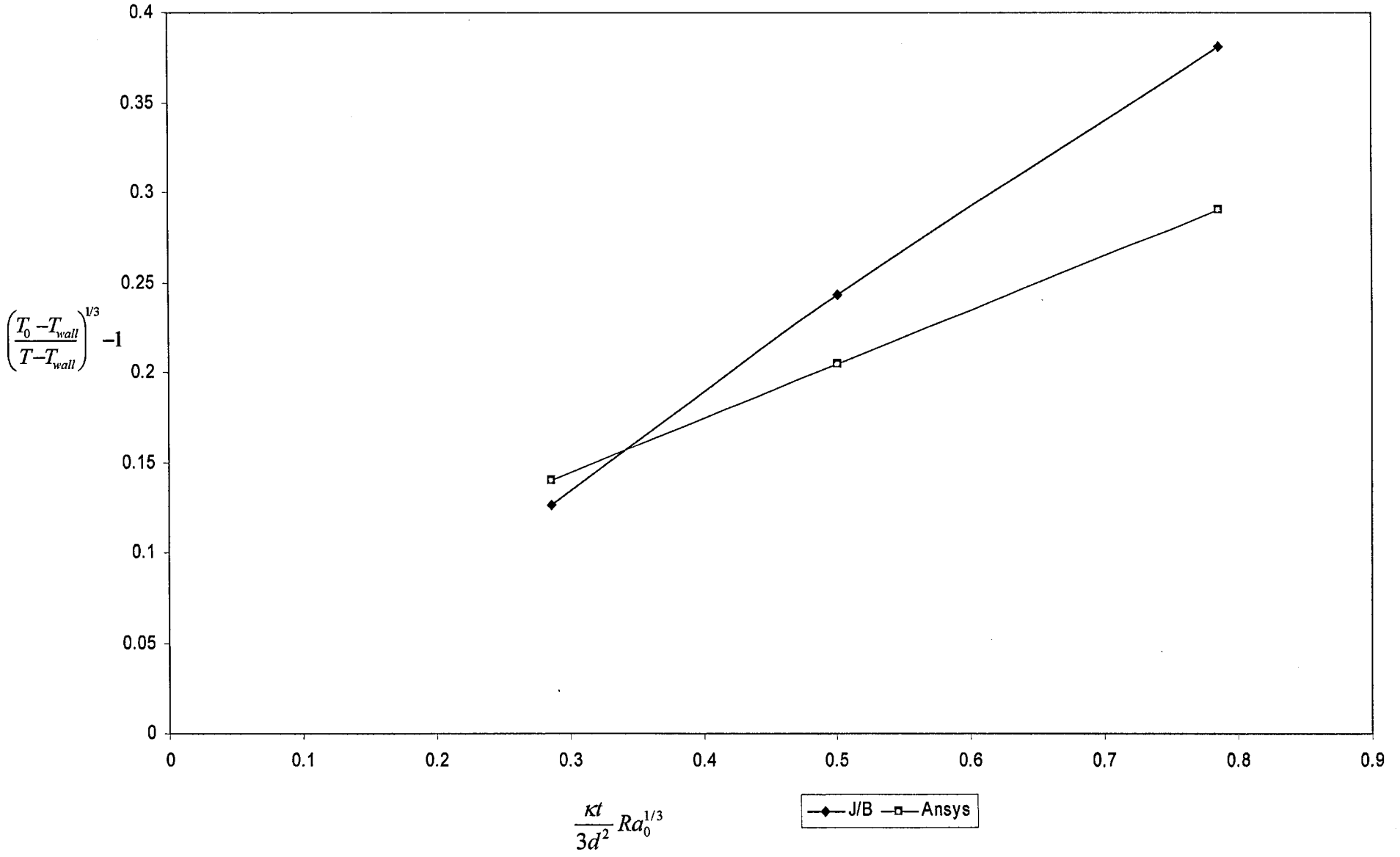

Figure 2.16 Comparing the Ansys F.E.A. model with J/B laboratory and theoretical models.

For these runs, a 4m × 1km model was used and the same mesh and initial and boundary conditions as in figure 2.2(a).

2.5.1.1 Results

Figure 2.17 shows the four 4 m × 500 m models illustrating vertical velocities, with the reds being positive (upward) velocities and the greens and blues showing the negative (downward) velocities. The following properties are varying with temperature:

a) density and specific heat capacity only

b) density and thermal conductivity only

c) density and viscosity only

d) density only

Where density only varies ,d), this can be taken as our control model with which to compare the others. Just observing the velocity distribution colours it can be seen that both a) and b) show a similar distribution to that of d). Also the magnitude of all these three are very similar. Now when c) is examined it is immediately clear that the velocity distribution is different and that the maximum positive velocity is much lower than that of the other models.

2.5.1.2 Summary

- Thermal conductivity and specific heat capacity have little effect on the thermal behaviour of the cooling dyke model
- Viscosity significantly affects the thermal behaviour of the cooling dyke model

2.5.2 Dimensions

As with conductive models, a systematic range of heights and widths were incorporated into the model. Dyke widths of 1 m to 20 m and heights of 10 m to 2 km were modelled. This was done in order to examine the effect of these parameters on the average temperature of the magma within the model. The temperature is averaged to minimize the effects of resolution.

2.5.2.1 Results

The first series of models involved running models of different widths and heights ranging from 1 m × 10 m to 20 m × 2 km and the boundary conditions were also

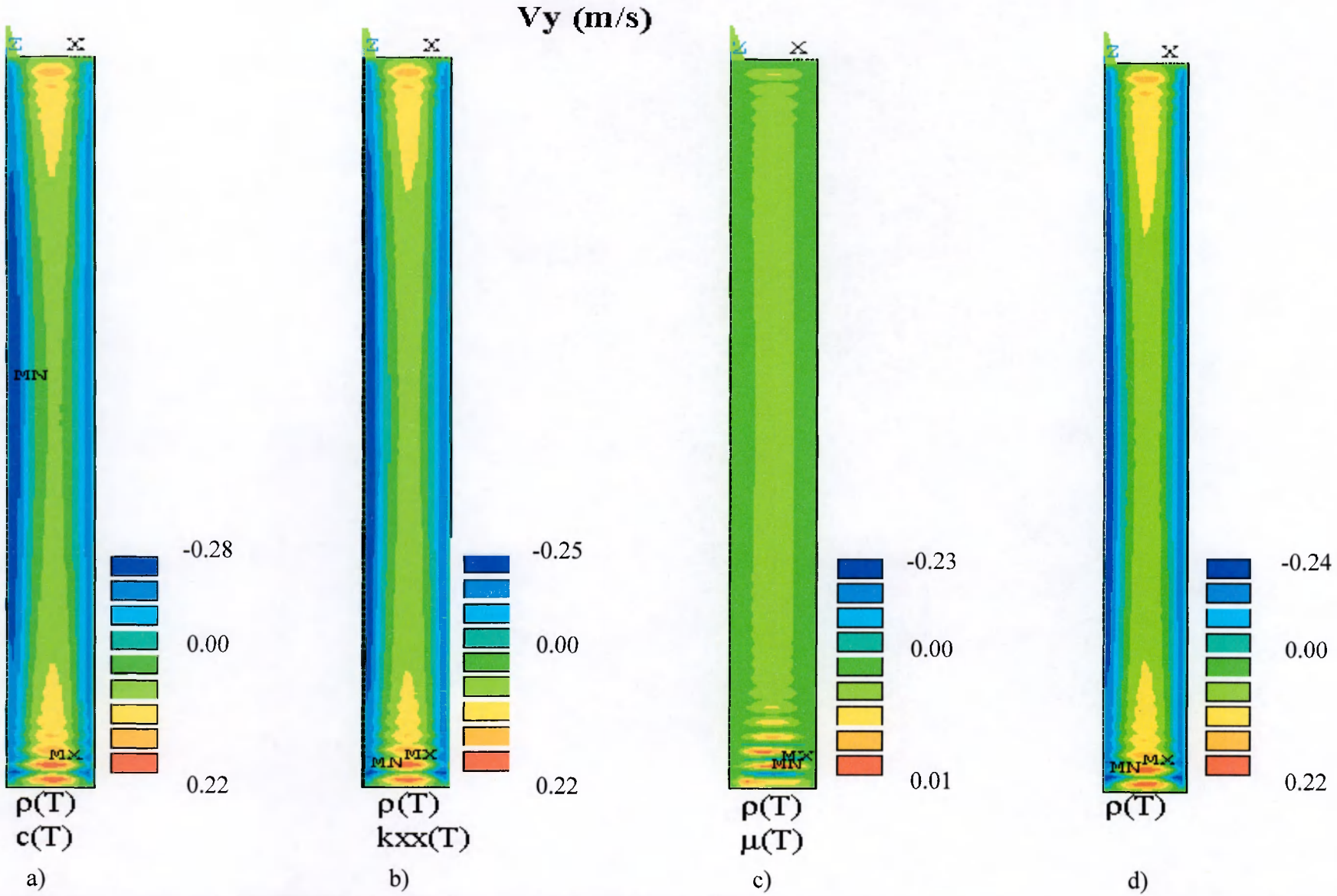

Figure 2.17 The effect of individual material properties varying with temperature (T). They are 4 x 500m models with boundary conditions as figure 2.2(a). Vertical velocity(m/s) is shown with greens, yellows and reds showing upward motion and blues as downward motion. a) density and specific heat capacity varying with T. b)density and thermal conductivity varying with T. c) density and viscosity varying with T and d) only density varying with T. this figure shows only vertical motion the oscillatory like appearance is dues to using a low resolution.

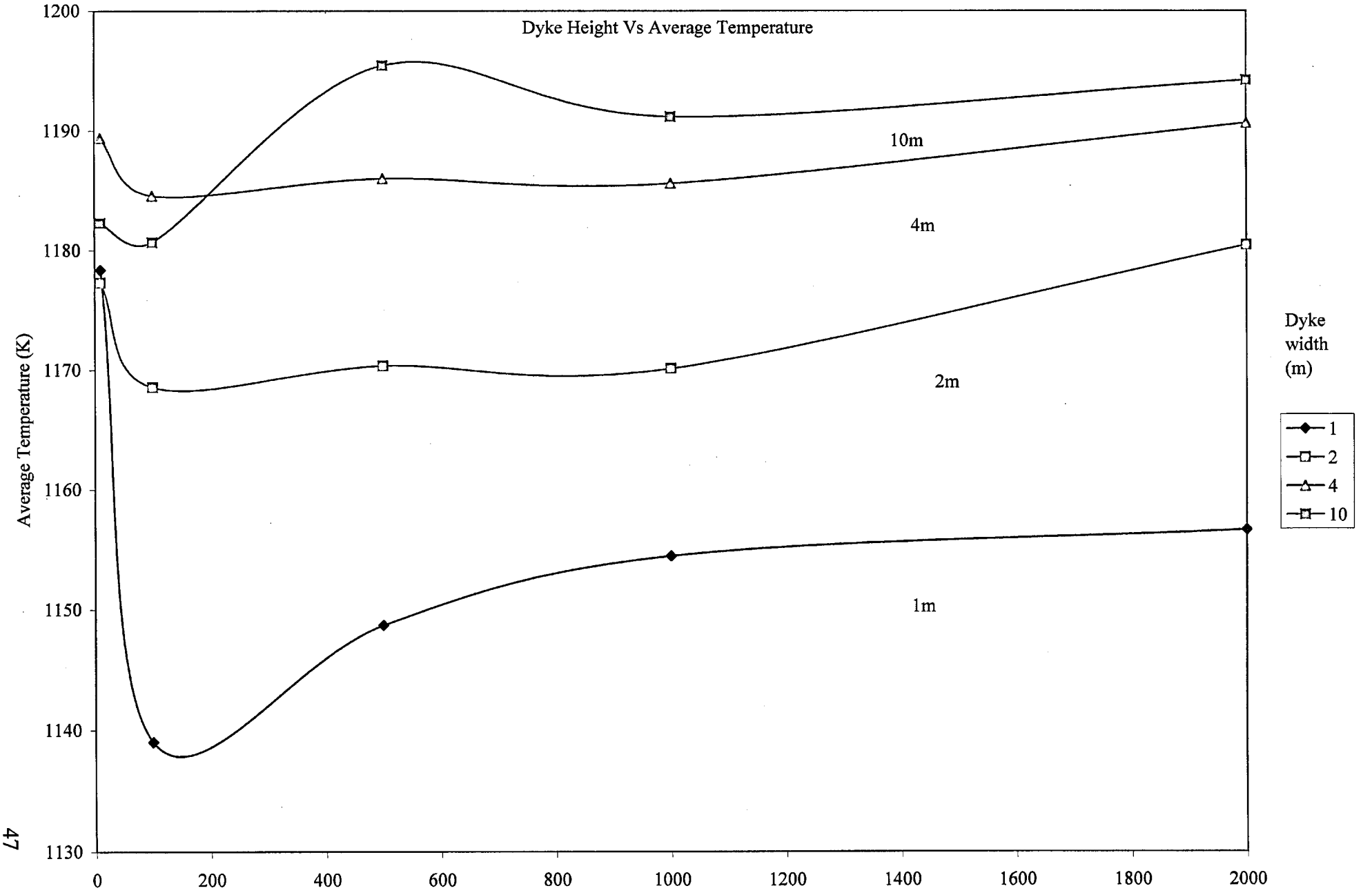

Figure 2.18 This graph shows the variation in temperature with height and width of a model dyke. The initial and boundary conditions are as in figure 2.2a).

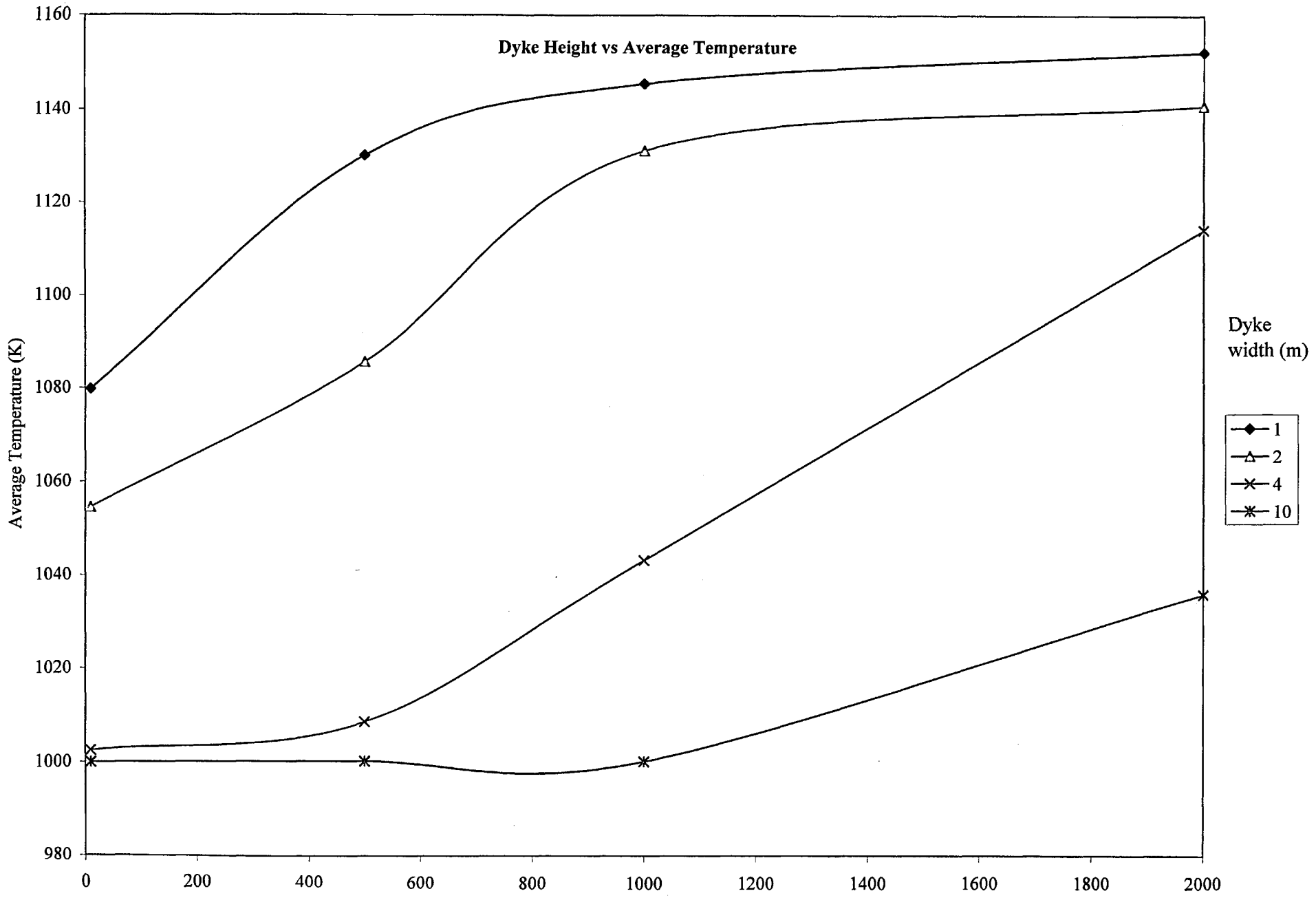

Figure 2.19 This figure shows the variation of temperature with height and width. The initial and boundary conditions are as in figure 2.2b).

varied. The first set of experiments used boundary conditions from figure 2.2(a) with a hot base; the second set used boundary conditions from figure 2.2(b) with all walls at the same temperature and were run for 86400s (1 day). The data from the models with the hotter base were plotted on figure 2.18. Each line represents a particular dyke width and along the x axis there is increasing height. From this it can be seen that for dykes over 400m height there is little variation in temperature. The wider the dyke the hotter it remains. The 10m high dykes remain quite hot and in all cases the 100m high ones are much cooler than their 10m equivalents. The model dykes with all walls at 1000K were plotted on figure 2.19. This figure has the same layout as figure 2.18. This figure shows the reverse trend with the narrower dykes retaining their heat better and with increasing height all dykes remain hotter. There is little difference in temperature between the 10m and 100m high dykes at widths of 4 and 10m. Above these heights the wider dykes have lost more heat in the same time period.

2.5.2.2 Summary

- The wider the dyke the higher the average temperature within it where there is a hotter base, this trend was reversed when there was no vertical temperature gradient.
- Increasing the height of a dyke does not significantly increase the average temperature within it.
- Boundary conditions are critical and can override the influence of the dyke size considerations.

The results were critically dependent on the dyke dimensions and the wall boundary conditions. Where the temperature was different at the bottom and top then the wider the dyke the higher the average temperature. This is because as the width increases more heat is transferred into the system. As the model height is increased, there is more hot material in the centre due to the increases in volume, but this increase is less than with increasing width. Where all the walls are at the same temperature then it is only this increasing area that increases the average temperature.

2.6 Conduction vs. Convection

As previously published models of magma cooling had assumed heat loss mainly through conduction; it was considered important to compare our conduction models

with the convective models. Firstly, two 4 m by 1 km models have been compared with boundary conditions as in figure 2.2 (a). Further pairs of conductive/convective models (i.e. pairs have same wall and initial magma temperatures) were then run with a variety of different wall temperatures i.e. all walls at 800 K, 1000 K, 1500 K. This range of boundary conditions was used so that we can see whether increasing the wall temperatures significantly affects the rate of temperature change. Also we wanted to examine how effectively the convective models can convect heat out of the model from the walls and how this affects the convective cooling rate compared with the conductive cooling rate. If this were a large effect then selection of boundary conditions would be even more important.

2.6.1 Results

The average temperature of the first two models has been plotted over 90 days (Figure 2.20). For the first 7-8 days the convective models cools very slightly quicker but then the cooling rate seems to stabilise. Models with wall temperatures less than that of the initial magma temperature show the same trends (figure 2.21) as before. Where the wall temperature is greater than the initial magma temperature the models gain heat with time. Although these initial and boundary conditions are unrealistic, this model was done for a systematic comparison to check how the model worked with a range of temperatures. The trend is the opposite to that of heat loss where the convective model gains heat quicker than the conductive model. In the cooling model runs after 90 days the difference between each pair of conductive/convective models is around 100K.

2.6.2 Summary

- Initially the convective models cools quicker than the conductive ones
- After around 7 days the convective models stay hotter than the conductive ones.
- The boundary conditions seem to have little effect on the above findings

This is surprising as generally convecting magmas are thought to cool more quickly than conductive ones. It originally looked if this was an artefact of the boundary conditions but the pairs of conductive/convective models show that this is not the case. It may partly be an effect that after the initial rapid heat loss a boundary layer of partially solid material forms which may act as an insulating layer between the

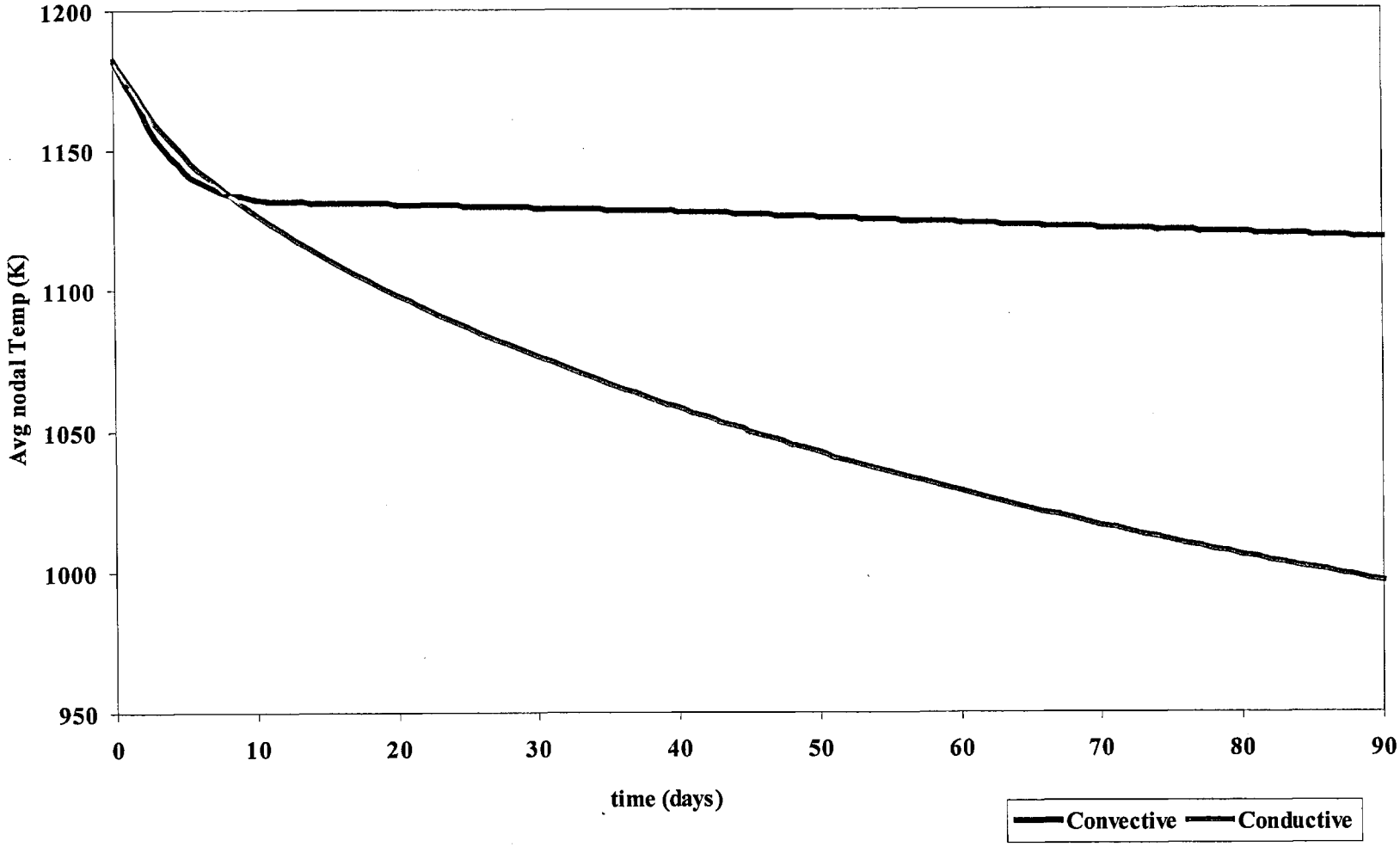

Figure 2.20 Convective vs conductive models over 90 days, 4m by 1km models. Boundary conditions as figure 2.2(a)

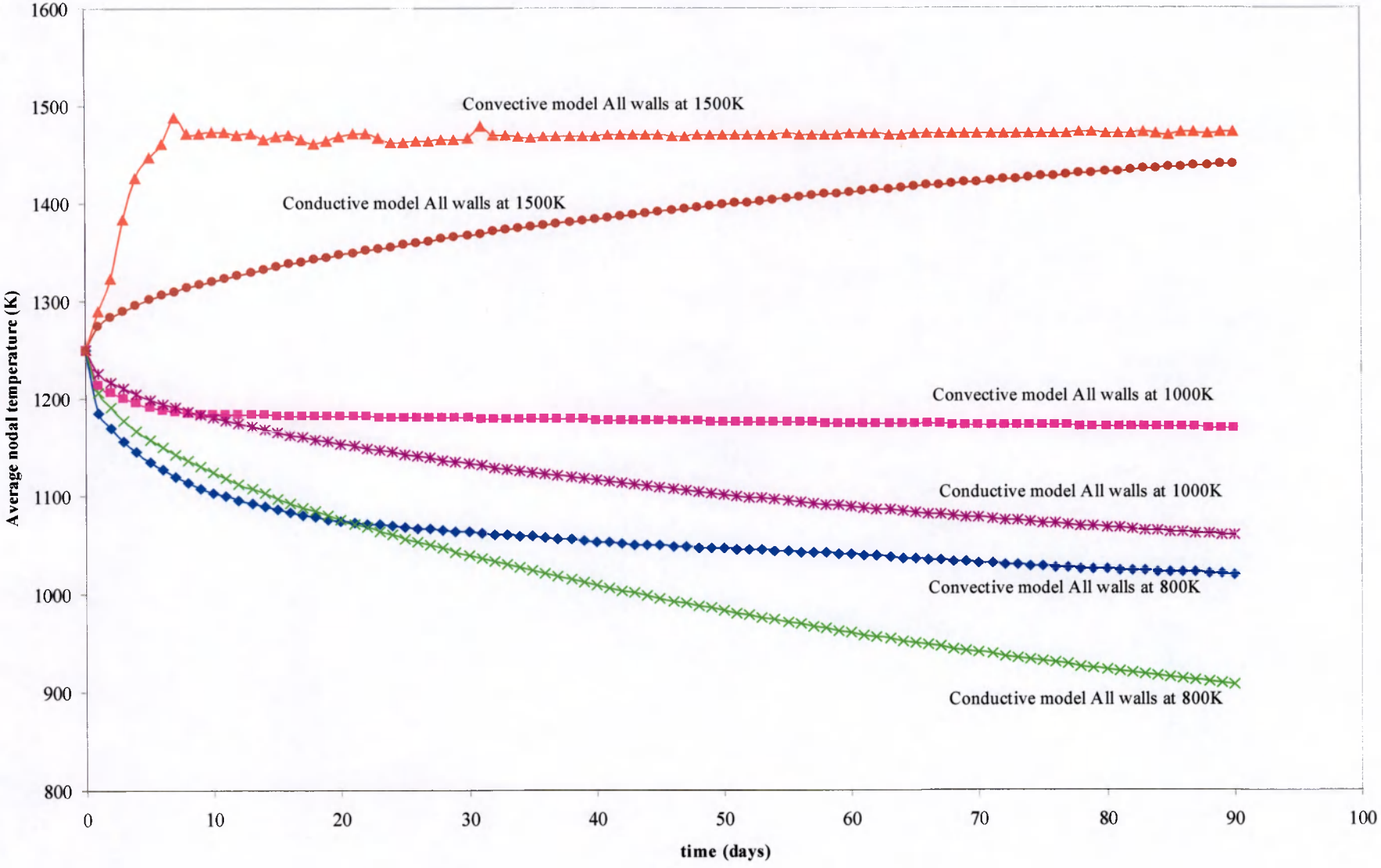

Figure 2.21 This shows pairs of conductive/convective models with the same boundary conditions cooling over 90 days

magma and the cooler surroundings. This would mean that the rate of heat loss would decrease further.

2.7 Summary and the way forward

The models in section 2.2 accurately reproduced the results of the earlier analytical work on conductive magma body cooling by (Carslaw and Jaeger, 1959). When the F.E.A. method was applied to convective models (sections 2.3 and 2.4) it was found that the models did not quantitatively match the laboratory experiment results of (Jaupart and Brandeis, 1986). Qualitatively and quantitatively comparing the F.E.A. models with both the theory and laboratory experiments showed that our models are very similar around the boundary layers. This may be because in the boundary layers conduction will dominate, so as our Ansys F.E.A. models agreed with the Carslaw/Jaeger models this is not suprising. The central part of the Ansys model of a convective layer was hotter than the J/B model, even after taking into consideration J/B laboratory errors. As yet, no explanation has been found as to why this part is too hot. This result was also shown when the conductive and convective models were compared. It was found that the convective models apparently stayed hotter for longer than the conductive ones.

This could possibly be the case despite general opinion being that convecting material should cool quicker. It is possible that as the material cools it forms an insulating layer of partially solidified material, as seen in lava tubes. Further work is needed to measure heat loss in features such as lava tubes so that these could be compared to the Ansys models. This work may be able to highlight areas of the models which may need modification.

A further step would be to introduce volatiles into the system. This would bring the models a little closer to simulating a real system. If this then showed the heat loss being too great to sustain the viability of dykes and other feeder systems it would be further evidence in favour of convective recharge. In the F.E.A. models after prescribed time periods new hot material could be introduced to see its effect on the thermal behaviour of the system.

An alternative to using F.E.A. would be to use physical analogue modelling to investigate the recharge. In the following chapter a physical model is created where a convective exchange can take place between a 'lava lake', a connecting feeder and a

deeper 'chamber' or source. One system could just be left to solidify and another could be heated from below to induce convection and then the two systems could be compared. From this it could be observed which stayed the hottest longest. The length and diameter of the feeder or depth and volume of the chamber could also be varied to see how, as in the F.E.A. models, dimension affected this process.

Chapter 3

Analogue and Mathematical Modelling of Lava Lakes

3.0 Introduction

The phonolitic lava lake on Mount Erebus on Antarctica has been active for decades (Kyle and Meeker, 1990; Harris et al., 1999). Persistently high heat and gas fluxes can be detected by remote sensing techniques and the number of reported persistently active volcanoes has increased over recent years (Tazieff, 1994; Kyle and Meeker, 1990). There have been many possible explanations about the longevity of some lava lakes. It had been thought that this may be due to large volumes of magma being constantly brought up and emplaced in the shallow plumbing of the volcano (Allard, 1997), but ground deformation studies carried out at places such as Kilauea indicate that this is not always the case (Harris et al., 1999). So how can periods of persistent volatile fluxes be maintained? Here we look at how the process of convective magma recharge may be responsible. This process involves hot volatile-rich magma from a deep chamber rising buoyantly up a conduit into a lava lake. As it rises, gases will exsolve. Escape of the gas to the atmosphere, and cooling and crystallisation of the degassed magma in the lave lake make the magma become denser. This degassed magma may then either sink to the bottom of the lava lake or be deposited on the walls of the conduit or sink back down to the magma chamber. Here it may be deposited or may possibly be re-gassed and heated to rise up the conduit and begin the cycle again. If this cycle continues then this could explain the persistent degassing and long-lived lava lakes seen at some volcanoes.

This investigation is aimed at understanding the factors that determine the rate of exchange driven by convection between a lava lake and magma chamber connected by a conduit. In this case the factors that are likely to influence the longevity of lava lakes are:

- The depth of the lava lake; Observations from lava lakes on Kilauea indicate that shallow lakes cool more rapidly than deep ones (Peck et al., 1979).
- The width of the conduit; conduit width will influence the rate of magma supply between lava lake and magma chamber. A wider conduit will generally

allow a greater supply of hot material to the lava lake and increase the rate of removal of cool crystallised magma from the lava lake to the magma chamber.

- The viscosity of the magma; the higher the viscosity of a magma the slower it would flow and hence heat will be lost more slowly by convection.
- The specific heat capacity of the magma; the higher the heat capacity the longer the magma will retain heat.
- Volume; The greater the volume of magma (for a given density), the more heat it will contain.

To identify whether there is convective recharge is important. A comparison of isolated cooling was made, between cooling of magma in a lake unconnected to sources of new material e.g. Alae on Kilauea (Peck et al., 1979), and with that of a lake which has free exchange with a magma chamber below e.g. Pu'u 'O'o (Heliker et al., 1998) on Hawaii. If the cooling gradients (rate of change of temperature with time) in a free exchange system differ from those in the isolated system it would mean that there are additional processes occurring. It is likely that these differences are due to convection taking place.

Considerable work has been done on convection in magma chambers using analogue models. (Huppert et al., 1986) examined the replenishment of magma chambers with light inputs. This involved injecting a variety of fluids into chambers containing a denser, more viscous fluid and examining the resultant buoyant plume. They also varied the aspect ratios of the chambers and conduits, from this they found a great diversity of effects that were dependent on the geometries. They also confirmed that the degree of mixing within the containers depended on the Rayleigh number. Similar work was carried out by (Weinberg and Leitch, 1998), they again examined the aspect ratios and different shaped tanks. Weinberg used waxes and much cooler temperatures such that some solidification took place. (Stevenson and Blake, 1998) developed a model of convective overturn between degassed magmas and fresh gaseous magmas. They constructed laboratory models in long narrow tubes with fluids of varying viscosities and densities. They found that the fresh gaseous magma ascended up the centre and the denser degassed magma descended along the walls.

3.1 Model

The system I wish to examine is that of a lava lake – conduit – magma chamber as show in figure 3.1.

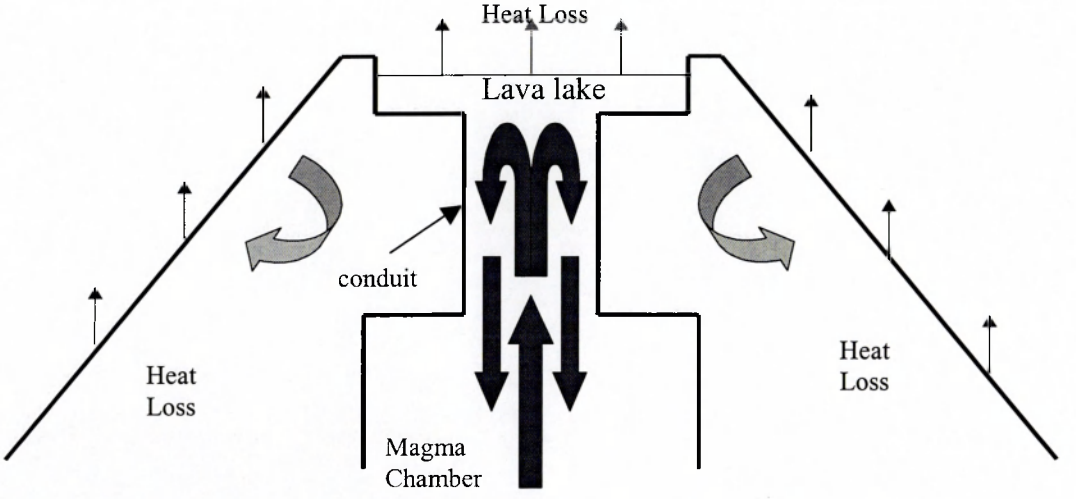

Figure 3.1 This shows a schematic cross section through a volcanic system. The arrows illustrate that heat is lost to the atmosphere and through any hydrothermal system within the volcano.

To create a mathematical model of this I needed to simplify the system, this simplification allowed a laboratory model to be built as shown in figure 3.2

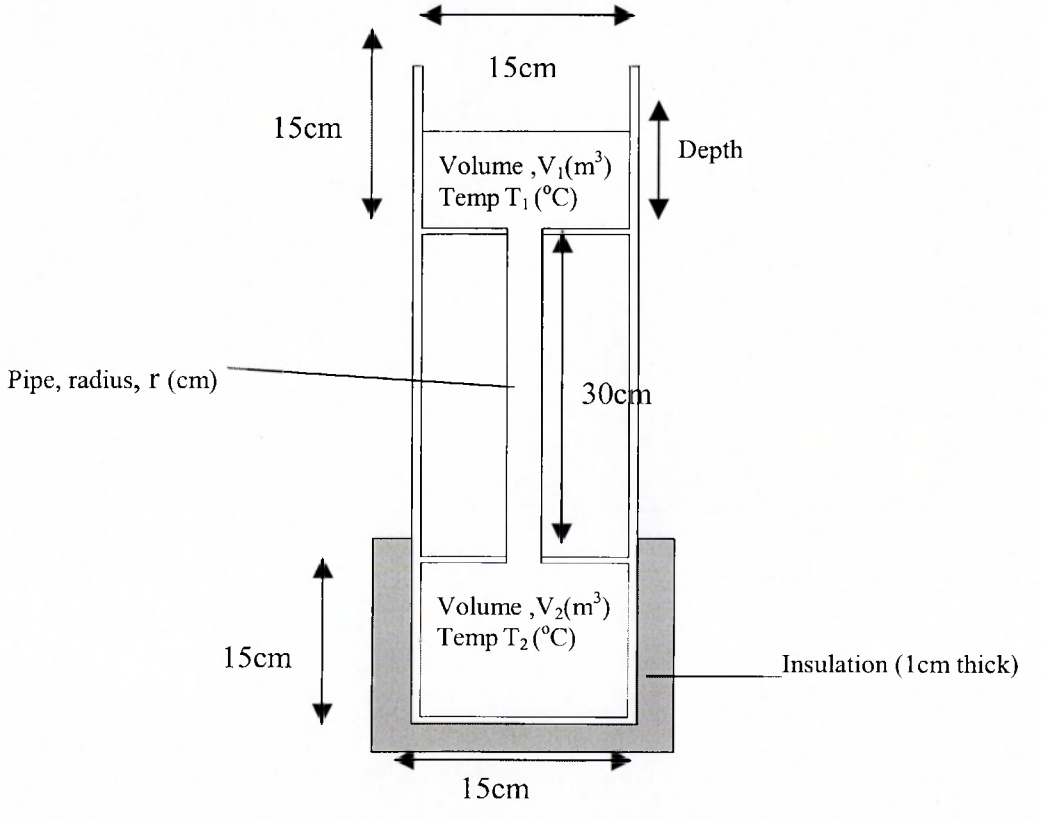

Figure 3.2 A schematic of the model. The Perspex walls were 1cm thick except for the pipe, which was 0.5cm thick.

In a real lava lake – conduit – magma chamber system the magma chamber is usually the hottest part due to better insulation (country rocks) and connections to a deeper magma. The lava lake loses heat to the atmosphere by conduction, convection and radiation. Also there can be heat loss where there is a hydrothermal system. Laboratory models could either be constantly heated at the base enabling convection or have one chamber insulated that differential cooling may occur. It is the latter that I have decided is the most practicable.

An isolated 'lava lake', of homogenous temperature, cools over time and so first I will establish a mathematical model for an isolated chamber to look at this process. Equations 3.1-3.5 are derived from (Kazahaya et al., 1994; Turcotte and Schubert, 1982)

$$\frac{dT_1}{dt} = -k_1 (T_1 - T_r)$$ **Equation 3.1**

Where T_1 = temperature (°C) in the upper chamber

T_r = room temperature (°C)

t = time (s)

k_1 = cooling constant ($°C^{-1}s^{-1}$) ; This is a function of the material properties of the fluid i.e. its specific heat capacity, thermal conductivity, density and viscosity and its mass and shape.

Assumptions

- The chamber is homogenous, so T_1 is representative of the whole chamber
- The room temperature T_r is constant

From figure 3.2 a magma chamber cools over time:

$$\frac{dT_2}{dt} = -k_2 (T_2 - T_r)$$ **Equation 3.2**

Where T_2 = temperature in the lower chamber (°C)

These differential equations can be solved for initial conditions at t=0 where $T_1 = T_0$ where T_0 = initial temperature of the fluid.

$\ln (T_1(t) - T_r) = \ln (T_0 - T_r) - kt$ **Equation 3.3**

Next this model will be expanded to examine the effects of free exchange. When there is free exchange between the lava lake and the magma chamber via the conduit, heat in the lava lake will be lost to the surroundings and gained from below. The flow

rate will be dependent on the density difference and hence the temperature difference between the lava lake and the magma chamber. The viscosity of the fluid will also have an influence as low viscosity fluids lose heat quicker than high viscosity fluids. The flow will also naturally be affected by the size of the pipe with wider pipes leading to larger volumetric flow rates. The upper chamber in the model is representative of a lava lake; it is connected to the magma chamber below by a conduit. The upper chamber (lava lake) is open to the air, which is where a lot of heat is lost.

$$\frac{dT_1}{dt} = \left[-k_1(T_1 - T_r)\right] + \left[\frac{Q_{up}T_2}{V_1} - \frac{Q_{down}T_1}{V_1}\right] \qquad \textbf{Lava lake Equation 3.4}$$

On the right hand side of equation 3.4 the first square brackets refers to heat lost to the surroundings as shown in the case of the isolated chamber. The second one refers to heat gained by convective exchange where an amount of magma from the magma chamber, Q_{up}, at temperature T_2 rises up in to the lava lake of volume, V_1, but heat is also lost by an amount Q_{down} at temperature of the cooling lava lake T_1 as a proportion of V_1.

Where Q = volumetric flow rate (m^3s^{-1})
up, down. $Q_{up} = Q_{down}$.

V_1 = Volume in the upper chamber (m^3)

V_2 = Volume in the lower chamber (m^3)

$$Q = \frac{cg\Delta\rho r^4}{\mu} \qquad \textbf{Pipe equation 3.4a}$$

Where c = constant, which is related to the fluids material properties and the shape of the pipe.

g = acceleration due to gravity (ms^{-2})

ρ = density (kgm^{-3}) $\Delta\rho$ is controlled by the temperature difference between the upper and lower chambers. $\Delta\rho = \rho_o\alpha(T_2\text{-}T_1)$ where

α = thermal expansivity ($^oC^{-1}$) ρ_o = reference density (kgm^{-3})

r = radius of the pipe (m)

μ = viscosity of fluid (Pas)

Assumptions

- Viscosity is high enough to control velocity
- Negligible heat is lost through the walls of the pipe

The magma chamber is represented in the model by the lower chamber, just as a real magma chamber is insulated by the country rock; the lower chamber is insulated too. Some heat will be lost to the insulation but a proportion of the hot magma will rise up to the lava lake and a proportion of the cooled lava lake will sink down to the magma chamber.

$$\frac{dT_2}{dt} = \left[-k_2(T_2 - T_1)\right] + \left[\frac{Q_{down}T_1}{V_2} - \frac{Q_{up}T_2}{V_2}\right]$$ **Magma Chamber Equation 3.5**

On the right hand side of equation 3.5 the first square brackets refers to heat lost to the surroundings, the second one refers to heat lost by convective exchange. Variables as in Equation 3.4.

3.2 Experimental Method

To test these models a Perspex model was built of the simplified volcanic system. This consisted of two 15 × 15 × 15cm cubes which represented the magma chamber and lava lake, these were then connected by pipes representing conduits. Volcanoes are not symmetrical, but using a symmetrical system should help isolate the effects of different conduit widths and lake and magma chamber volumes. As initial plans were to build a system whereby the model could be overturned (like an egg-timer) it was decided that this would be a practical size. These pipes were 30cm long and of varying widths and were interchangeable. The Perspex walls are 1cm thick everywhere except in the pipes. The pipe walls had thickness of 3mm for the medium pipe and 5mm for the wide pipe. The diameters of the pipes used were 2.5cm (medium pipe) and 5cm (wide pipe). The pipes were interchangeable screwing into the fittings cushioned by an O-ring to keep it fluid tight. The lower chamber was insulated with a 1cm thickness of polystyrene sheet so that V_1 cools quicker than V_2 therefore creating differing densities to drive convective exchange. Pico type K thermocouples were used to measure the temperatures in the fluids. Up to five thermocouples were used for a full convective exchange experiment down to just two for some of the isolated chamber experiments. For the full exchange experiments two

thermocouples were inserted through rubber sealed holes in the base of the lower chamber so that the ends of the thermocouples were 5cm above the base of the chamber. The holes were situated as is figure 3.3 below, 5cm either side of the centre on a diagonal.

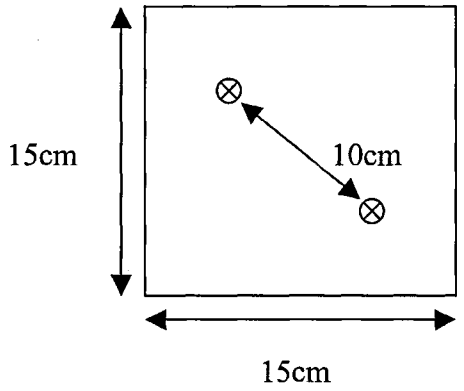

Figure 3.3
This shows the plan view of the base of the lower chamber and the position of the rubber sealed thermocouple holes.

The thermocouples in the upper chamber were placed one over the centre of the open pipe held in place with a clamp. The other was directly overhead of one of the lower chamber thermocouples and was held in place by a specially made bracket, which was attached to the side of the upper chamber. The upper chamber thermocouples were placed at a depth of halfway into the relevant depths; the depth of fluid used was either 5cm, 7.5cm or 10cm. A final thermocouple was placed to measure the room temperature; it was placed away from the influence of the heat loss from the chambers. The thermocouples were connected through a data logger to PC recording the temperature over time direct on to a spreadsheet.

Before each experiment was run warm water was run through the system and then it was dried. This was to help thermally equilibrate the Perspex to experiment temperatures. The fluids were heated and placed into large containers, from these containers the system was filled to the appropriate level. The containers were used to mix thoroughly the fluids to minimise cooling whilst the next batch was heated, so that the experiments could begin with a uniform fluid temperature. Initial test experiments showed that the thermocouples were sensitive to extremes in the weather. In particular hot sunny days lead to an increase in measured temperature. Where this occurred experiments were repeated during more uniform conditions. Another problem was the electrical noise in the laboratory building lead to noisy results, this was minimised by applying a smoothing filter which was included in the data logger

software. Where experiments began with non-uniform starting temperatures in the upper and lower chambers the results were redefined. The data were plotted and the time was zeroed to where the upper and lower chamber temperatures were equal. To test the mathematical models the following experiments were set up. Three fluids were used water and two different dilutions of golden syrup, Mix a and Mix b. The viscosities of these fluids were measured over a range of temperatures using the falling sphere method. Mix b was the most viscous, then mix a, water was the least viscous. A variety of volumes were used, the lower chamber, when used, was always completely filled with 3.375 litres of fluid. The upper chamber was filled with three different volumes; 1.125, 1.688 and 2.25 litres.

3.2.1 Isolated Chambers

The experiments for the isolated upper chamber were carried out by closing off the top of the pipe(the base of the upper chamber) and filling the upper tank with the required volume of warmed fluid. For the experiments looking at the isolated lower chamber, the lower chamber was completely filled with fluid and then the bottom of the pipe (the top of the lower chamber) was closed off. These were then left to cool, the temperatures in the appropriate chamber were then measured over time using a Pico Data-logger with thermocouples both in the fluid and exposed to room conditions. The temperature was sampled at either 1 or 10 second intervals as shown in Appendix.

3.2.2 Free Exchange

The equipment was set up with one of the interchangeable pipes and filled up to a set volume of one of the fluids in the upper chamber. The thermocouples were placed in both the upper and lower chambers as well as again measuring the room temperature. The sample rates were at 1 and 10s intervals.

3.3 Results

For the graphs which have the vertical axis as ln (T_1-T_r) all graphs have been normalized to 3 for comparison purposes. This number was chosen as it was the nearest whole number and was intended as a working figure to be refined if time allowed.

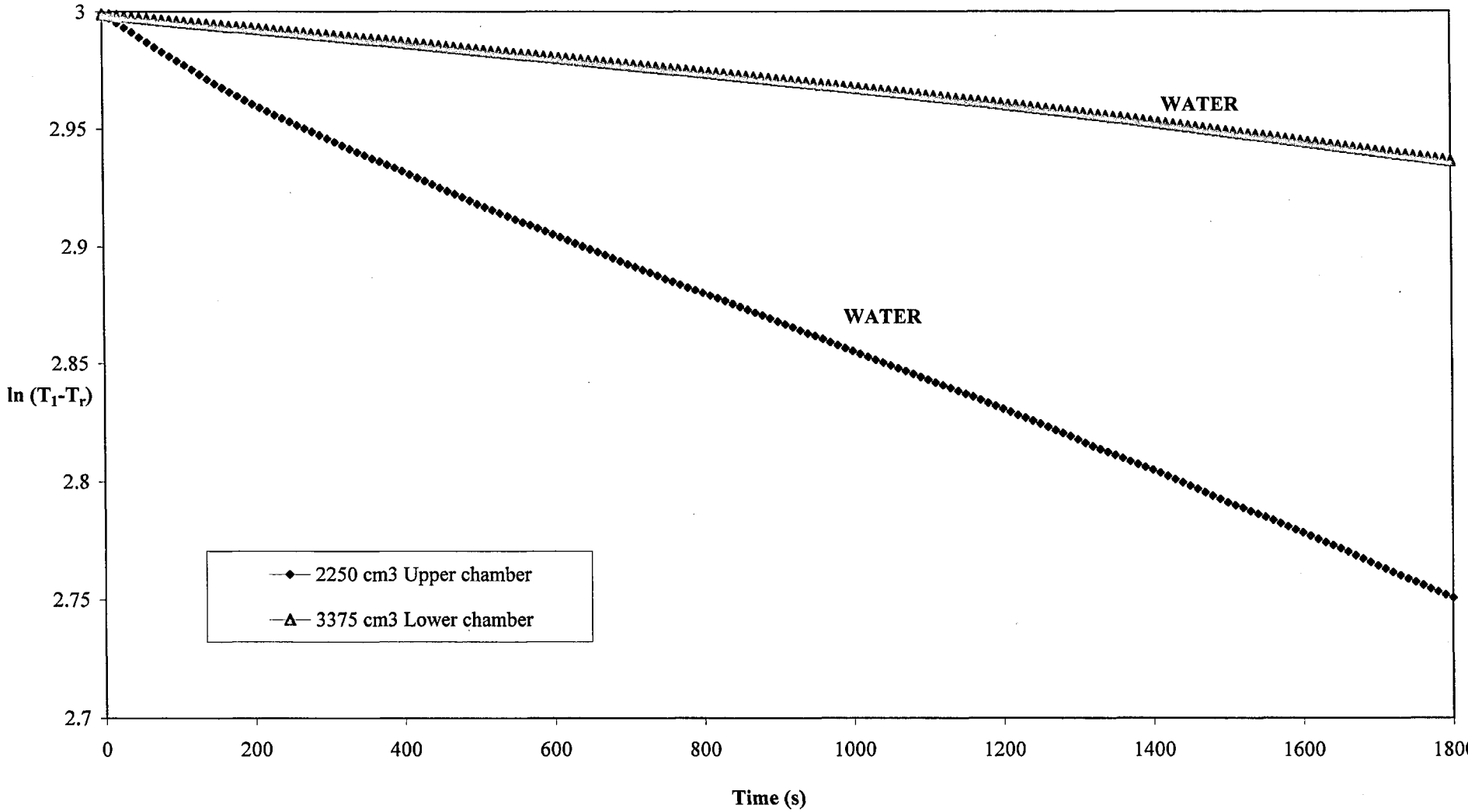

Figure 3.4 This illustrates the difference in cooling rates between the upper and lower chambers when isolated from one another.

3.3.1 Isolated Chambers

Firstly the isolated upper and lower chambers were filled with water to test equations 3.1 and 3.2. figure 3.4 shows the lines for these experiments. Along the vertical axis we have ln (T_1-T_r) and along the horizontal axis time. The lines on this graph are clearly straight with the line of the insulated isolated lower chamber being much shallower than that of the isolated upper chamber. This experiment was also carried out with the other two fluids, mix a and mix b. Three different volumes were used; 1125 cm^3, 1687.5 cm^3 and 2250 cm^3. For each of these experiments a graph was plotted of the same format as figure 3.4. From all of these experiments the gradient of the lines was calculated. The gradient of these lines is equal to k_1 which should be different for each experiment as each of the fluids has different material properties. These values of k_1 are shown in the figure 3.5 below and graphed in figure 3.6.

	Upper Volume (cm^3)			Lower (cm^3)
	1125	1687.5	2250	3375
Water k_1	2.11×10^{-4}	1.90×10^{-4}	1.60×10^{-4}	6.20×10^{-5}
Mix a k_1	1.80×10^{-4}	1.60×10^{-4}	1.40×10^{-4}	6.00×10^{-5}
Mix b k_1	1.62×10^{-4}	1.40×10^{-4}	1.20×10^{-4}	5.7×10^{-5}

Figure 3.5 This table shows the experimentally derived values of k_1, this is the cooling constant as shown in equations 3.1 and 3.2.

All the values of k_1 as shown in figure 3.5 have been plotted on figure3.6. This graph shows volume of the fluid along the horizontal axis and k_1 up the vertical axis.

This graph show that for the upper chambers the value of k_1 decreases with increasing volume. All three of the upper chamber lines show the linear correlation expected. The position of the lines also show a relationship. Water, the least viscous fluid, shows higher values of k_1, and mix b the most viscous shows the lowest values of k_1. The values of k_1 for mix a fall between the two.

For the lower chamber only full isolated chamber experiments were carried out. This means k_1 is shown by only 3 data points. The values of these points show that the k_1 values of the lower chamber experiments were much smaller than those of the upper chamber. Like the lines in the upper chamber experiments they show an order with the water data point demonstrating the highest value of k_1 and again the mix b data point showing the lowest of all.

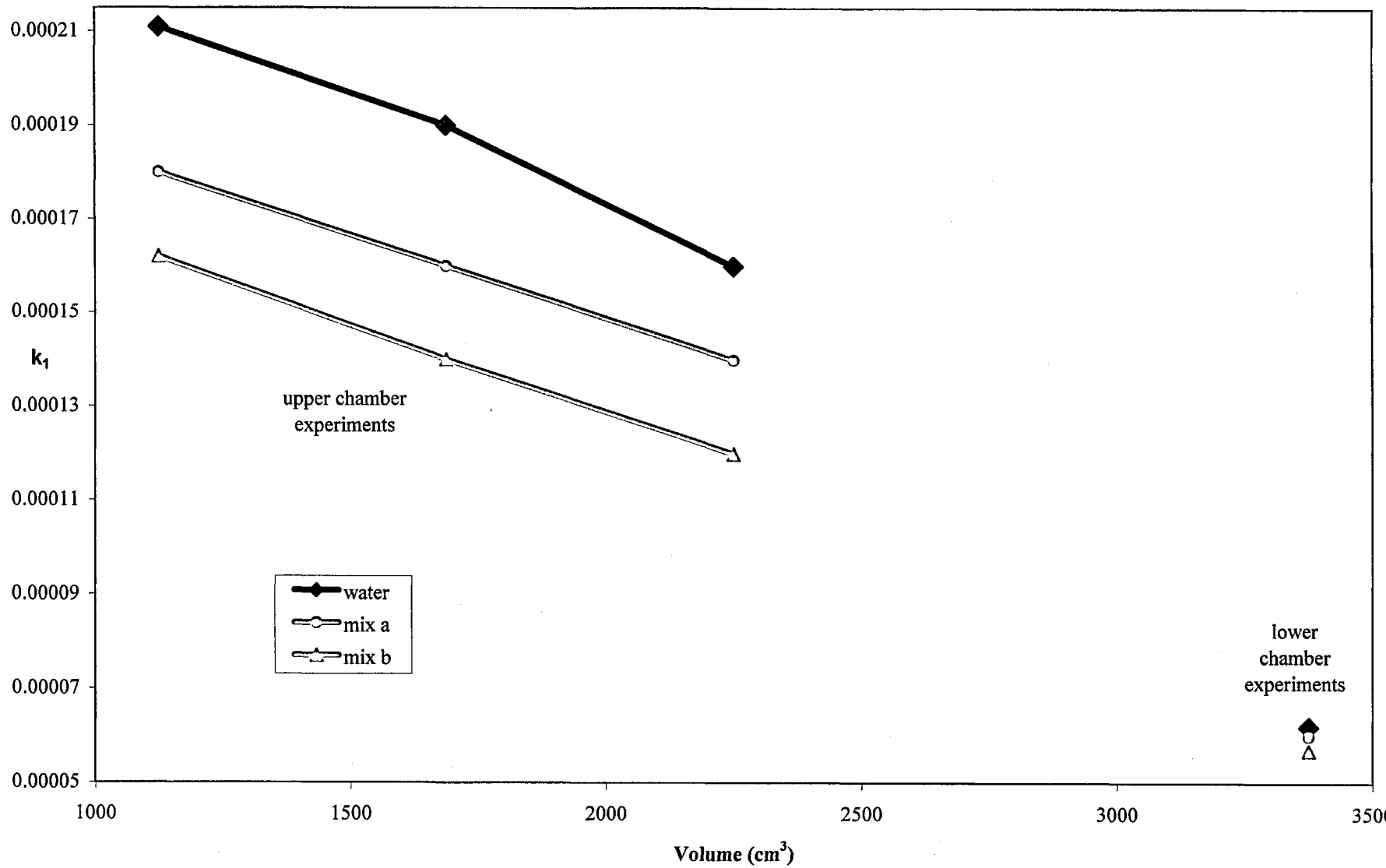

Figure 3.6 This illustrates the variation of the cooling constant k_1 with volume.

3.3.2 Convective Exchange

These experiments varied one of the influencing factors and held the others constant namely lave lake volume, conduit width and magma viscosity. The results will be examined firstly as a selection of cooling curves to illustrate cooling over time. From all of the data the gradients were measured, where experiments were repeated averages were taken. These averages are shown in figures 3.5, 3.13 and 3.14.

3.3.2.1 Pipe Width

Figure 3.7 shows a series of results for water cooling in chambers connected by pipes of differing diameters; 2.5 cm (medium), 5 cm (wide) and 0 cm (isolated). This was for both the upper and lower chambers. These experiments shown here used a constant volume of water in the upper chamber. Figure 3.7 shows the lower chamber. Again ln (T_l-T_r) is shown along the vertical axis and time (s) is shown along the horizontal. In figure 3.7 it shows that the experiment with the widest pipe has the steepest gradient. The next steepest gradient belongs to the medium pipe experiments with the isolated chamber experiment showing the shallowest gradient of all.

Figure 3.8 has the same layout as figure 3.7 but it shows the lines for the upper chamber. In this graph the shallowest gradient belongs to the experiment using the widest pipe. The steepest gradient was that of the isolated chamber, the experiment with the widest pipe had the shallowest gradient and the medium pipe between the others. This implies that the isolated chamber cooled the quickest.

3.3.2.2 Volume of the Upper Chamber

Again figure 3.9 has the same layout as figure 3.4. This graph shows the two chambers connected by a medium pipe, filled with water. The upper chamber contained three different volumes in three different experiments; 1.125 litres, 1.6875 litres and 2.25 litres. The lines showing the lower chamber displayed the shallowest gradient did indeed belong to the experiment with the greatest upper chamber volume and the steepest gradient belonged to that of the experiment with the lowest volume in the upper chamber. The lines for the upper chamber do not show the same pattern. Once again the largest volume in the upper chamber related to the shallowest gradient but the smallest volume had a shallower gradient than that of the medium volume experiment.

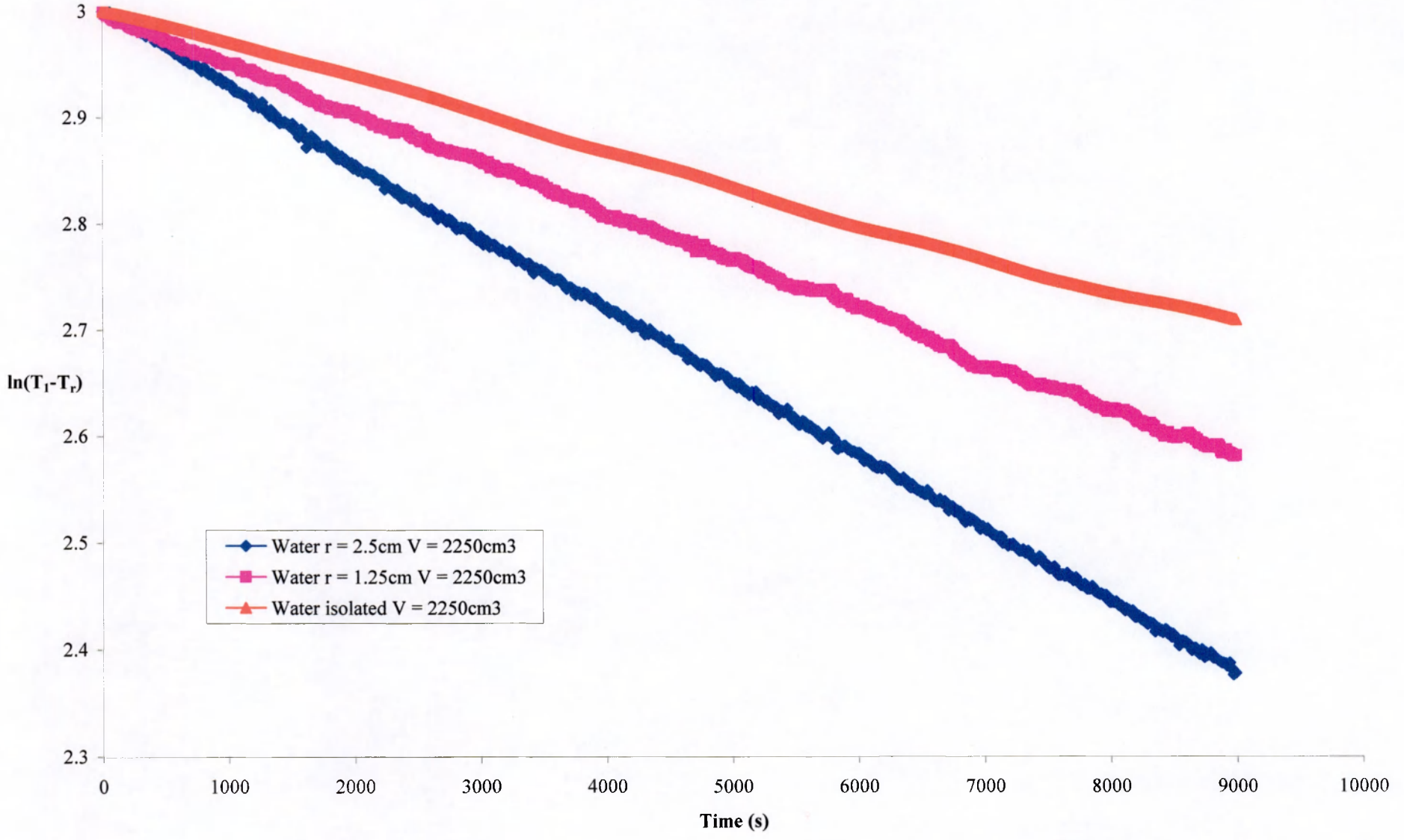

Figure 3.7 This illustrates how the cooling rates of water vary with conduit width in the lower chamber.

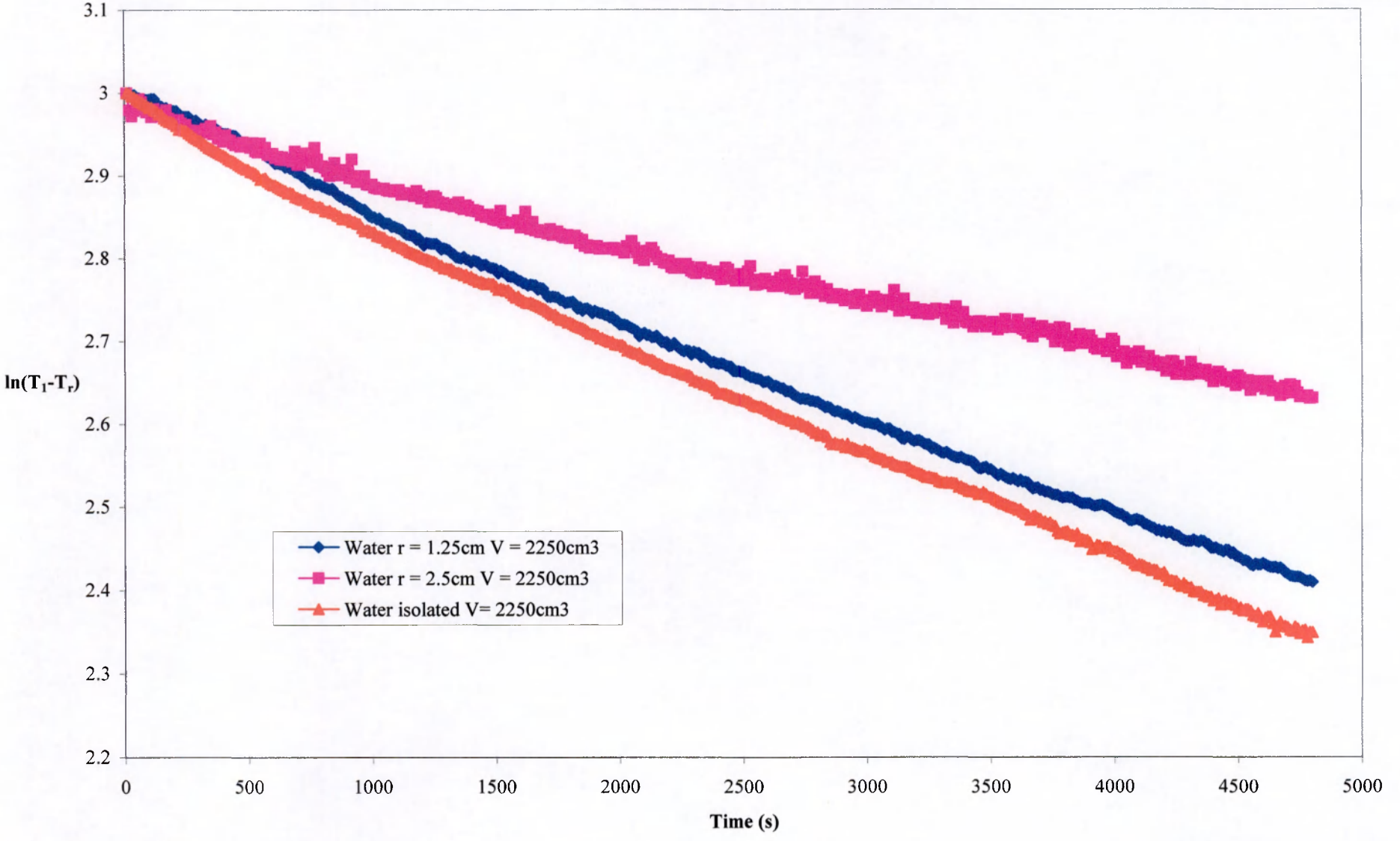

Figure 3.8 This illustrates how the cooling rates of water vary with conduit width in the upper chamber.

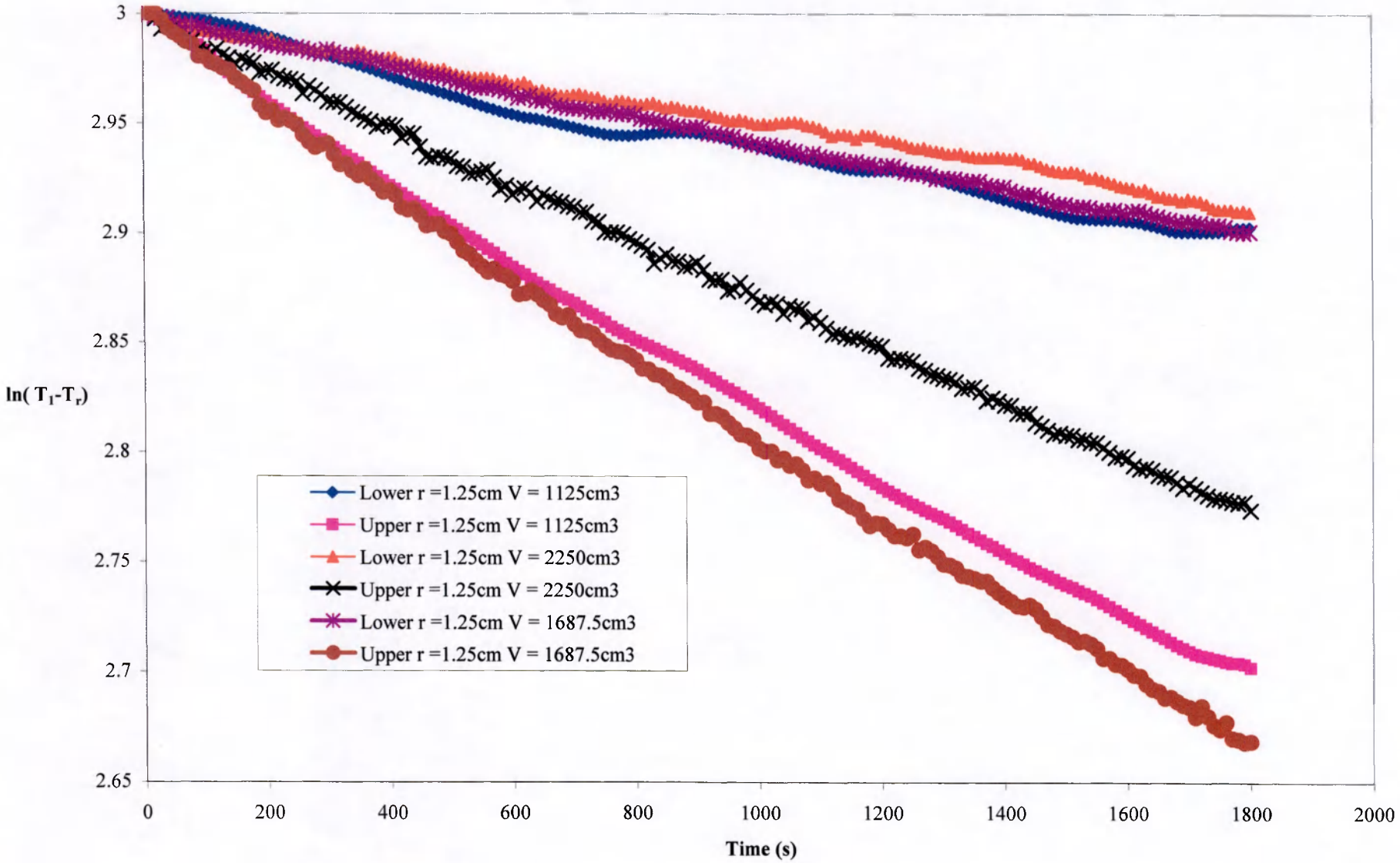

Figure 3.9 This illustrates how the cooling rates of water vary with volume in the upper chamber.

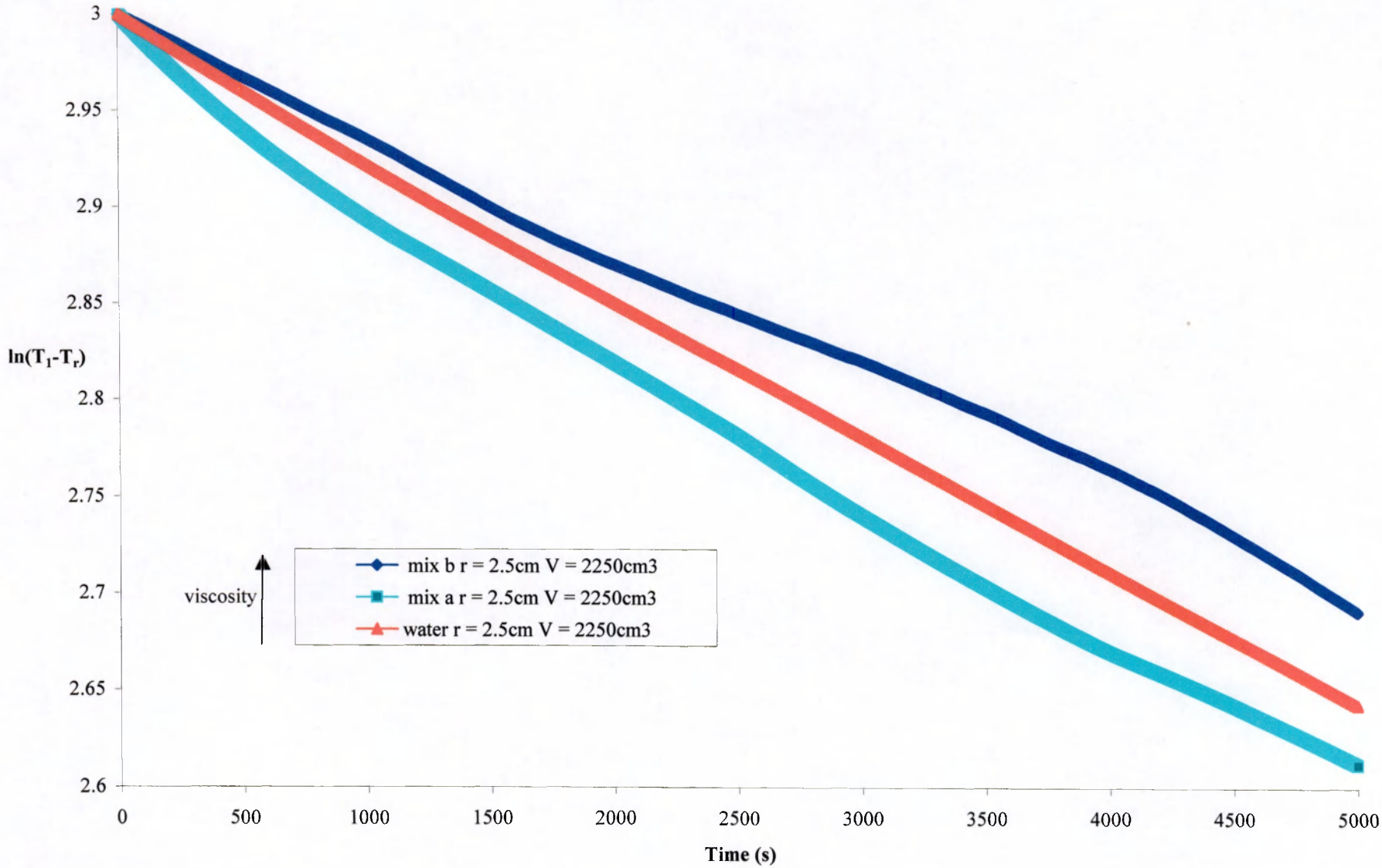

Figure 3.10 This illustrates how the cooling rate varies with viscosity in the upper chamber.

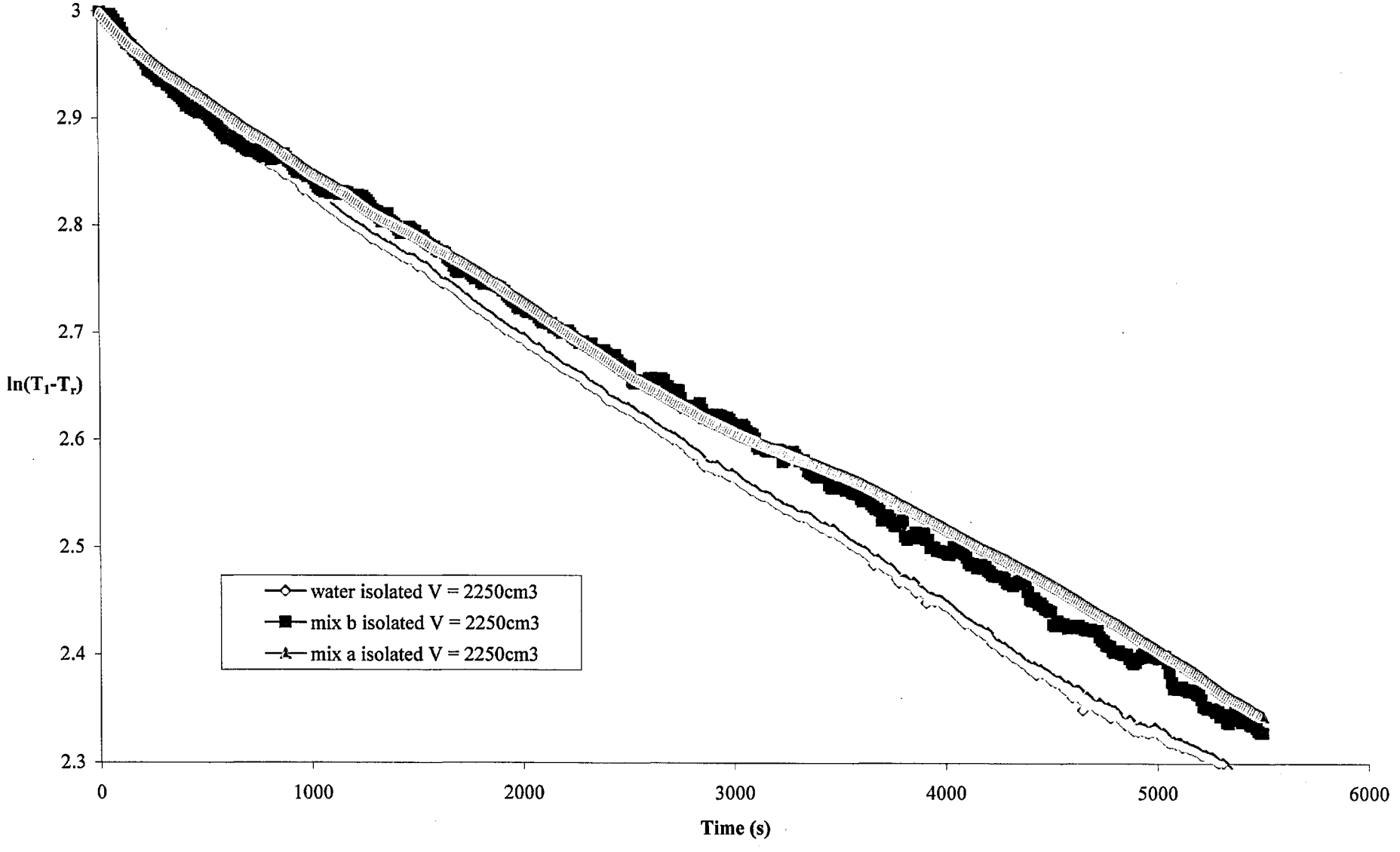

Figure 3.11 This illustrates how the cooling rates vary with viscosity in an isolated chamber.

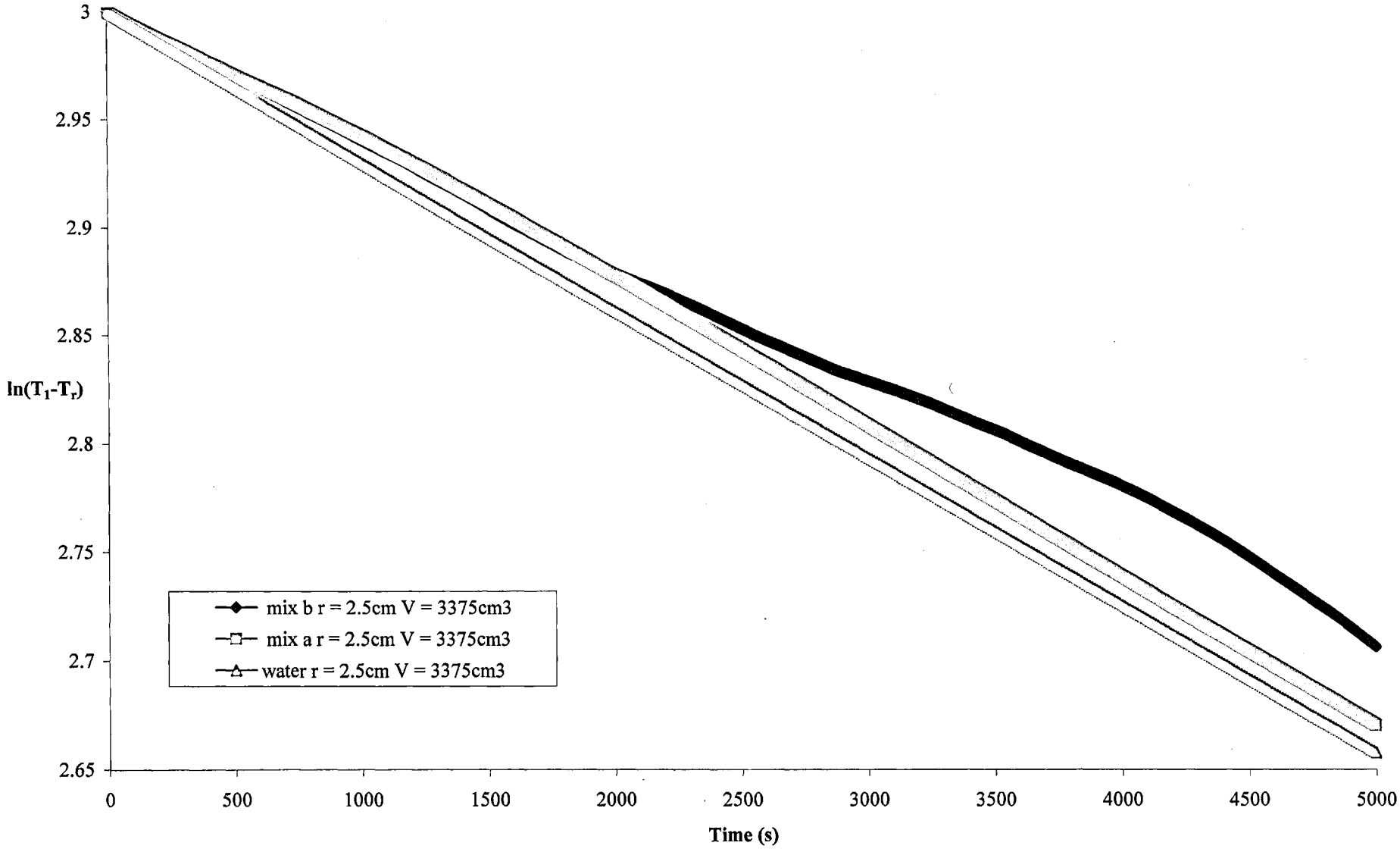

Figure 3.12 This illustrates how the cooling rates vary with viscosity in the lower chamber.

3.3.2.3 Viscosity of Fluids

Figure 3.10 and 3.11 demonstrate how the viscosities of the fluids affect how the system cools over time. Figure 3.10 shows how the upper chamber cools with differing viscosity fluids; mix b being the most viscous, mix a the next most viscous and the least viscous water. These experiments shown had a constant volume of 2.5 litres and the chambers were connected by the wide pipe. Mix b was the most viscous fluid and was found to have the shallowest cooling gradient. The next most shallow gradient was demonstrated by the water experiment, water is less viscous than both mix a and mix b. The steepest gradient and hence the fastest cooling rate was shown in the mix a experiment. Figure 3.11 shows experiments using mix a, mix b and water for an isolated tank. This shows that the experiment with water cools the quickest. Mix a and b cool at a similar rate. Figure 3.12 shows again the three fluids with a constant volume connected by a wide pipe. Mix b, the most viscous fluid, again cooled the slowest with the shallowest gradient. The next shallowest gradient was that belonging to the mix a experiment and the fluid that cooled the quickest with the steepest gradient was water. The most viscous fluid mix b shows a slight deviation from the trends of the other fluids. Further repeats of this experiment are required to see if there is an error within the experiment or a real effect.

	Water- wide	Mix a - wide	Mix b -wide	Water- medium	Mix a - medium	Mix b - medium
1125 cm^3	1.6×10^{-4}	1.38×10^{-4}	1.2×10^{-4}	3.6×10^{-4}	3×10^{-4}	1.85×10^{-4}
1687.5 cm^3	1.35×10^{-4}	1.22×10^{-4}	1.1×10^{-4}	2.5×10^{-4}	2.4×10^{-4}	1.87×10^{-4}
2250 cm^3	1.2×10^{-4}	1.0×10^{-4}	7×10^{-5}	8×10^{-5}	6×10^{-5}	1.1×10^{-4}

Figure 3.13 Values of the cooling constant k_1 which refers to the cooling in the upper chamber

	Water- wide	Mix a - wide	Mix b -wide	Water- medium	Mix a - medium	Mix b - medium
1125 cm^3	1.22×10^{-4}	1.1×10^{-4}	1.0×10^{-4}	1.2×10^{-4}	7×10^{-5}	6×10^{-5}
1687.5 cm^3	8.8×10^{-5}	8.6×10^{-5}	8.55×10^{-5}	1.0×10^{-4}	6.45×10^{-5}	5×10^{-5}
2250 cm^3	6.5×10^{-5}	6.4×10^{-5}	6.2×10^{-5}	7.1×10^{-5}	5.7×10^{-5}	4×10^{-5}

Figure 3.14 Values of the cooling constant k_2 which refers to the cooling in the lower chamber

3.3.3 Cooling Constants k_1 and k_2

Figure 3.15 shows a series of lines relating the cooling constant k_1 (upper chamber) up the vertical axis to the volume (cm^3) in the upper chamber along the horizontal axis. There are basically two sets of lines; one set is that relating to convective exchange with a wide pipe (r = 2.5 cm), the other relates to using the medium pipe (r = 1.25 cm). The lines relating to the wide pipe show that as volume increases the cooling constant k_1 decreases but only by a little. The line for the water experiments illustrate that k_1 is higher than that of mix a which in turn is higher than that of mix b. The lines relating to the medium width pipe are not so clear.

As the volume increases the cooling constant decreases. Water has the highest cooling rate with the next highest being mix a followed by mix b. Over lower volumes the cooling constants are higher for the medium pipes but as the volume increases the cooling constants become similar to those of the wide pipe.

Figure 3.16 shows a series of lines relating to the cooling constants k_2 (lower chamber) to the volume of the upper chamber (cm^3) along the horizontal axis. Again like figure 3.15 there are two sets of lines, the medium and the wide pipe experiments. Both sets of lines sit close to each other. Again the medium pipe experiments show the higher cooling constants. As before, as the volume in the upper chamber increases the cooling constant in the lower chamber decreases. This is shown for both the medium and the wide pipe. Also as shown in the upper chamber analysis the more viscous the fluid the lower the cooling constant.

3.3.4 Errors

There are many potential sources of errors. One source was from the set up, the equipment had to be warmed to help thermally equilibrate the Perspex with the fluid so that the temperature gradient between the two were minimized. Filling the equipment was also difficult to control to enable $T_1 = T_2$, this was done by premixing the whole batch of fluid in one go. The thermocouples were threaded onto a metal bracket which attached to the outside of the upper chamber and this could be affected by people entering the room causing the bracket to vibrate, on the whole though this was a small effect. It showed as a sharp deviation from the trend, but within a few minutes the trend re-established itself as shown in figure 3.17. The thermocouples themselves held the largest error with them being able to measure to an accuracy of

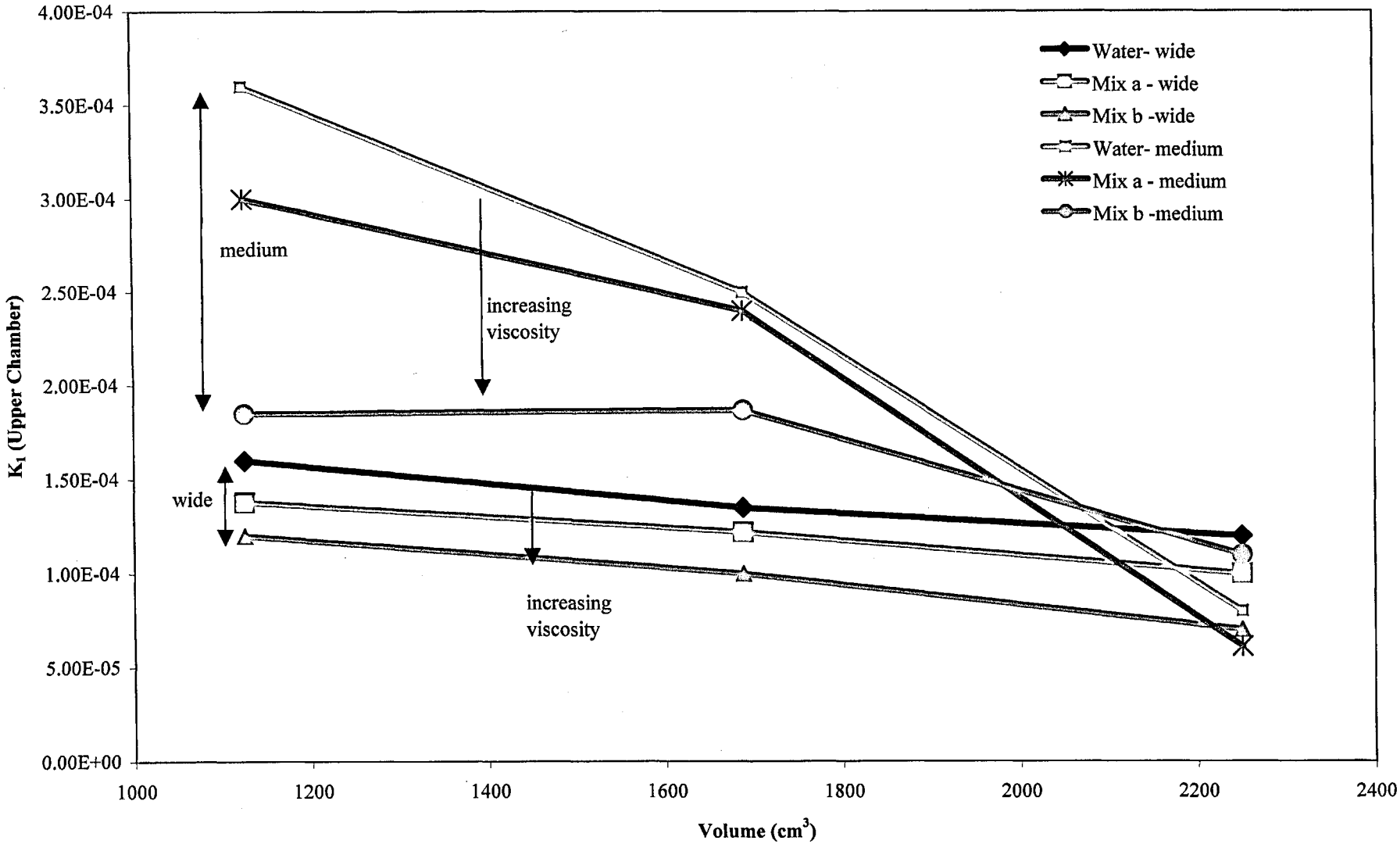

Figure 3.15 This graph illustrates how K_1 varies with volume, pipe width and viscosity.

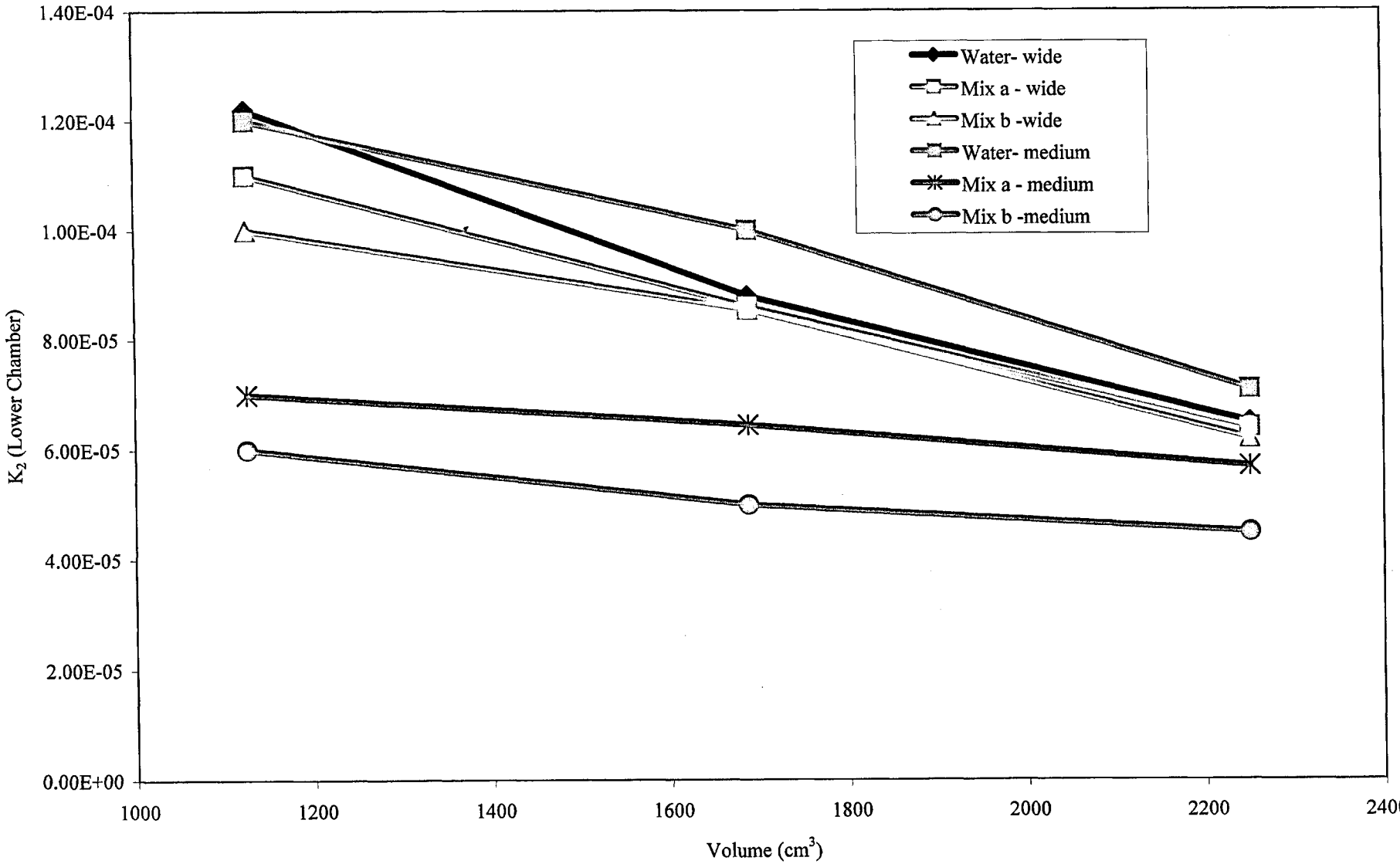

Figure 3.16 This graph illustrates how K2 varies with volume, pipe width and viscosity

+/- 0.1 °C. This error generally was much more significant than the set up errors. The Pico program could be set to filter the data so that some of the interference could be eliminated. During the processing of the data I used a moving weighted average to smooth the data further, this did not affect the trend of cooling just smoothed the curve.

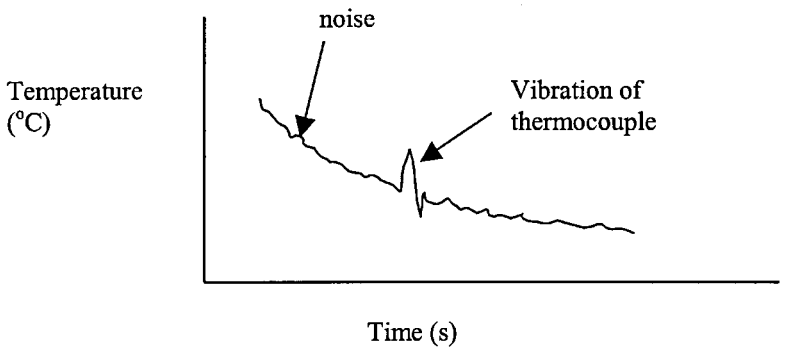

Figure 3.17 This shows a schematic of potential errors as seen from the data logger trace. Electrical noise and interferences shows as a low amplitude deviation. The large amplitude deviation showed when the thermocouples were vibrated for example when someone enters the room and knocks the table on which the equipment stands.

3.4 Interpretation

3.4.1 Isolated Chamber

Figure 3.4 showed that the lower isolated chamber cooled slower than the upper isolated chamber. This will be due to the insulation on the lower chamber and that the upper chamber is open to the surroundings. Figure 3.6 shows the variation of the cooling constant with volume in the upper chamber. All three lines show a decrease in the cooling constant with increasing volume (and mass). So for a given heat energy H we can use the energy relationship:

Equation 3.6

$$\frac{H}{mc} = \Delta T$$

Where: H = heat energy (J), m = mass (kg), c= specific heat capacity ($Jkg^{-1}K^{-1}$),

ΔT = change in temperature (K)

Therefore increasing the mass of a fluid decreases the change in temperature. In the lower chamber the slower cooling rate will be due the reduced heat lost to the surroundings.

3.4.2 Convective Exchange –Cooling over time

We can combine equations 3.4 and 3.4a to get:

Equation 3.7

$$\frac{dT_1}{dt} = -k_1(T_1 - T_r) + \frac{cg\Delta\rho r^4 T_2}{\mu V_1} - \frac{cg\Delta\rho r^4 T_1}{\mu V_1}$$

Where the variables are as Equations 3.4 and 3.4a. This can be used to see if the results are reasonable.

3.4.2.1 Pipe Width

Increasing the radius of the pipe will increase the amount of heat gained by convective exchange so this will offset the effect of heat lost to the surroundings. The effect of the radius in equation 3.7 is quite powerful as it is to the power 4. The cooling trends in figure 3.7 for the lower chamber does indeed show that with increasing pipe width the cooling rate is indeed slower. This relationship is confirmed in figure 3.8 which shows the cooling trends for the upper chamber.

3.4.2.2 Volume of the Upper Chamber

From equation 3.7 it would suggest that increasing the volume would increase the heat lost as the effect of heat gain by convective exchange would be lessened, but from figure 3.9 shows that this is clearly not the case. Another approach is to look at the heat loss related to the surface area to volume ratio.

The larger this ratio the larger the heat loss should be i.e. a large flat area will lose heat quicker than smaller deep area would. So if we examine the surface area to heat ratio of the three volumes used, a) 1125 cm^3, b) 1687.5 cm^3 and c) 2250 cm^3, we get:

a) surface area = (5 cm ×15 cm) x 4 + (15 cm × 15 cm) × 2 = 750 cm^2

volume = 5 cm × 15 cm ×15 cm = 1125 cm^3

∴ ratio = 0.666 cm^{-1}

b) surface area = (7.5 cm × 15 cm) × 4 + (15 cm × 15cm) × 2 = 900 cm^2

volume = 7.5 cm × 15 cm ×15 cm = 1687.5 cm^3

∴ ratio = 0.533 cm^{-1}

c) surface area = (10 cm × 15 cm) × 4 + (15 cm × 15cm) × 2 =1050 cm^2

volume = 10 cm × 15 cm ×15 cm = 1687.5 cm^3

$\therefore$ ratio = 0.466 cm^{-1}

This examination of the surface area to volume ratio show that a higher cooling rate could have been expected for the smaller volume. The larger the surface area for a given volume would mean a larger heat loss.

3.4.2.3 Viscosity of the Fluids

The effect of viscosity on the rate of cooling can be examined by looking at the Reynolds number: $\mathrm{Re} \propto \frac{\rho r u}{\mu}$. The Reynolds number is a dimensionless number which measures the ratio of viscous to inertial forces. Fluid flow will move from a laminar flow for flow in a pipe towards a turbulent flow as the critical Reynolds number is approached. $Re_{cr} \approx 2300$. The higher the Reynolds number the quicker a fluid will cool.

Figures 3.10, 3.11 and 3.12 show the effect of viscosity in the upper, isolated and lower chambers. In the upper chamber they have similar cooling rates with water cooling quicker than the most viscous mix b. This was expected as water is the least viscous of the fluids and therefore has the largest Reynolds number. So the larger the viscosity the smaller the Reynolds number and hence the slower the cooling. Figure 3.11 shows the cooling of fluid in isolated chambers; this demonstrates that as in the upper and lower chambers the least viscous fluid, water, cools the quickest.

3.4.3 Cooling constants k_1 and k_2

Graph 3.9 shows how the cooling constants vary with volume. The cooling rates of the medium pipe are higher than those of the wide pipe. This is probably due to the efficiency of the mixing in the pipes and chambers. The wider pipes will allow more hot material to ascend. From qualitative mixing experiments of two different viscosity/density fluids in the medium pipe the less dense fluid rose into the upper chamber creating a distinct flat mushroom plume going straight to the open surface i.e. the coolest surface, where cooling would be most rapid. Whereas with the wider

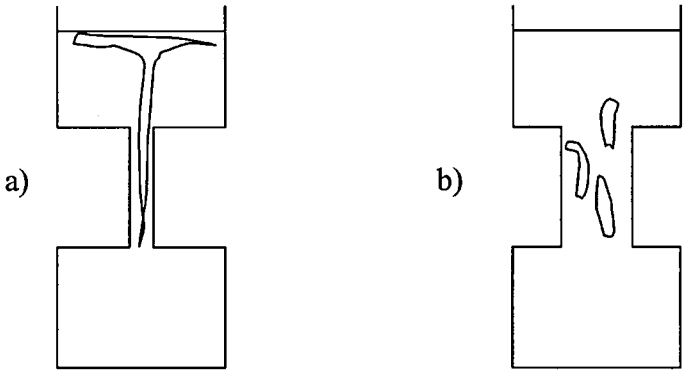

Figure 3.18 This shows a) is the medium pipe and b) is the wide pipe. The lower part of the chambers was filled with a warm coloured fluid and sealed off. The seal was then released and the warm fluid buoyant rose and mixed with the cooler clear fluid in the upper chamber and conduit. In a) mixing took place in the upper chamber, in b) the mixing began in the pipe.

pipe more mixing took place in the upper half of the pipe which then rose in a more pulse like fashion, which would lead to slower cooling. In the lower chamber the medium pipe generally showed the slower cooling rate except for the water cooling trend. This may be expected as water would be much more likely to illustrate turbulent behaviour with its low viscosity and hence higher Reynolds number.

3.5 Conclusions

- Wider conduits decrease heat loss in lava lakes, so volcanoes with wide conduits could be expected to remain active for longer.
- The larger the volume and mass of a lava lake the slower it will cool. This is dependent on the surface area, the larger the surface area for a given volume the larger the heat loss.
- From these experiments it was found that the more viscous the fluid the slower it will cool.

Chapter 4

4.1 Conclusions and Applications

In this final chapter I discuss whether the aims from chapter 1 have been achieved. They were:

- Whether dykes can remain molten over long periods of time without a heat influx.
- Whether natural convection occurs in dykes when it is a closed system.
- How the dimensions of dyke can affect their convection and cooling rate.
- Which material properties are the most influential in enabling convection and the effect on the cooling rate.
- How the dimensions of a lava lake – conduit – magma chamber system affects the cooling rate of both lava lake and magma chambers.
- How the cooling rate is affected by convection within the system.
- The material properties of a magma and how this affects the cooling rate

4.1 Magma Cooling in Dykes

Chapter 2 used finite element analysis (F.E.A.) to model the cooling of dykes. I first examined heat loss by conduction and found that the F.E.A. model almost exactly replicated the (Jaeger, 1968) theoretical model, therefore this was deemed a success allowing progression to models of convection.

The next step was to build an F.E.A. model which allowed natural convection. All these models used temperature-dependent material properties which was an advance over previous work on magma cooling. The Ansys F.E.A. models were compared to the experimental models of (Jaupart and Brandeis, 1986) and the theoretical models of (Deardoff et al., 1969). These comparisons showed that the Ansys models were a limited success. It was decided that there were enough similarities to allow the program of Ansys F.E.A. experiments to continue.

One set of experiments examined the effect of making the material properties vary as a function of temperature. These experiments demonstrated that viscosity and density had a significant effect on convection. This was not unsurprising considering their effect on the Rayleigh number and hence convection. Other experiments investigated

the effect of height and width on the cooling of magma in dykes. These models showed that where there was a temperature gradient, with a hotter base and cooler top, then the wider the dyke the hotter the average temperature. They also demonstrated that the height of a dyke had little effect on the average temperature. This was not unexpected; the cooler country rock would be the greatest area of heat loss and as this would be dominantly a process perpendicular to the walls, so the effect of width would be the most significant.

In the case of the dykes that fed the 1991-93 eruption on Mount Etna it was estimated that they were between 1 and 5m wide and they erupted a basaltic magma with a viscosity of the order of 10^2 Pas. These were relatively narrow dykes with a fairly low viscosity, the models suggest that in a closed system the magma would solidify in a matter of days or weeks. Clearly they did not or they would not have been able to feed the eruption. Tolbachik (Kamchatka) is similar, again the dyke was approximately 5m wide and basaltic in composition. This dyke has stayed hotter for much longer than the Etnean feeder dykes, so what can account for this difference? (Connor et al., 1997) has suggested that the Tolbachik dyke may have remained hot for so long mainly because of the insulating effect of the surrounding scoria and the re-distribution of heat by convective transfer. It is possible that the Etnean dykes have shown these effects to a lesser degree. The Tolbachik dyke was emplaced into a cinder cone whereas on Mount Etna the magma was intruded into pre-existing fractures in denser country rock. This would imply that the thermal conductivity of the country rock is clearly an important factor.

A comparison was made between the conductive and convective models of Ansys, this showed that both models and hence dykes could stay hotter longer than previously thought. The most notable part of this graph (figure 2.20, page 51) was that after the first week the convective model cooled much slower than the conductive one. It is generally thought that convecting magma cools faster than conducting magma. For the convective model to be correct, additional processes must be taking place, perhaps as the convecting model shows initially a faster cooling rate and an insulated boundary forms quicker so after this period the temperature gradient is greatly reduced. The conductive model may take much longer to form this layer hence the faster cooling rate, but further work is required to resolve this.

4.2 Cooling in Lava Lakes

In Chapter 3 I built an analogue model from a mathematical model. The mathematical model was based on a combination of equations from (Kazahaya et al., 1994; Turcotte and Schubert, 1982) and a simplified model of a lava lake-conduit-magma chamber system. This lava lake-conduit-magma chamber system was used to build the laboratory model with which to conduct the experiments. I was able to examine different conduit widths, different volumes of both the upper and lower chambers. The viscosity of a magma is clearly important therefore I used fluids of varying viscosities. I examined the effect on cooling of both the upper lake and lower chamber in isolation to see how they cool without any convective exchange of fluid. Then I examined how the cooling is effected by exchange of fluid between the lake and chamber. Systematic combinations of these parameters were used to run the experiments. The results from these experiments showed that there were variations between repeated experiments but on the whole the cooling trends were consistent. The cooling trends in the isolated chambers were shown to be different to those where there was an exchange of fluid. There was also a difference between the upper lake and lower chamber.

From these experiments several aspects became apparent. The lava lakes remained hotter where the conduits were wider, for lakes of the same surface areas the higher the volume of the lake the longer they took to cool. It would be expected for larger surface areas there would be a larger heat loss. Varying the viscosity of the fluids led to the conclusion that the more viscous the fluid the slower the rate of cooling. Isolated chambers showed a fast cooling rate, heat was only being lost and not added to the system. When exchange was allowed it appeared that the lake had a slower cooling rate than when it was isolated, this may be explained by cooler material being removed and warmer material buoyantly rising to take it place.

4.2.1 Application to Inactive Lava lakes

When looking at the longevity of lava lakes I first examined inactive lava lakes. These are defined in Chapter 3 as ponds of lava with no direct connection to the magmatic system. I obtained rough estimates of properties of the Hawaiian basaltic lava ponds, Alae, Makaopuhi and Kilauea Iki from various sources such as (Peck et al., 1979). These estimates included volume, temperature of the lava lake, solidus temperature and the lifespan of the lava lake. The details for Makaopuhi were fairly

sketchy but were estimated to be between those of Alae and Kilauea Iki as the volume and lava temperature was between the two. This led to values of k_1, the cooling constant as defined in chapter 3, from 0.23×10^{-9} to 5.6×10^{-9} Ks^{-1} and when these values are plotted against estimated volume, the relationship shown in Figure 4.1 was obtained. In this example the magma source should be fairly similar so any effects due to differing composition and material properties of the magma should be minimal. I believe this to show that these are comparable to the isolated chamber experiments where, as volume increases, the value of the cooling constant decreases which results in slower cooling (Chapter 3, figure 3.6).

4.2.2 Application to Active Lava Lakes

4.2.2.1 Volume in the Lava Lake

It is clear from the section above there is an inverse relationship between cooling rate lava lake volumes. On Mount Erebus the lava lake's surface area varied from 11000 m^2 in 1983 to 2800 m^2 in 1987, implying that there must be an element of forced convection. Erta 'Ale has been much more consistent and steadily active with a reasonably steady volume. On Nyiragongo it appears to have filled to a high volume in 1977, then drained and refilled to a much lower level by 1982. Lava lakes on Kilauea also show variation in their volumes.

Although my experiments show that there is a relationship between volume and cooling rate it is difficult to demonstrate this with active lava lakes as their volume is rarely constant.

4.2.2.2 Conduit Width

Again like with volume the experiments show that there is a relationship between conduit width and heat loss. The experiments show that a wider conduit will keep a lake hotter for longer.

Many people have inferred the widths of conduits (Allard, 1997; Giggenbach et al., 1973; Rymer et al., 1995; Tazieff, 1994) and again they vary over time. Obviously if conduits are very narrow then they will solidify relatively rapidly if they have no regular influx and conversely if they are very wide they will be more difficult to block. However Erta 'Ale has recently been estimated to have a conduit width of

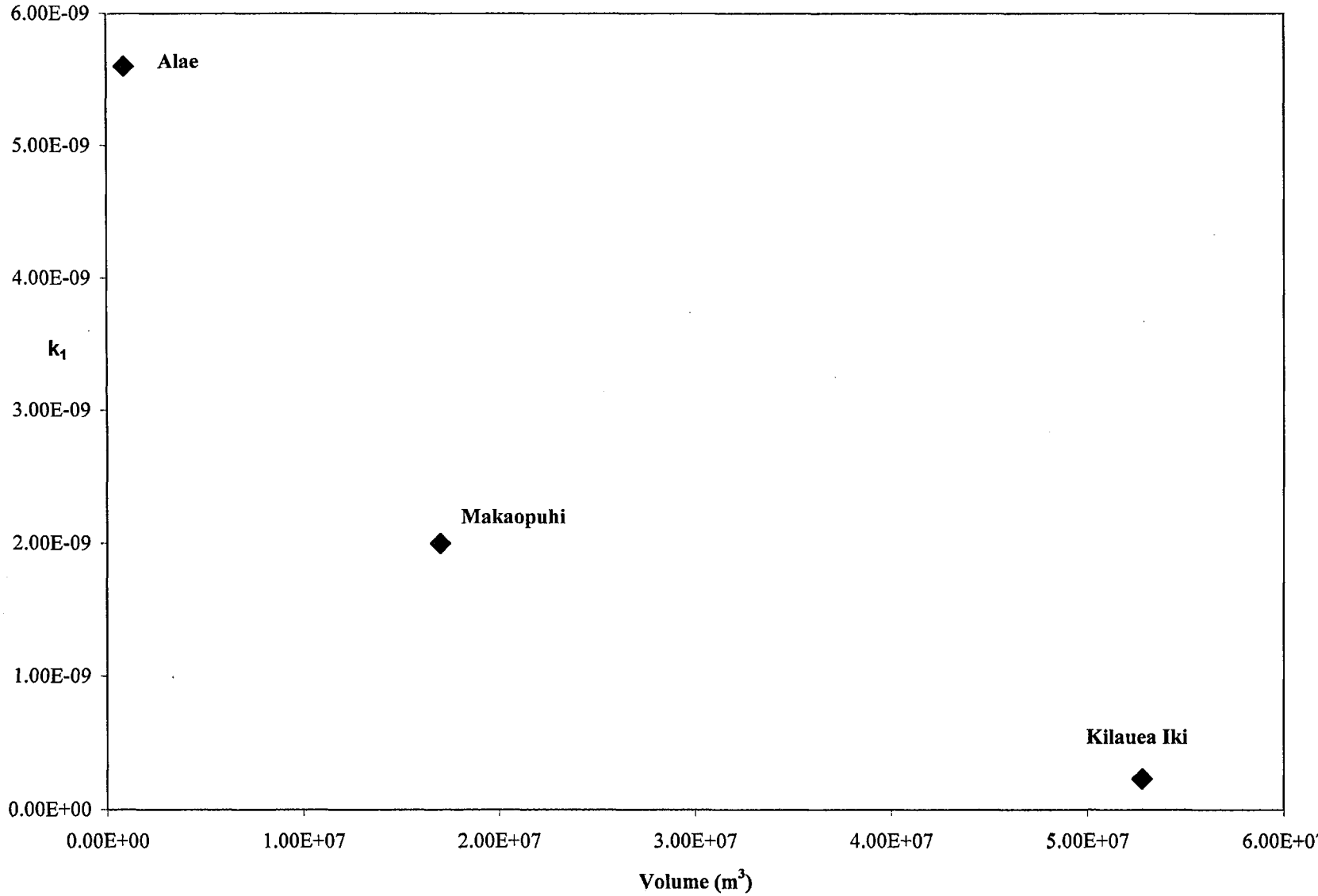

Figure 4.1 This illustrates how an estimate of the cooling constant k_1, decreases with the increase in the lava lake volume.

about 1.5m to 5m (Burgi et al., 2002) and the lava lakes here are thought to be around a hundred years old. A conduit in Kilauea's east rift zone has an estimated conduit width of about 7.5m (Hardee, 1988); Etna's conduit has been modelled at about 25m (Rymer et al., 1993). As with lake volume there is variability in conduit width over time and this makes the relationship hard to test with existing data.

4.2.2.3 Magma Viscosity

Both Mount Erebus and Erta 'Ale have been active for a considerable time, but the viscosity of their magmas is very different. The viscosity of phonolite from Mount Erebus can be up to 10^4 Pas (Aster et al., 2003) and viscosity of basalt from Erta 'Ale is more like 10^1 to 10^2 Pas. As mentioned in Chapter 1.3.2 Mount Erebus and Erta 'Ale have different styles of activity due to their viscosity differences. The surface area of Mount Erebus has varied considerably over time, it has regular mild strombolian bursts and occasional more violent strombolian outbursts. The reasonably high viscosity would allow for slower cooling aided by some recharge. Erta 'Ale with its lower viscosity magma reacts differently; there were noticeable and consistent currents across the surface. This would suggest that the lake should cool quickly but it is one of the longest-lived known lakes. As the currents flow rapidly it suggests that cooled magma could be efficiently removed and replaced by new hot magma. So although these two magmas have very different viscosities they may work in different ways to achieve the same result.

4.3 Suggestions for Further Work

Another concern was that the Ansys F.E.A. model was inherently flawed, many people examined this model and no obvious error was found. One way to check this would have been to use a different package to create the model hopefully in the process eliminating any systematic error. Due to time constraints and uncertainty this part of the modelling was not continued.

The work in this thesis leads to a number of further questions.

Further testing and expansion of the F.E.A. models may answer questions such as:

- How would the inclusion of volatiles affect the cooling rate? This could also apply to the laboratory experiments.

- The temperature of the walls in the F.E.A. models was held constant, how would a time-dependent temperature affect the cooling rate?
- I examined conduction and natural convection, what effect would forced convection and an open system have on the cooling rate?
- Latent heat was not included in the F.E.A. model, so what effect would this have?

The laboratory experiments were also just a starting point for more advanced models. Potential future issues could be:

- The effect of volatiles in the system and their effect on cooling.
- The heating and / or cooling of fluids during the experiment could be set up to examine any increased convection.
- The equipment was designed to overturn like an egg-timer so that two fluids of differing viscosity could be placed within, then overturned and their intermingling examined.
- Pumping fluid into the system would simulate an open system instead of the closed system used here. As real dykes and lava lakes are generally open systems this would be a useful set of experiments to carry out.

There is enormous potential for further work in this field. The next step would be to investigate the injection of fresh magma into the system. In this study, active systems have been assumed to be connected to a deeper magma source supplying heat and volatile-rich magma, but the system has been essentially 'closed'. A system that is 'open' at the base to fresh magma supplies (and perhaps able to remove gas-depleted and cooler magma) would be expected to behave slightly differently. It would be interesting to see how often and how much hot material would need to be added to the system to minimise solidification and enable activity to continue.

The replenishment of magma chambers can have implications for various aspects of the volcanic system. (Rymer and Williams-Jones, 2001) suggests that magma entering a magma chamber at low Reynolds numbers i.e. low velocity/high viscosity and low turbulence will not interact significantly with the magma already resident in the chamber. This intrusion would therefore not be expected to precede a catastrophic degassing of magma and explosive eruption. It might however lead to quiet effusive

eruptions or feed a persistent lava lake (Rymer and Williams-Jones, 2001). In systems where the fresh magma intrusion has a higher Reynolds numbers then the more turbulent system may lead to super-heating and significant vesiculation of the magma causing expansion of the chamber. This build up of gas pressure in the chamber can lead to explosive eruptive activity.

It would be interesting to see how different Reynolds numbers can lead to different regimes of mixing within magma chambers and the wider volcanic system. Questions that arise from this investigation are:

- What ranges of Reynolds numbers lead to significant interaction within a magma chamber? Hence aiding greater understanding of eruption precursors.
- How does the Reynolds number of the incoming material affect temperatures in the lava lake?
- What set of conditions could lead to an extended lifespan of a lava lake?
- What happens to the cooling rate of a lava lake if hot material is added for a period and then after a while some more is added.
- How does this situation of adding material compare to systems where the mass is constant.

The existing laboratory model equipment of a magma chamber/conduit/lava lake system should be sufficient to continue this investigation. The base plate of the equipment has a tap through which it would be possible to pump material into the system. To vary the Reynolds number (the ratio of density to viscosity multiplied by the velocity) only input flow rate need be changed. So experiments can be done for a range of flow rates and hence Reynolds numbers. Whether the host material is initially stationary or convecting is another question so that would need to be looked at.

It would be expected that by increasing the Reynolds number there would be increased turbulence within the chamber and hence increased mixing as suggested by others (Huppert et al., 1986). In a chamber where convection is already taking place the host magma may then entrain inputs of material and therefore mix at lower Reynolds numbers than in cases where the host is stagnant. Therefore the initial conditions within the magma chamber is naturally critical if entrainment is taking place.

For the more advanced models a series of possibilities are likely. The higher the Reynolds number the faster the mixing. This may lead to an increased temperature gradient between the chamber and the lava lake and so this may initiate stronger convection and the cooling rate in the lake would decrease. While material is being added, an overall increase in temperature of the system would be expected providing the heat coming in exceeds that lost to the surroundings.

These experiments should be able to tell us about mixing regimes which may be able to affect the temperatures of lava lakes and also give an idea of what kinds of conditions lead to vesiculation and hence possible eruptive conditions.

References

Allard, P., 1997. Endogenous magma degassing and storage at Mt Etna. Geophysical Research Letters, 24(17): 2219-2222.

Ansys.Inc, 1994. Ansys Workbook.

Armienti, P. et al., 1994. The long-standing 1991-1993 Mount Etna eruption: petrography and geochemistry of lavas. Acta Vulcanologica, 4: 15-28.

Aster, R. et al., 2003. Very Long Period Oscillations of Mount Erebus Volcano. Journal of Geophysical Research, 108(B11): 2522.

Bailey, E.B., Clough, C.T., Wright, W.B. and Wilson, G.V., 1924. Tertiary and post-Tertiary geology of Mull, Loch Aline, and Oban. Scottish Geological Survey Memoirs: 445.

Barbieri, F., Bertagnini, A. and Landi, P., 1990. Mount Etna: the 1989 eruption. Giradini.

Brown, G.C. and Musset, A.E., 1995. The Inaccessible Earth, 2nd Edition. Chapman and Hall, London.

Bruce, P.M. and Huppert, H.E., 1989. Thermal Controls of basaltic fissure eruptions. Nature, 342: 665-667.

Burgi, P., Caillet, M. and Haefeli, S., 2002. Field temperature measurements at Erta 'Ale Lava Lake, Ethiopia. Bulletin of Volcanology: online.

Buttner, R., B.Z., Blumm, J. and Hagemann, L., 1998. Thermal conductivity of a volcanic rock material (olivine-melilitite) in the temperature range between 288 and 1470K. Journal of Volcanology and Geothermal Research (80): 293-302.

Carrigan, C.R., 1983. A Heat Pipe Model for Vertical, Magma-filled Conduits. Journal of Volcanology and Geothermal Research, 16: 279-298.

Carrigan, C.R., Schubert, G. and Eichelberger, J.C., 1992. Thermal and dynamical regimes of single- and two-phase magmatic flow in dikes. Journal of Geophysical Research, 97(B12): 17377-17392.

Carslaw, H.S. and Jaeger, J.C., 1959. Conduction of Heat in Solids. Oxford University Press, Oxford, pp. 92-132.

Connor, C.B. et al., 1997. Cooling of an Igneous dike 20 yr after intrusion. Geology, 25(8): 711-714.

Deardorff, J.W., Willis, G.E. and Lilly, D.K., 1969. Laboratory experiments of non-steady penetrative convection. Journal of Fluid Mechanics, 35: 7-31.

Emery, A.F. and Lee, J.W., 1999. The effects of property variations on natural convection in a square enclosure. Journal of Heat Transfer, 121: 57-62.

Fagan, M.J., 1992. Finite Element Analysis Theory and practice. John Wiley & Sons.

Francis, P., Oppenheimer, C. and Stevenson, D., 1993. Endogenous growth of persistently active volcanoes. Nature, 366: 554-557.

Giggenbach, W.F., Kyle, P.R. and Lyon, G., 1973. Present Volcanic Activity on Mt Erebus, Ross Island, Antarctica. Geology (1): 135-136.

Hardee, H.C., 1988. Heat and Mass Transport in the East-Rift Zone Magma Conduit of Kilauea Volcano. USGS Professional Paper (1350).

Harris, A.J.L., Flynn., L.P., Rothery, D.A., Oppenheimer, C. and Sherman, S.B., 1999. Mass Flux measurements at active lava lakes: Implications for magma recycling. Journal of Geophysical Research, 104(B4): 7117-7136.

Heliker, C.C., Mangan, M.T., Mattox, T.N., Kauahikaua, J.P. and Helz, R.T., 1998. The character of long-term eruptions: inferences from episodes 50-53 pf the Pu'u 'O'o-Kupainaha eruption of Kilauea Volcano. Bulletin of Volcanology, 59: 381-393.

Ho-Liu, P., Hager, B.H. and Raefsky, A., 1985. An improved method for computing heat flux in convection calculations. EOS Transactions, Am.Geophysical Union, 66: 1070.

Huppert, H.E. and Bruce, P.M., 1990. Solidification and melting along dykes by the laminar flow of Basaltic Magma, Magma Transport and Storage.

Huppert, H.E., Sparks, R.S.J., Whitehead, J.A. and Hallworth, M.A., 1986. Replenishment of Magma Chambers by Light Inputs. Journal of Geophysical Research, 91(B6): 6113-6122.

Incropera, F.P. and DeWitt, D.P., 1990. Introduction to Heat Transfer. John Wiley & Sons.

Jaeger, J.C., 1964. Thermal effects of Intrusions. Reviews of Geophysics, 2(3): 443-466.

Jaeger, J.C., 1968. Cooling and solidification of igneous rocks. In: Hess.H.H and Poldervaart.A. (Editors), Basalts: The Poldervaart Treatise on rocks of basaltic composition. John Wiley &Sons, pp. 503-536.

Jaupart, C. and Brandeis, G., 1986. The stagnant bottom layer of convecting magma chambers. Earth and Planetary Science Letters, 80: 183.

Kazahaya, K., Shinohara, H. and Saito, G., 1994. Excessive degassing of Izu-Oshima volcano: magma convection in a conduit. Bulletin of Volcanology, 56(3): 207-216.

Keszthelyi, L., 1994. Calculated effect of vesicles on the thermal properties of cooling basaltic lava flows. Journal of Volcanology and Geothermal Research, 63: 257-266.

Kyle, P.R. and Meeker, K., 1990. Emission Rates of Sulfur Dioxide, Trace Gases and Metals From Mount Erebus, Antarctica. Geophysical Research Letters, 17(12): 2125-2128.

LeGuern, F., 1987. Mechanism of energy transfer in the lava lake of Nyiragongo (Zaire), 1959-1977. Journal of Volcanology and Geothermal Research, 31: 17-31.

LeGuern, F., Carbonnelle, J. and Tazieff, H., 1979. Erta'Ale lava lake : Heat and gas transfer to the Atmosphere. Journal of Volcanology and geothermal research, 6: 27-48.

Maaloe, S., 1998. Shape of Ascending Feeder Dikes , and Ascent Modes of Magma. Journal of Volcanology and Geothermal Research, 81(3-4): 207-214.

McLeod, P. and S.Tait, 1999. The growth of dykes from magma chambers. Journal of Volcanology and Geothermal Research, 92: 231-246.

Mohr, P., 1962. The Ethiopian Rift System. Bulletin Geophysics(5): 33-62.

Oppenheimer, C. and Francis, P., 1998. Implications of longeval lava lakes for geomorpholgical and plutonic processes of Erta 'Ale volcano, Afar. Journal of Volcanology and Geothermal Research, 80: 101-111.

Otway, P.M., Blick, G.H. and Scott, B.J., 1994. Volcanic Deformation Monitoring on Mount Erebus: Methods and Results of Geodetic Surveys, 1980-1985. Volcanological and Environmental Studies of Mount Erebus, Antarctica, 66: 57-68.

Parfitt, E.A., Gregg, T.K. and Smith, D.K., 2002. A comparison between subaerial and submarine eruptions at Kilauea Volcano, Hawaii: implications for the thermal viability of lateral feeder dikes. Journal of Volcanology and Geothermal Research, 113(1-2): 213-242.

Peck, D.L., Wright, T.L. and Decker, R.W., 1979. The lava lakes of Kilauea. Scientific American, 241(4): 114-128.

Pollard, D.D. and Delaney, P.T., 1982. Solidification of Basaltic Magma during Flow in a Dike. American Journal of Science, 282(6): 856-885.

Rymer, H., Cassidy, J., Locke, C.A. and Murray, J.B., 1995. Magma Movements in Etna Volcano associated with the major 1991-1993 lava eruption: evidence from gravity and deformation. Bulletin of Volcanology, 57: 451-461.

Rymer, H., Murray, J.B., Brown, G.C., Ferrucci, F. and McGuire, W.J., 1993. Mechanisms of magma eruption and emplacement at Mt Etna between 1989 and 1992. Nature, 361: 439-441.

Rymer, H. and Williams-Jones, G., 2001. Detecting volcanic eruption precursors: a new method using gravity and deformation measurements. Geophysical Research Letters, 27(16): 2389-2392.

Sanderson, T.J.O., 1982. Direct gravimetric detection of magma movements at Mount Etna. Nature, 297: 487-490.

Stevenson, D.S. and Blake, S., 1998. Modelling the dynamics and thermodynamics of volcanic degassing. Bulletin of Volcanology (60): 307-317.

Swanson, D.A., Duffield, W.A., Jackson, D.B. and Peterson, D.W., 1972. The complex filling of Alae crater, Kilauea Volcano, Hawaii. Bulletin of Volcanology, 36: 105-126.

Tazieff, H., 1994. Permanent lava lakes: observed facts and induced mechanisms. Journal of Volcanology and geothermal research, 63: 3-11.

Turcotte, D.L. and Schubert, G., 1982. Geodynamics. John Wiley and Sons, 450 pp.

Wada, Y., 1994. On the relationship between dike width and magma viscosity. Journal of Geophysical Research, 99(B4): 17743-17755.

Weinberg, R.F. and Leitch, A.M., 1998. Mingling in mafic magma chambers replenished by light felsic inputs: fluid dynamical experiments. Earth and Planetary Science Letters (157): 41-56.